CHALMERS
UNIVERSITY OF TECHNOLOGY

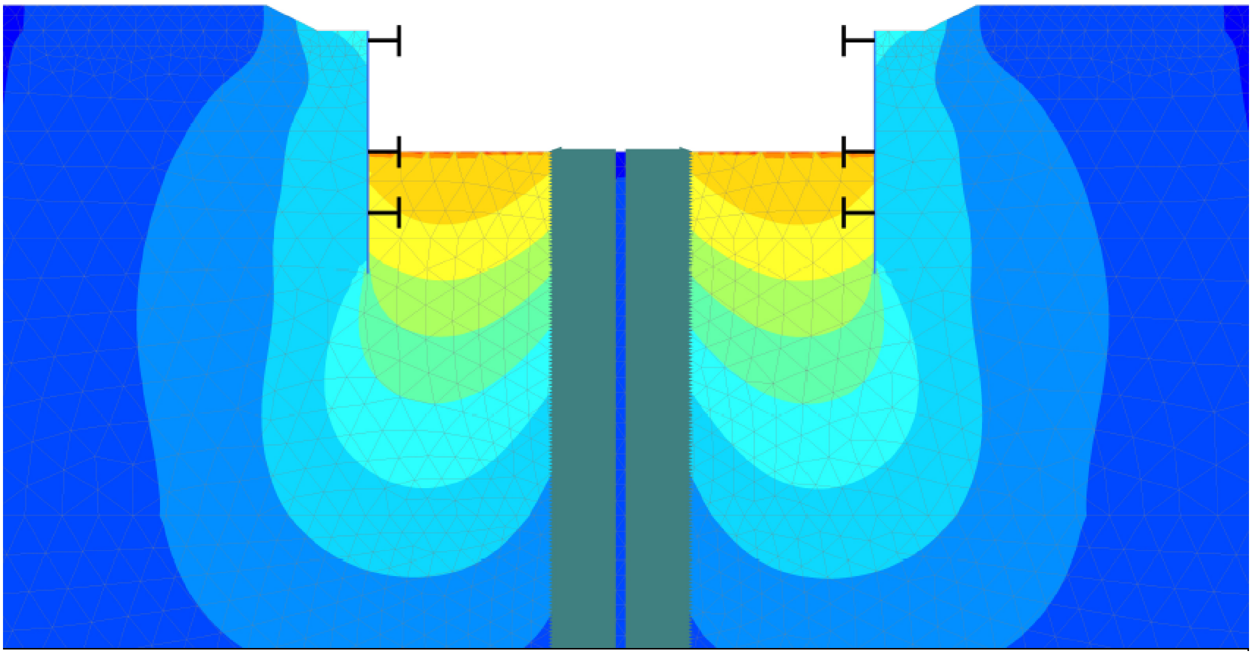

Mass displacement due to pile installation in soft and sensitive clay

The influence pile installation with precast concrete displacement piles has on adjacent areas

Master's Thesis in the Master's Programme Infrastructure and Environmental Engineering

GILA EDVARDSSON
PAULA MELIN-NYHOLM

Department of Architecture and Civil Engineering
Division of Geology and Geotechnics
Geotechnical Engineering Research Group
CHALMERS UNIVERSITY OF TECHNOLOGY
Master's Thesis ACEX30-18-31
Gothenburg, Sweden 2018

Master's Thesis ACEX30-18-31

Mass displacement due to pile installation in soft and sensitive clay

The influence pile installation with precast concrete displacement piles has on adjacent areas

Master's Thesis in the Master's Programme Infrastructure and Environmental Engineering

GILA EDVARDSSON
PAULA MELIN-NYHOLM

Department of Architecture and Civil Engineering
Division of Geology and Geotechnics
Geotechnical Engineering Research Group
Chalmers University of Technology
Göteborg, Sweden 2018

Mass displacement due to pile installation in soft and sensitive clay
The influence pile installation with precast concrete displacement piles has on adjacent areas

Master's Thesis in the Master's Programme Infrastructure and Environmental Engineering
GILA EDVARDSSON
PAULA MELIN-NYHOLM

Examensarbete ACEX30-18-31
Institutionen för arkitektur och samhällsbyggnadsteknik
Chalmers tekniska högskola, 2018

Department of Architecture and Civil Engineering
Division of Geology and Geotechnics
Geotechnical Engineering Research Group
Chalmers University of Technology
SE-412 96 Göteborg
Sweden
Telephone: +46 (0)31-772 1000

Cover:
Plane strain model in PLAXIS, where the cross section 475+480 of the project Västlänken Station Centralen is modelled. The illustration shows the total displacement around and in the excavation, for more information see *Chapter 5*.

Göteborg, Sweden, 2018

Mass displacement due to pile installation in soft and sensitive clay

The influence pile installation with precast concrete displacement piles has on adjacent areas

Master's Thesis in the Master's Programme Infrastructure and Environmental Engineering

GILA EDVARDSSON

PAULA MELIN-NYHOLM

Department of Architecture and Civil Engineering
Division of Geology and Geotechnics
Geotechnical Engineering Research Group
Chalmers University of Technology

Abstract

The installation of displacement piles is known to lead to disturbances in soft sensitive clays as found in Gothenburg, i.e. deformations, excess pore water pressures and loss of strength and stiffness. In this Thesis the mass displacement and pore pressure build up due to installation of precast concrete displacement piles is investigated for the construction of the Central Station project within Västlänken. A numerical plane strain cavity expansion approach is adopted using a 2D Finite Element code with a suitable constitutive model for soft soils. The modelling approach was first validated against field measurements from nearby projects, i.e., a bridge support for the *Partihallsbron* and a project on the lowering of the highway *E45* between Lilla Bommen and Marieholm before the Västlänken case is studied in detail.

The results indicate that for a well calibrated model the trends and magnitudes of the vertical component of the mass displacements can be obtained with a maximum error of approximately 10 millimetres. Over time the initial settlements double in magnitude due to consolidation and creep. The location and construction sequence of the piling works was further investigated for the Västlänken case by simulating pile installation before and after excavation of the building pit and with or without pre-augering. For these scenarios the maximum vertical mass displacement of the ground surface was largest when piling after construction of the retaining walls and excavation, but the impact area was smallest. The lowest vertical mass displacement occurred when a pre-augering/pile-block was used. Adjacent support structures that confined the piled soil volume deformed due to the mass displacement from pile installation. Furthermore, the excess pore pressure was largest adjacent close to the cavity directly after piling, with an excess pore water front moving outwards during consolidation over a total period of 80 years.

Keywords: Mass displacement, superpile, prescribed line displacement, pile installation, PLAXIS 2D.

Massundanträngning som en följd av installation av pålar i lös och känslig lera
Påverkan som pålinstallation med färdiggjutna betongpålar har på närliggande områden
Examensarbete inom masterprogrammet Infrastruktur och Miljöteknik
GILA EDVARDSSON
PAULA MELIN-NYHOLM
Institutionen för Arkitektur och Samhällsbyggnadsteknik
Avdelningen för Geologi och Geoteknik
Forskargruppen för Teknisk Geologi och Geoteknik
Chalmers Tekniska Högskola

Sammanfattning

Vid pålning av massundanträngande pålar i lös och känslig lera, som den i Göteborg, är kända för att orsaka störningar i jorden. I examensarbetet är massundanträngningen och uppbyggnaden av porvattentrycket som en konsekvens av pålning av färdiggjutna massundanträngande betongpålar, för konstruktionen av *Västlänken* Station Centralen undersökt. Detta med numerisk modellering, PLAXIS 2D, plane strain antagande, superpåle och en tolkning av Cavity Expansion Method. Den odränerade responsen av jorden var modellerad med den konstitutiva modellen Soft Soil och långtidsfallet med Soft Soil Creep. Modellen validerades mot fältdata från andra byggprojekt i området, närmare bestämt ett av brostöden till *Partihallsbron* och nedsänkningen av *E45:an*, mellan Lilla Bommen och Marieholm. Modellen skapades för att fånga den nuvarande stresshistoriken, sättningshastigheten och porvattenövertrycket i området. Pålningen modellerades som en ihålighet fylld med ett poröst linjär-elastiskt material, vilket expanderade med en föreskriven linjeförskjuten. Härledd från en ekvation som gav den procentuella ökningen av superpålen, med antagandet att leran ej skulle genomgå någon volymförändring, då den i princip är ogenomsläpplig. Resultatet visade att modellen fångade trenden och storleken på massundanträngningen, med felvärden på maximalt tio millimeter. Beträffande långtidssättningarna gav modellen, med hänsyn till krypning, nästan dubbelt så höga sättningar vid 80 års konsolidering. Effekten på massundanträngning och uppbyggnaden av porvattenövertryck beroende på var pålinstallationen skedde undersöktes i *Västlänken*, då med pålning från schaktbotten eller innan schaktningen utfördes, med eller utan knektning eller dragning av lerproppar. Slutsatsen var att den maximala hävningen av markytan skedde då pålningen utfördes från schaktbotten, men påverkningsområdet var minst. Den lägsta hävningen gavs då lerproppar drogs eller knektning utfördes. Intilliggande stödkonstruktioner deformerades som en konsekvens av massundanträngnigen. Porvattenövertrycket var direkt efter pålningen som högst intill superpålen och vandrade sedan till de horisontella gränserna under konsolideringen och hade efter 80 år konsoliderat bort.
Nyckelord: Massundanträngning, superpåle, föreskriven linjeförskjuten, pålinstallation, PLAXIS 2D.

Acknowledgements

This Master's Thesis was conducted at the Division of Geology and Geotechnics at Chalmers University of Technology and in collaboration with Tyréns. The Thesis was written between February and June 2018.

Firstly would we like to thank our supervisor Tim Björkman at Tyréns for all the help, knowledge and encouragement throughout the work with this Master's Thesis. We would also like to thank Jelke Dijkstra, our supervisor and examiner at Chalmers, for your honest opinions and advices. Further would we like to thank Tara Wood for your expertise and all the colleagues at Tyréns for the help.

Finally, would we like to thank our families and friends for their support during this process.

Gila Edvardsson and Paula Melin-Nyholm, Gothenburg, June 2018

Contents

List of Figures

List of Tables

Notations

Roman upper case letters

E'	Effective Young's modulus
E'_{oed}	Constrained modulus
G	Shear modulus
K_0	Earth pressure coefficient at rest
K_0^{NC}	Earth pressure coefficient for normally consolidated soils
M_{MC}	Modified Mohr-Coulomb
P_i	Inner pressure acting on a spherical cavity
P_u	Outer pressure acting on the spherical cavity
R_{inter}	Interface factor
S	Point source
S'	Mirror image sink
V_p	Pile volume

Roman lower case letters

a_{sp}	Area of superpile
a_{pa}	Piling area
b	Width of the piling area
c'	Effective cohesion
c_{ref}	Reference cohesion
d	Depth of the pile below the ground surface or excavation bottom
e_{init}	Initial void ratio
k_x	Horizontal permeability in PLAXIS
k_y	Vertical permeability in PLAXIS
l	Length of the piling area
p'	Mean effective stress
r	Radius
v'	Poisson's ratio for drained conditions
v_{ur}	Poisson's ratio for loading and unloading
w_{sp}	Width of superpile
x	Mass displacement within the piling area
x_{max}	Maximum horizontal boundary in PLAXIS
x_{min}	Minimum horizontal boundary in PLAXIS
y_{max}	Maximum vertical boundary in PLAXIS
y_{min}	Minimum vertical boundary in PLAXIS

Greek letters

α	Relative weight of constructions in Rehnman
β	Relative weight of constructions in Rehnman
γ	Relative weight of constructions in Rehnman
γ_s	Deviatoric strain
γ_{sat}	Saturated unit weight
γ_{unsat}	Unsaturated unit weight
δ	Relative weight of constructions in Rehnman
ΔV_{pr}	Volume of removed clay with pre-augering
ε_1	Axial strain
ε_v	Volumetric strain
η	The heave factor
κ_1^*	Modified swelling index in PLAXIS
κ_2^*	Modified swelling index in PLAXIS
κ^*	Modified swelling index
λ^*	Modified compression index
μ^*	Modified creep index
σ_c'	Pre-consolidation pressure
σ_v'	Effective vertical stress
ϕ_c'	Effective friction angle
ψ	Dilatancy angel

Abbreviations

CEM	Cavity expansion method
CRS	Constant rate of strain
FEM	Finite element method
IL	Incremental loading
LE	Linear elastic
MC	Mohr-Coloumb
NCS	Normal compression surface
OCR	Over consolidation ratio
POP	Pre-overburden pressure
SPM	Strain path method
SS	Soft Soil
SSC	Soft Soil Creep
SSPM	Shallow strain path method

"It is not the beauty of a building you should look at; it's the construction of the foundation that will stand the test of time."

- David Allan Coen

1 Introduction

A global trend and contemporary challenge is growing urbanisation, which puts pressure on already densely populated areas. The cities must grow and space effective solutions need to be utilised to cope with the increasing demand on housing and infrastructure. As a global challenge this is highly relevant, not least in Sweden, as the population in South West of Sweden is growing rapidly. Therefore, an infrastructural investment is made with the city of Gothenburg as hub, called *Västsvenska Paketet* [Västsvenska paketet, nda]. The investment incorporates several infrastructural investments such as highways, railroads, bridges and commuting traffic. This to ensure more reliable transport for industry, smaller environmental impact and better commuting options. The aim is to make the city more accessible to everyone who wants to work or study in Gothenburg and enable the city to grow by making the commuting more efficient.

To enable these infrastructural projects, the need for a stable and efficient foundation method is crucial. One of the most common foundation methods, with the purpose to transmit the loads from the constructions down in the sub-layers with adequate strength, is the pile [Knappett and Craig, 2012]. Piles are often used when constructing bridge approach abutments, road embankments and buildings on soft and sensitive soil. One soft soil type is the sensitive clay that in large parts of Scandinavia can be found along coastlines and near lakes, areas which are commonly densely populated [Massarsch and Wersäll, 2013]. Hence, prone to have large and heavy constructions, which is the case in Gothenburg. The installation of piles in such areas can result in horizontal and vertical mass displacement of the soil, depending on the used pile type and piling technique.

Investigations and predictions of mass displacement and the influence it has on adjacent constructions can be carried out with several different methods, such as empirical, analytical and numerical. The different calculation methods have their advantages and disadvantages, where the complexity of the problem and the level of accuracy needed to be obtained decides which method is most appropriate. Methods based on empirical relationships often give rough predictions, whereas semi-analytical and analytical methods give better predictions and a higher level of accuracy. Numerical methods such as the finite element method is commonly used for modelling geotechnical problems when deformations are of importance.

1.1 Background

The biggest individual investment in *Västsvenska Paketet* is *Västlänken*, an eight kilometres long double tracked railway, which mainly is going to be constructed as a tunnel under the central parts of Gothenburg, see *Figure 1.1*. Three stations will be constructed underground, one besides the existing Central Station, one at the junction Korsvägen and one in the district of Haga [Västsvenska paketet, ndb]. Both commuter trains and regional trains will traffic the railway which will link together the railway system in the South West of Sweden.

Figure 1.1: *Illustration over Västlänken with the area around the Central Station marked with a rectangle, modified from [Trafikverket, 2014].*

In addition to *Västlänken* being constructed adjacent to the existing Central Station, are several other infrastructural projects constructed constructed, projected for the area. A number of them as part of the *Västsvenska paketet* [Västsvenska paketet, nda]. A new bridge, *Hisingsbron*, is constructed to replace the old bridge *Götaälvbron* and connect Hisingen with the main land, see *Figure 1.2*. Adjacent to this is the highway *E45* is to be lowered, a stretch of 900 metres between Lilla Bommen and Marieholm, where approximate half of the stretch will be built as a tunnel, see *Figure 1.2* [Sabattini and Wallgren, 2018]. Between the lowering of the highway *E45* and *Hisingsbron*, a part of the new city district, *Platinan*, will be constructed.

The city district is planned to emerge around the Central Station through construction of new housing, business premises and offices, and is called *Centralenområdet* [Västsvenska paketet, ndc]. Another large construction being built as part of *Centralenområdet*, is the building *Regionens Hus*, which is built alongside the lowering of the highway *E45*, see *Figure 1.2*.

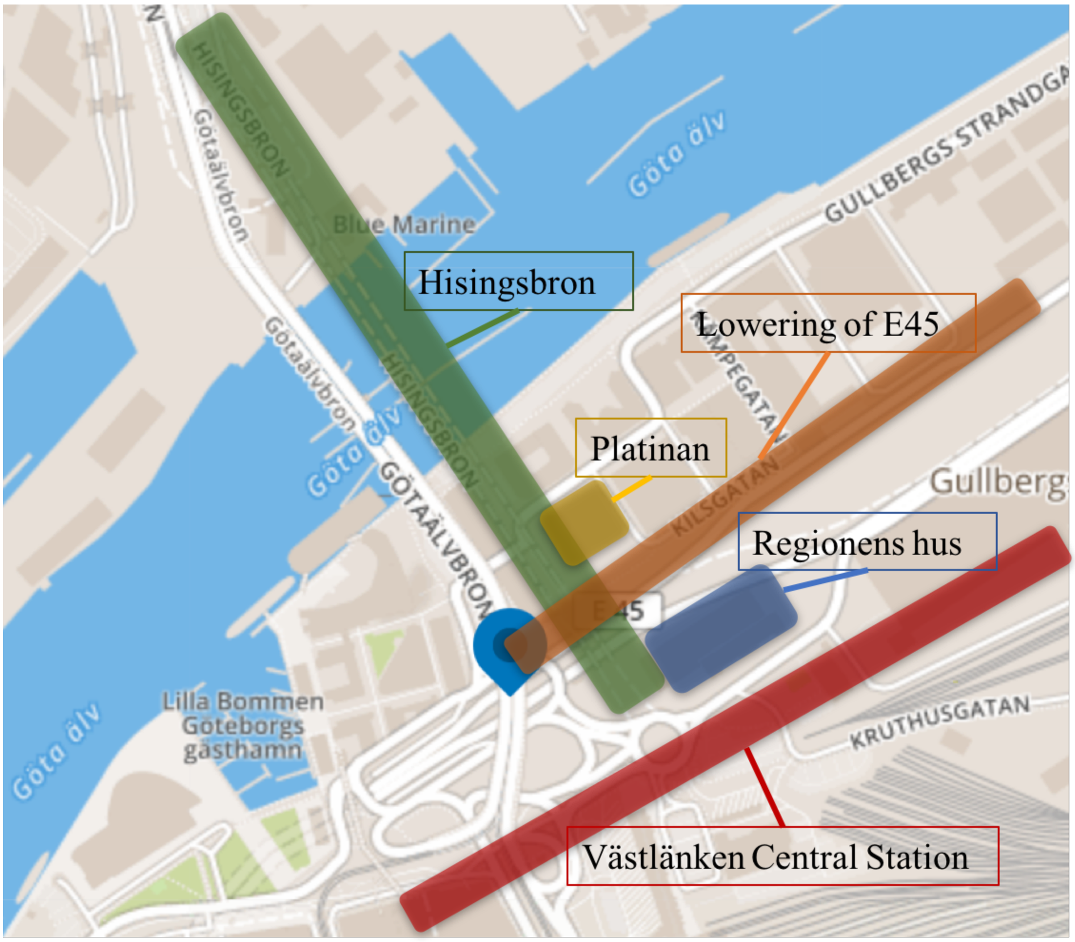

Figure 1.2: *Illustration over the construction projects taking place around the Central Station in Gothenburg, modified from [Google Maps, 2018].*

As the city of Gothenburg is partly located on deep deposits of soft and sensitive clay it is crucial to consider and execute good foundations which can control the rate and occurrence of settlements. The chosen foundation method is, to a large extent, precast concrete piles which is classified as a displacement pile, due to the consequently mass displacement that occurs when installing them. Thus, it is problematic when a large number of piles are driven in a confined area, in a number of parallel projects with different contractors. Therefore, in the area around Gothenburgs Central Station the contractors have started a project group where consultants from the projects discuss the movements and measures that should be taken, called *Project Navet*. This has enabled the contractors to take part of each other's field measurements of the mass displacement, among other things.

1.2 Aim

The aim of the Master's Thesis is to investigate numerical methods to predict the magnitude of mass displacement, as a consequence of pile installation with precast concrete displacement piles. The focus is on a case study of *Västlänken Station Centralen*.

The aim is divided into the following objectives:

- Evaluate the derived model parameters, with consideration to parameters which influence the result most.
- Derive and evaluate an equation for the prescribed line displacement, which is based on the area of the piles being installed.
- Perform numerical calculations on the chosen projects with PLAXIS 2D.
- Compare the result with field measurements and analyse the differences.
- Compare numerical models with or without consideration to time dependent behaviour such as creep, and analyse how this influence the result.
- Investigate how the excess pore pressure varies in the model with consideration to time and distance to the piling area.
- Compare the difference in the resulting mass displacement, when installing the piles from the ground surface with or without pre-augering/pile block or from the excavation bottom.

1.3 Limitations

In the Thesis is not the whole pile installation modelled, instead is the installation modelled as the expansion of a filled cavity in soft and sensitive clay. Ignoring the penetration of the pile into the soil, and other soil types.

1.4 Scope

The Thesis investigates the horizontal and vertical mass displacement occurring due to the installation of precast concrete displacement piles in three projects; *Partihallsbron*, the lowering of the highway *E45* and *Västlänken Station Centralen*. Considering how the influence pile area, installation technique and the geometry from which the piles are going to be installed have on adjacent areas. The calculations are carried out numerical with the finite element method, PLAXIS 2D and the constitutive models Mohr-Coulomb, Soft Soil and Soft Soil Creep. Furthermore, investigations are carried out concerning the change in excess pore water pressure, the influence creep have on long term settlements and how the deviatoric strains are captured in the model.

2

Pile installation and its effect on surrounding soil

There are two types of foundations, shallow foundations and deep foundations, see *Figure 2.1*. The latter is the foundation type considered in this Thesis. The characteristics of a deep foundation is that it consists of elements extending to a large depth into the ground, whilst occupying a small area in the plan. The most common version of this, hence deep foundation, is the pile [Knappett and Craig, 2012].

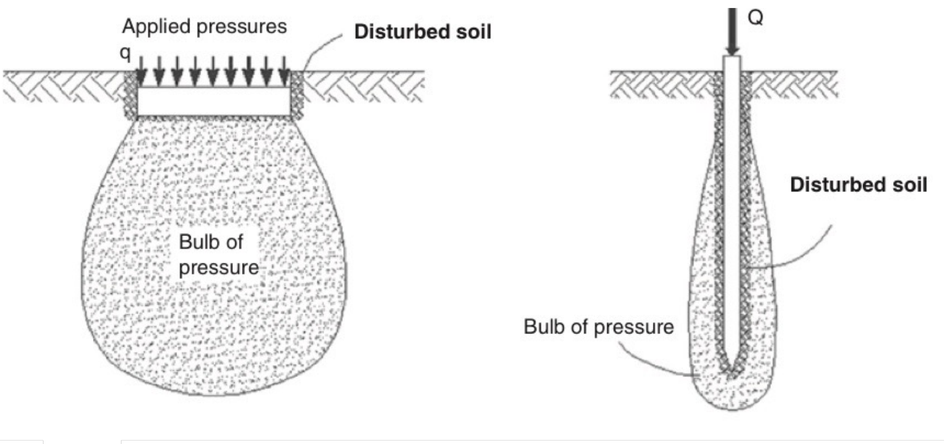

Figure 2.1: *Schematic illustration over a shallow foundation to the left and a deep foundation to the right, modified from [Viggiani et al., 2014].*

Physical processes occur in connection to the pile during its lifetime, which can be divided into the three phases: installation, equalisation and loading, see *Figure 2.2* [Ottolini et al., 2014].

During the installation phase will large strains, mass displacement, soil disturbance and excess pore water pressure occur consequently to the rapid change in void ratio and stresses in the soil [Abu-Farsakh et al., 2015]. When the pile penetrates the soil, the soil below the pile toe will be pushed downward, and then moved horizontally. Therefore, the initial soil structure and stress history will be destroyed. For nearly impermeable clays, during undrained conditions, will there be almost no volume change. Hence, the pile volume driven will correlate to the volume of mass displacement. During the pile installation in undrained conditions will the pore pressure in the soil change as soft clays contracts with no volume change. Which directly influence the total stresses in the soil [Randolph et al., 2011].

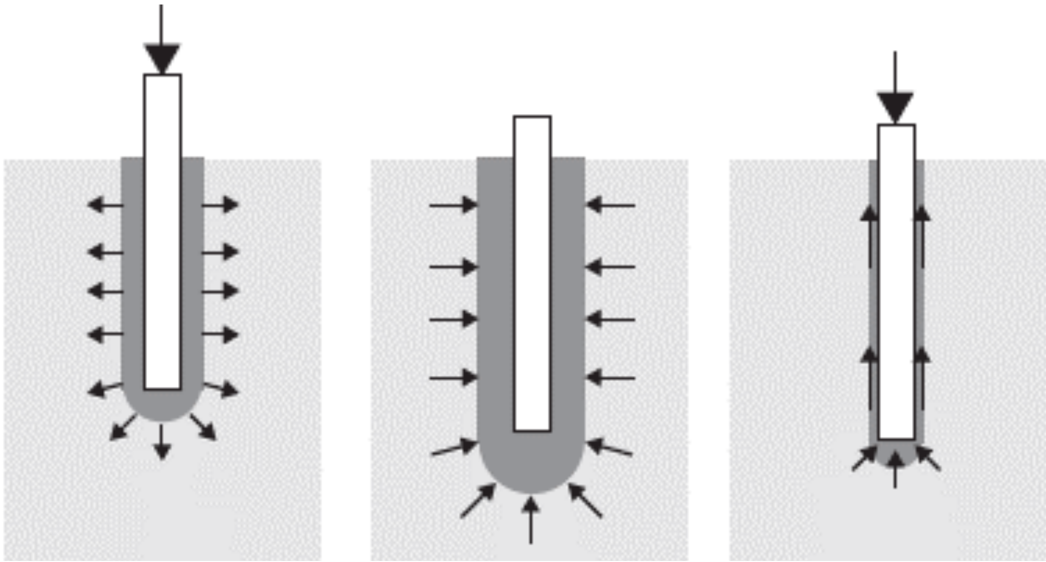

Figure 2.2: *Illustration of the phases that occurring during pile history, from left to right; installation, equalisation and loading, modified from [Ottolini et al., 2014].*

Following the installation phase is the equalisation phase, also called the set-up period, where the soil moves back towards the pile due to dissipation of the excess pore pressures induced, consolidation, and the rearrangement of soil particles, thixotropic effects [Abu-Farsakh et al., 2015]. The equalisation of pore pressure, creep and thixotropic effects means that the bearing capacity of the soil starts to recover [Augustesen et al., 2006]. The time it takes for the bearing capacity to recover, called the set-up period, is dependent on the hydraulic conductivity and stiffness of the clay. In Gothenburg clay is the empirical knowledge that the equalisation time is between three to six months [Fellenius, 1972]. Adjacent to the pile shaft will the decrease of void ratio in the clay lead to an increase of the undrained shear strength.

In the following loading phase is the load on the pile head transmitted through the pile into the soil. Where the bearing capacity of the pile is directly proportional to the interface friction angle at the pile-soil interface and the normal effective stresses [Randolph et al., 2011].

2.1 Pile types and installation techniques

Different piles and piling techniques will have different effect on the mass displacement [Knappett and Craig, 2012]. Mass displacement occurs when the volume of piles installed pushes away corresponding volume of soil [Olsson and Holm, 1993]. To counteract mass displacement can soil be removed through drilling, decreasing the total volume of soil which is being pushed away, commonly known as pre-augering.

Piles can be installed through several techniques; a simple division is driven piles or bored piles [Fleming et al., 2008]. The choice of piling method depends on the soils characteristics, groundwater conditions, the consequences the mass displacement could have etcetera. Driven piles can further be divided into dropping weight, explosive, vibration and jacking against a reaction. The dropping weight, more commonly known as a drop hammer, is the traditional method of pile driving. The pile is driven through the soil by striking the pile head. Bored piles, also known as drilled piles, is installed by using rotary augering machines, and therefore causes no mass displacement as the soil is removed. When the piles cutting level is beneath ground surface, hence the pile head is out of reach from the piling machine, can a pile-block be used [Olsson and Holm, 1993]. A pile-block is an extension with the approximate same area as the pile head, which enables the machine to continue driving the pile to its intended cutting level. When the pile is installed the pile-block will be drawn back up, leaving a cavity, which the soil can fall back into, decreasing the moved soil volume.

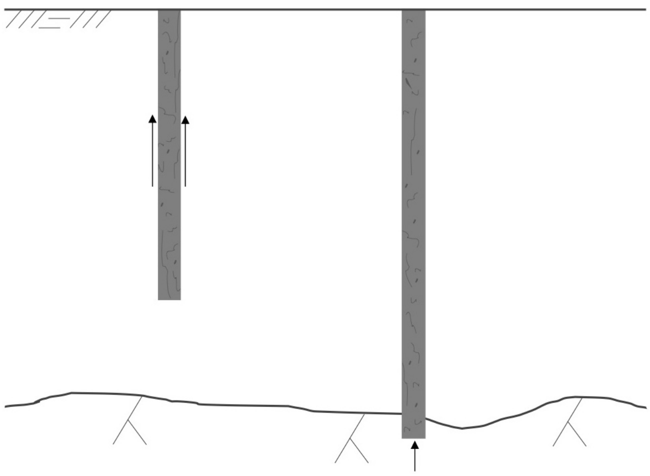

Figure 2.3: *Schematic illustration showing to the left a floating pile and to the right an end bearing pile.*

Piles can be made of materials such as concrete, steel and wood [Fleming et al., 2008]. Further, can piles be divided into displacement or non-displacement piles, where the former is piles with a large cross sectional area, and the latter have smaller cross sectional areas or hollow cross sections. Therefore, causing less mass displacement when installed. The chosen pile type in the Thesis is precast concrete piles, which is a displacement pile, and the most common pile type in Sweden [Edstam, 2011].

Furthermore, piles can be end bearing or floating, see *Figure 2.3*. End bearing piles are installed with the toe of the pile either on solid bedrock or in a stiff soil layer with adequate strength. Floating piles relies on the adhesion between the soil and the pile shaft. Depending on the soil type can the adhesion be friction or cohesion. In this Thesis floating cohesion piles are investigated.

2.2 Soil mechanics interpreted with constitutive models

Soil is a complex material as it is compounded of three individual materials; grains, water and air in the voids [Lade, 2005]. Thus, when subjected to stress and stress change, e.g. pile installation, the soil will show highly non-linear, anisotropic and time dependent behaviour [Knappett and Craig, 2012]. To capture this behaviour, different constitutive soil models can be used, which will lead to different degrees of accuracy, depending on the model.

The concept of a constitutive model is to describe the soil mechanics through a set of equations which give the relationship between stress and strain in a single element [Lade, 2005]. The more accurate a model captures the soil mechanics, the complexity increases, as well as the number of input model parameters. The field data of the soil is often limited and retrieved through basic field test; hence, the data is often too insufficient to select all the parameters needed for the more advanced models. The simplest constitutive models assume that the soil behaves linear-elastic, only showing reversible deformations, therefore, implying that the soil is infinitely strong. The applied shear strain is directly proportional to the applied shear stress [Knappett and Craig, 2012]. For total stress, the relationship between stress and strain is given by Hooke's law. However, soil is a highly non-linear function of shear strain and effective confining stress.

To be able to model the failure of the soil the Mohr-Coulomb failure criterion can be applied, which is based on that the soil is a frictional material exposed to three dimensional states of stress. The Mohr-Coloumb (MC) model can also be called the linear elastic perfectly plastic model, as the soil is assumed to be elastic until it reaches a defined failure condition, illustrated by when the Mohr circle touches the failure envelop in one point in the plane, see *Figure 2.4*. Thus, only experience reversible deformations and no irreversible deformations before failure. So, in some numerical models a yield function can be introduced that models the plastic deformations for the model [PLAXIS, 2017a]. However, in soil there is not elastic and plastic deformations, only a small span of reversible deformations and then irreversible deformations. But, as much of the theories and the constitutive models is built on the simplification of elastic and plastic deformations is these terms used in the Thesis. Furthermore, to capture the undrained response of the soil, which is a necessity when looking at the short-term response of soft clays, must the model be adapted, as the shear strength of the soil is different with comparison to drained conditions which the model is based on. The undrained behaviour is further defined with a friction angle (ϕ') of one, which means that the shear strength should be constant in an undrained soil [Knappett and Craig, 2012]. This could lead to inaccurate predictions of the soils strength. The model further fails to capture the softening or hardening of the soil after it has reached its peak strength.

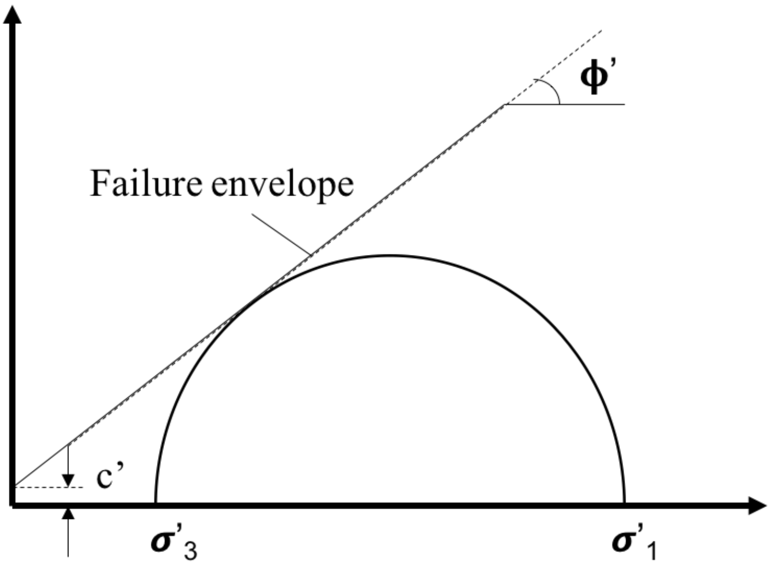

Figure 2.4: *The Mohr-Coulomb failure criterion, defined as the failure envelop and the principal stresses defining the Mohr-Coulomb circle.*

Two additional models which adapts the Mohr-Coulomb failure criterion are the Soft Soil (SS) model and Soft Soil Creep (SSC) model. Where both models adapt an isotropic assumption, which many of the constitutive models do with the hydraulic conductivity. Whilst, soil in reality is anisotropic as no soil consist of perfectly spherical grains. The SSC model further aims to capture the secondary consolidation, creep, and is a development of the SS model. Both models consider the elastic and plastic deformations of the soil, reversible and irreversible deformations, in contrast to the MC model. The models further work with non-linear elasticity in contrast to MC. Besides the creep is the main difference between the models, the way they interpret the yield surface, the boundary between small strains and large strains. Were in SSC has the yield surface been replaced with a Normal Compression Surface (NCS), see *Figure 2.5* [Karstunen and Amavasai, 2017]. The NCS boundary in SSC is falsely assumed to be the contour of constant volumetric creep, thus have the drawback of reproducing unrealistic creep strains for nearly all stress paths [Olsson, 2013]. Another drawback with the SSC model is how the (false) creep is modelled, as it models non-plausible excess pore pressures. Which in turn will influence other processes in the model.

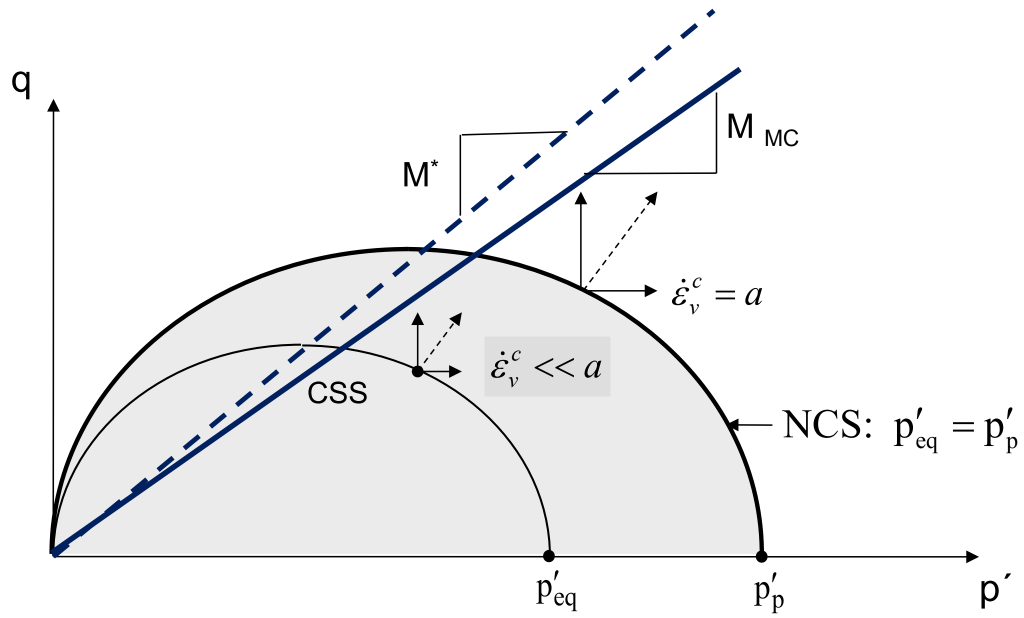

Figure 2.5: *SSC model, the NCS illustrating the boundary between small and large strains. The Mohr-Coulomb failure criterion is illustrated through the M_{MC} line, with permission from [Karstunen and Amavasai, 2017].*

2.3 Empirical and analytical calculation methods

To calculate and predict the soil behaviour due to pile installation, e.g mass displacement, as the increase in excess pore pressure and strain response, can empirical, analytical and numerical calculation methods be used.

2.3.1 Rhenman's method

Empirical calculations rely on patterns observed in the field and laboratory, and so, do not account for the small variations that can occur. Giving rough predictions as best. One empirical calculation method which is used for the calculation of mass displacement is Rhenman's method. The method contains several simplifications and assumptions. The method is based on the assumption that the vertical mass displacement of the ground surface occurs within an area of one pile length away from the piling area, see *Figure 2.6* [Hintze et al., 1997]. Other assumptions are that the ground surface is horizontal and that the volume of vertical mass displacement is proportional to the volume of the piles installed. The vertical mass displacement of the ground surface is calculated through *Equation 2.1*.

$$x = \frac{\eta(V_p - \Delta V_{pr})}{d[(\alpha+\beta)(\frac{l}{2}+\frac{d}{3})+(\gamma+\delta)(\frac{b}{2}+\frac{d}{3})+\frac{bl}{d}]} \tag{2.1}$$

Where:
x = Mass displacement within the piling area
d = Depth of the pile below the ground surface or excavation bottom
b = Width of the piling area
l = Length of the piling area
η = Heave factor, ranging between 0.5 to 1.0, often 0.75
V_p = Pile volume
ΔV_{pr} = Volume of removed clay with pre-augering
$\alpha, \beta, \gamma, \delta$ = Relative weight of constructions A, B, C and D,

The calculation method only considers the mass displacement of the ground surface. The model is built on volumetric ratios and geometry, ignoring the soil behaviour. Thus, the method is useful if a fast and rough prediction of the mass displacement of the ground surface is sought. But if information on additional processes in the soil and a higher accuracy is sought the method cannot be used.

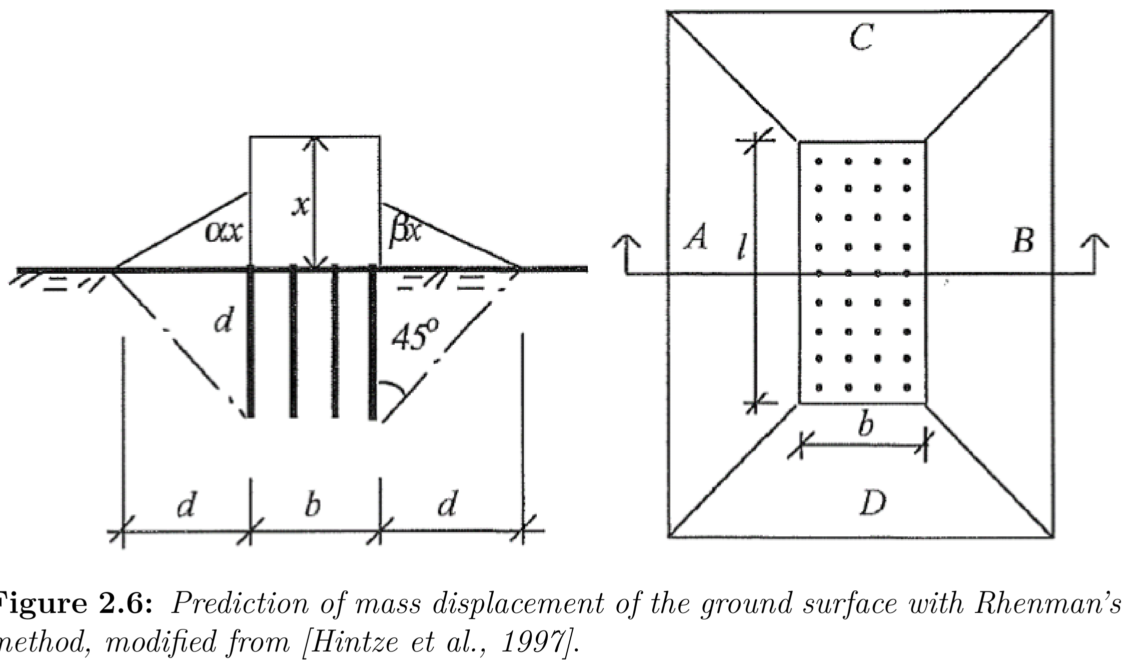

Figure 2.6: *Prediction of mass displacement of the ground surface with Rhenman's method, modified from [Hintze et al., 1997].*

2.3.2 Shallow Strain Path Method and Cavity Expansion Method

Different analytic methods can be used to model and predict the mass displacement and soil disturbance due to piling, e.g. cavity expension method (CEM) and the strain path method (SPM). One semi-analytical method based on SPM is the Sagaseta's method, which can be referred to as the shallow strain path method (SSPM) [Sagaseta and Whittle, 2001]. SPM assumes that the soil deformations and strains occurring due to deep pile installation in undrained clays is independent of the shear strength. The method further model the mass displacement that occur due to the irrational flow of an ideal fluid. Although, this assumption ignores that different soils can have highly different penetration resistance and soil stresses. Field observations, tests and empiric knowledge shows a link between pile driving and ground heave, whereas SPM analysis of pile penetration calculates that all soil elements undergo a net downward movement. Thereof, is SPM suitable for calculating strains near the pile toe, but not for far field conditions where the ground surface can affect the soil deformations. These limitations are addressed in the SSPM analysis through the incorporation of the effects from a stress free ground surface.

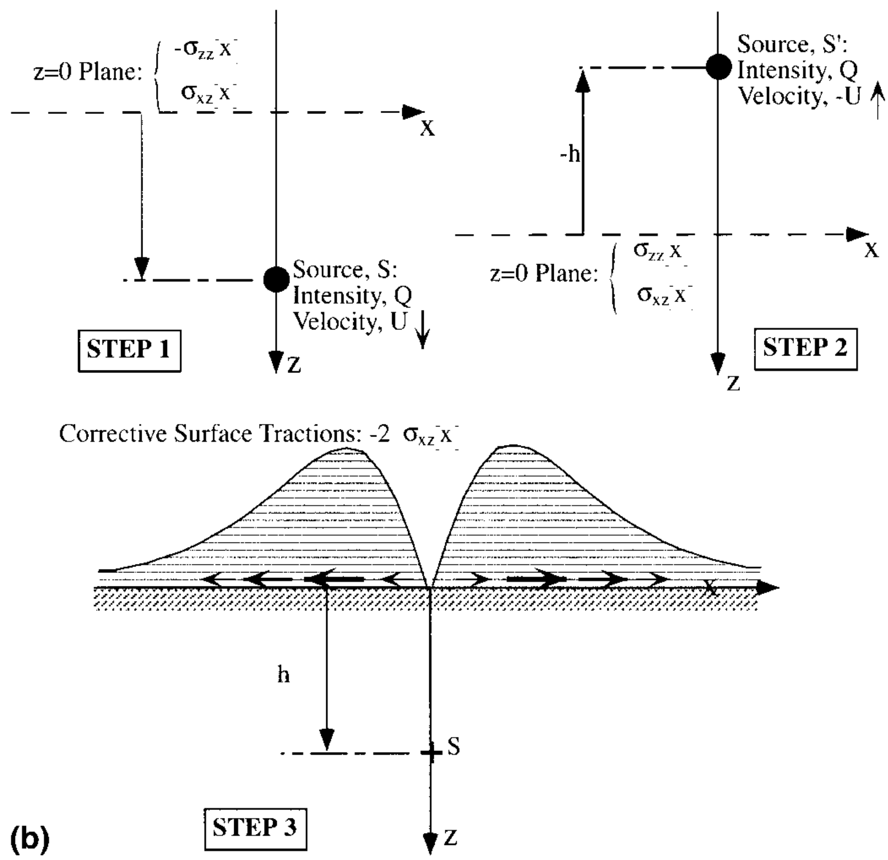

Figure 2.7: *Conceptual model for SSPM representing the three steps used to simulate a single pile penetration, modified from [Sagaseta and Whittle, 2001]*

.

Mass displacement is calculated in four steps with SSPM. The installation of a single pile is simulated in three steps, see *Figure 2.7*. The result from these simulations is then combined for a final analysis of the mass displacement. The first step, see *Figure 2.7*, entails the assumption of a point source (S), which penetrates the soil throughout the pile length [Sagaseta and Whittle, 2001]. S is thought to discharge an ideal fluid throughout the penetration. Thus, creating a spherical flow which causes the mass displacement. The presence of a ground surface is ignored and the soil is assumed to be in-compressible. In the second step is a mirror image sink (S') introduced, which moves in the opposite direction, see *Figure 2.7*. Cancelling out the normal stresses, whilst the shear stress doubles. Hence, do not corresponds to an unloaded ground surface. To counteract this is a set of corrective radial shear forces added in step three, see *Figure 2.7*. The method works for predictions with floating cohesion piles in deep deposits of clay, which the method was designed for but cannot be applied for end bearing piles or floating cohesion piles which are driven close to the bedrock, as the displacements will behave differently [Sagaseta and Whittle, 2001].

CEM studies the soil's reaction to pile installation, i.e. excess pore pressure, change in stresses and mass displacement, through the use of an expanding or contracting cylindrical cavity, instead of an ideal fluid as in SPM and SSPM [Yu, 2013]. The method was first introduced from research on copper, where it was concluded that deep penetrations lead to large strains and consequently hardening of the material [Bishop et al., 1945]. There are several approaches when using the CEM, as the spherical or cylindrical cavity can be modelled with constitutive models such as linear elastic (LE), elastic-perfectly plastic or strain hardening/softening plasticity. When using LE models the soil will be modelled to have infinite strength. Whereas, the elastic-perfectly plastic models will have constant strength during both the loading and unloading [Yu, 2013]. Therefore, do not consider the variation of the soil's strength due to deformation history. As pile installation is a rapid process, and the low permeability of soft clays, is the undrained response of the soil modelled. The solution in LE, isotropic models, is often to assume that the inner (P_i) and outer (P_u) pressure acting on the sphere or cavity starts from zero, see *Figure 2.8*. Where the soils deformations occur purely plastic. For the elastic-perfectly plastic models a yield surface is introduced, often Trescas, von Mises or Mohr-Coulomb depending on if it is cohesion or friction soil, and a plastic radius, see *Figure 2.8*. As the soil first will behave elastic due to the initial pressure, before initial yielding occurs at the cavity wall leading to plastic deformations around the inner cavity wall and increased P_i, see *Figure 2.8*, [Yu, 2013]. To fully capture the behaviour and the influence from softening/hardening due to strains these kind of constitutive models should be applied.

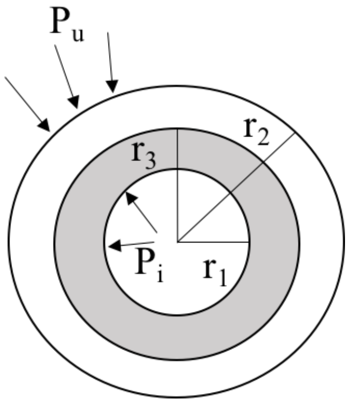

Figure 2.8: *Cavity with inner and outer pressure, P_i and P_u respectively, and the inner, outer and plastic radius denoted r_1, r_2 and r_3 respectively.*

Both the CEM, SPM and SSPM can be applied with numerical methods, which is a necessity when more advanced constitutive material models are used, due to the complexity of the problem.

2.4 Numerical calculation methods

There are several numerical calculation methods which in combination with constitutive soil models can be used to predict the response of the soil due to pile installation. Numerical calculation methods are characterised by the discretization of continua and the use of algorithms; which allows for calculation of non-linear and time dependent material behaviour, arbitrary geometries, initial or in situ conditions, multiphase media, different types of loading i.e. static and cyclic loading, and the impact of environmental factors, i.e. temperature and fluids [Desai and Gioda, 1990]. Thus, can numerical modelling be used for geotechnical problems, such as pile installation and mass displacement, that can be complex to solve by using empirical or analytic methods. There are several numerical methods that can be used for these problems such as the finite element method, boundary element method, discrete element method and finite difference method.

The finite element method (FEM) solves differential equations approximately where complex problems are divided into several finite elements. These elements are then approximated separately, but in relation to each other [Ottosen and Petersson, 1992]. Hence, can the approximation of these elements be assembled to a complete system, thus the solution for the unit. Two FEM-based software programs that can be used for the modelling of geotechnical problems, such as mass displacement, are PLAXIS 2D and PLAXIS 3D.

Furthermore, analytical calculations can be adapted with numerical methods, such as SPM and CEM. The latter have been adopted with FEM in different scientific reports and research. In the report *Numerical simulations of stone column installation* is the FEM based software program PLAXIS used [Castro and Karstunen, 2010]. Whereas, in the report *Evaluating pile installation and subsequent thixotropic and consolidation effects on setup by numerical simulation for full-scale pile load tests* is the FE based software programme Abaqus used [Abu-Farsakh et al., 2015]. In PLAXIS 2D either a plane strain or an axisymmetric model can be used. The different approaches have different advantages and disadvantages. The main difference between the two models is the geometry, where the plane strain assumption should be used for models with a uniform cross section, where the stress state and loading scheme is fairly constant for a significant length perpendicular to the cross section, i.e. roads [PLAXIS, 2018a]. When it comes to the strains and displacements in the perpendicular direction, the z-direction, they are assumed to be zero, whereas the normal stress is still accounted for. The axisymmetric model is instead used for circular structures, where the radial cross section is uniformed. The deformation and stress state are assumed to be equal around the central axis. In the axisymmetric model is the x-coordinate the radius and the y-coordinate the axial line of symmetry, hence no negative x-coordinates. The difference of the plane strain model and axisymmetric model can be seen in *Figure 2.9*.

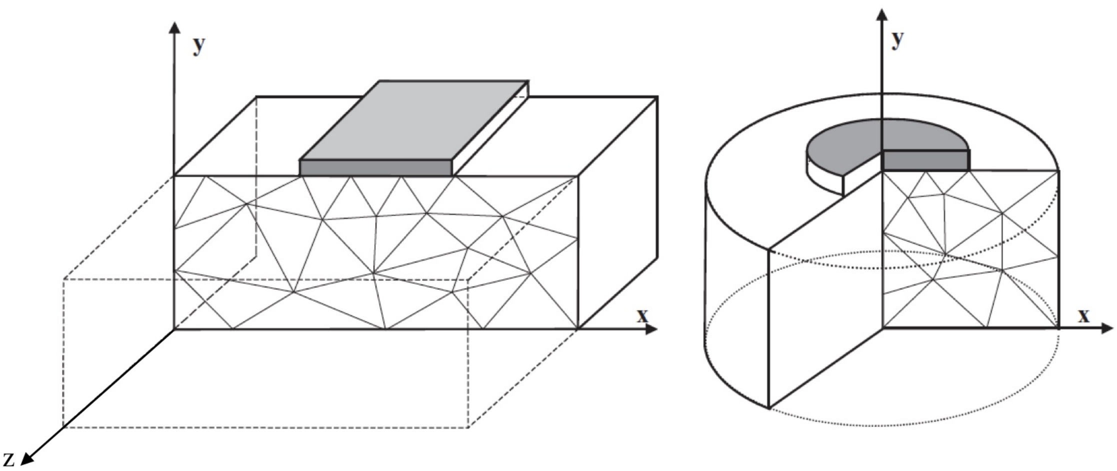

Figure 2.9: *Difference between a plane strain model, to the left, and an axisymmetric model, to the right, both on a Cartesian coordinate system, modified from [PLAXIS, 2018a].*

Both models have their advantages and disadvantages when modelling pile installation. One disadvantage with the plane strain model is that it will model a piling area which is constant in the z-direction. Thereof, entails that the pile will become an infinity long wall if the pile is modelled as a soil polygon/cluster. However, in an axisymmetric model can only one pile be modelled.

Pile installation can be modelled with the use of CEM, through the activation of a prescribed displacement. In PLAXIS this function is called prescribed line displacement, entailing a load that acts horizontal and/or vertical in the soil with a prescribed movement [PLAXIS, 2017b]. The prescribed line displacement can be applied on a soil cluster, a structure or by itself in/on the soil. The prescribed line displacement will occur in the direction and magnitude applied, either fixed, free or prescribed in the horizontal and/or vertical direction. When using a prescribed line displacement is a restriction that an initial cavity must be modelled with a radius over zero, even if this is not the case in reality where the expansion starts from a cavity with a radius of zero. However, should this not influence the result [Castro and Karstunen, 2010].

If only the influence on the surrounding soil is of interest the cavity can be left empty, as there is no reason to model the pile material [Castro and Karstunen, 2010]. However, is the drawback that no interaction between the soil and the pile in the form of interfaces etcetera can be modelled. If the cavity instead is filled with a material acting as the pile, the interaction can be better captured. Favourable could a LE material be used as this would not collapse due to the high applied strains [Abu-Farsakh et al., 2015].

Another way to model the expansion of a soil cluster in PLAXIS is through volumetric expansion, which corresponds to the displaced volume of soil that occurs during the pile installation [PLAXIS, 2017b]. Through, the function volumetric strain, where a positive volumetric strain corresponds to an expansion and a negative shrinkage. The software adjusts the stresses and forces that occurs in the surrounding soil. Therefore, the total volumetric strain may not be applied to the cluster. Hence, the resulting deformations is dependent on the ratio of stiffness between the cluster with volumetric strain and the surrounding soil. Thus, sometimes a larger volumetric strain must be applied in order to reach a specific final expansion, if the clusters have different properties. The prescribed line displacement is therefore more numerically stable [Castro and Karstunen, 2010].

To simplify the modelling of mass displacement as a consequent of pile installation it can be beneficial to model a group of piles as one superpile. This simplification has proven to work well when soil movements far from the piling area is of interest [Edstam, 2011]. The use of a superpile can be executed in several ways, either a number or a single superpile can be modelled, where the superpile has the same cross sectional area as the sum of the piles it replaces. The superpile is then placed in the centre of the piling area. Another way to make a superpile is to model the whole piling area as a superpile and applying the rule of mixture on the superpile material, making a mix of the pile material and the soil which correlates to the volume ratio. The problem is that only mass displacement occurring outside of the piling area can be predicted. Both volumetric strain and prescribed line displacement can be used on the superpile to model the mass displacement. When making model calculations in two dimensions with a plane strain assumption can this be a good simplification, as the distance between the piles in the z-direction cannot be modelled anyway.

3

Prediction of mass displacement due to pile installation, using PLAXIS 2D

There are different ways to model pile installation in PLAXIS 2D and PLAXIS 3D, but no method is fully established or verified. Therefore, to decide the optimum way to model the consequences of pile installation, in relevance with the Thesis aim, were different approaches evaluated in PLAXIS 2D. All the models were constructed with a pre-installed pile in the soil, which then was expanded with different functions. The constructed pile was either a cavity or contained a linear elastic material. Hence, were the models based on the CEM. The influence of the disturbance from the pile installation was not investigated, e.g. the influence of the installation technique. Only the volume-change in the soil due to the pile installation. The constitutive models used were Linear-Elastic, Mohr-Coulomb, Soft Soil and Soft Soil Creep. The reason to investigate several constitutive models were that the simpler models such as LE and MC would cope with larger deformations before collapse, hence did the trials started with these before the more advanced models were used.

3.1 Investigation and chosen modelling technique

To decide which model and modelling technique was best suited for the calculations in PLAXIS, in the Thesis, a number of models were carried out. Firstly, was an axisymmetric model constructed with a general soil profile and model parameters. In which three different versions to model mass displacement were carried out. The first model contained a cavity with a prescribed line displacement. The problem were either the occurrence of soil collapse or that the prescribed line displacement tugged in the nodes. Hence, not giving an accurate distribution of the mass displacement and deformation of the mesh. Another drawback was that no interaction between the soil and the pile could occur. Whereas, when modelling a soil cluster with a LE material an interaction could be obtained. Furthermore, did the deformation of the mesh occur smoother, resulting in a more plausible mass displacement.

The plane strain model was, as the axisymmetric model, constructed with a general soil profile. Where, compared to the axisymmetric model, more than one pile could be modelled. Therefore, it was investigated if the influence of the pile order could be captured. This were done both with prescribed line displacement and volumetric strain. Firstly, three soil clusters were constructed, which the prescribed line displacement or volumetric strain were activated upon. One pile at a time was activated in three following phases, mimicking the pile order. As the piles were constructed as soil clusters the mesh was deformed when the first pile was installed, including the not yet activated piles. Hence, resulting in deformed piles before activation. To counteract this problem were different measures carried out, including embedded beam rows in the soil clusters which would not deform before activation, with varying results.

Furthermore, it was investigated if the deformed piles nevertheless would cause unsymmetrical deformations and displacement of the soil; which could be linked to the pile order. A couple of additional piles were therefore constructed in the model, to give large deformations. The result showed minor unsymmetrical deformations that could be linked to the mesh as well as the pile order and the technique was ruled out.

The main problem when modelling mass displacement with the function volumetric strain, was the uncertainty of how much the soil cluster would expand, as the applied volumetric strain can be overruled due to other parameters in the model. As the depth entails higher stresses and strains in the surrounding soil can it be assumed that the volumetric expansion will decrease with the depth if the same volumetric strain is set for the entire soil cluster. A scenario where the volumetric strain increased with depth were therefore carried out, resulting in some difference in the outcome. However, the uncertainty of the amount of volumetric strain which had been applied remained.

When investigating the function prescribed line displacement, it was set to occur horizontal and uniformed. Whereas, the movement in the vertical direction were either set to free or fixed. Both with and without the use of interfaces. Thus, could the interaction between the surrounding soil and pile be somewhat captured. When not using interfaces, letting the prescribed line displacement move in the vertical direction there was a significant drag down of the pile, even when the unit weight of the pile was the same as the soil.

The chosen model technique for this Thesis was to use a plane strain model, with a superpile and prescribed line displacement. A plane strain model was chosen as unsymmetrical geometries could be modelled and the scenarios investigated in the Thesis correlates well with the plane strain assumption. A superpile was chosen as the modelling of individual piles and pile order gave small to zero differences in deformation. Lastly was prescribed line displacement used as displacement is more numerical stable, in contrary to the function volumetric strain.

3.2 Deriving model parameters

It is important to distinguish between soil properties and model parameters, as soil properties give information on how the soil reacts in different situations, depending on loading/unloading and soil characteristics to name a few. Whereas model parameters are input values used in different constitutive models to capture the behaviour of the soil. As no constitutive model fully captures the soils behaviour it is important to choose parameters that will make the model act in the way that is sought.

3.2.1 Study site

The Thesis investigates the mass displacement occurring in Gothenburg and more specific in the area around the Central Station, due to the installation of precast concrete displacement piles. The area around the river *Göta älv*, were the Central Station is located, consist of soft sensitive clay underlying a layer of fill which was placed in the area around 200 years ago. Before this both the north and the south side of *Göta älv* were reed areas, see *Figure 3.1*.

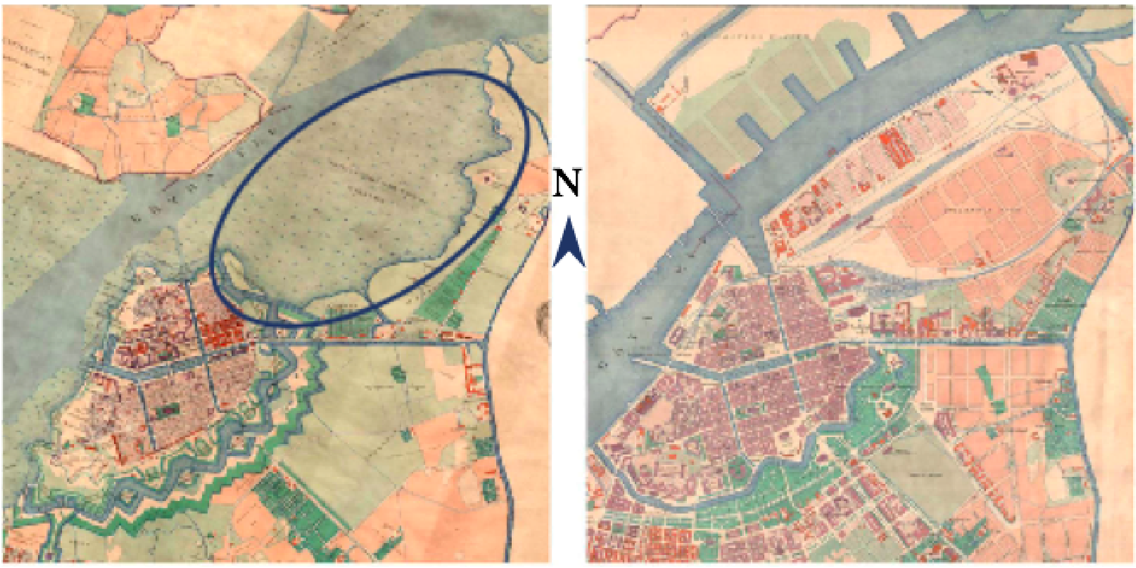

Figure 3.1: *Map over the area around Gothenburg Central Station, inside the circle, in 1790, to the left and in 1890 to the right. After the fill of dredged material was placed, modified from [Ramböll AB et al., 2015].*

The thickness of the clay layer is up to 100 metres on both sides of the river. On the South side is the layer of fill between three to four metres, consisting of both friction fill and dredged material [Sabattini and Wallgren, 2018]. Underlying the clay is a layer of friction material which varies from zero to two metres in thickness, before solid bedrock. The groundwater level varies in the area depending on the distance to *Göta älv*, as the groundwater varies with the water level in the river.

Most of the model parameters used in the calculations are retrived from investigations made for *Regionens Hus* and from the *Design Base - Geoteknik* made for *Västlänken Station Centralen* [Wood, 2017]. From here on after referred to as the *Design Base* in the Thesis. Parameters further come from field and laboratory tests carried out for *Västlänken Station Centralen*.

For the clay the constitutive models SS and SSC were chosen, and for the fill and friction material was MC used. Whereas, the superpile was modelled with a LE material, so it could cope with the large strains occurring when the prescribed line displacement was activated. The material was a concrete material retrieved from *PLAXIS Tutorial Manual*, Tutorial 13, where the unit weight was modified to correlate with the clay, to prevent drag down [PLAXIS, 2018b]. All parameters for the fill, friction material and clay materials can be found in *Appendix A*, *Table A.1* and *Table A.2*, respectively.

3.2.2 Pre-consolidation pressure

The pre-consolidation pressure (σ'_c) is in more advanced models a key parameter, that changes throughout the soil profile [Karstunen and Amavasai, 2017]. In the SS and SSC models is the variable especially sensitive in relation to over consolidated ratio (OCR) and pre-overburden pressure (POP). To derive the parameter the OCR and the POP from the *Design Base* were used, and the vertical effective stress, instead of using e.g. the Casagrande method. σ'_c was plotted against the vertical effective stress, where the difference between them is either OCR or POP, see *Appendix A*, *Figure A.1*. The values derived were used as an input parameter in the PLAXIS SoilTest for both the IL Oedometer and Triaxial compression tests, see *Chapter 4.3*.

3.2.3 Poisson's ratio for loading and unloading

Poisson's ratio for loading and unloading (v_{ur}) is an elastic parameter which in PLAXIS is set to be constant, commonly assumed to range between 0.1 and 0.2 [Karstunen and Amavasai, 2017]. In the Thesis it was set to 0.15 for all clay layers. The SS models tend to not be especially sensitive to the assumed v_{ur}, but when it comes to models and predictions where the horizontal stresses are of importance it is advised to perform a sensitivity analysis of the parameter. Hence, as the Thesis investigates both the horizontal and vertical mass displacement was a sensitivity analysis performed on the v_{ur}, see *Chapter 4.3*.

3.2.4 Modified compression, swelling and creep index

In the SS and SSC models are the modified parameters for compression (λ^*) and swelling (κ^*) the key parameters for the soils stiffness [Karstunen and Amavasai, 2017]. In the SSC model is also the modified creep index (μ^*) a vital stiffness parameter. Both λ^* and κ^* can be derived from either IL Oedometer tests or CRS tests.

The parameters can be derived directly from graphs by plotting the logarithmic relationship between volumetric strain (ε_v) and mean effective stress (p') [PLAXIS, 2017a], see *Figure 3.2*.

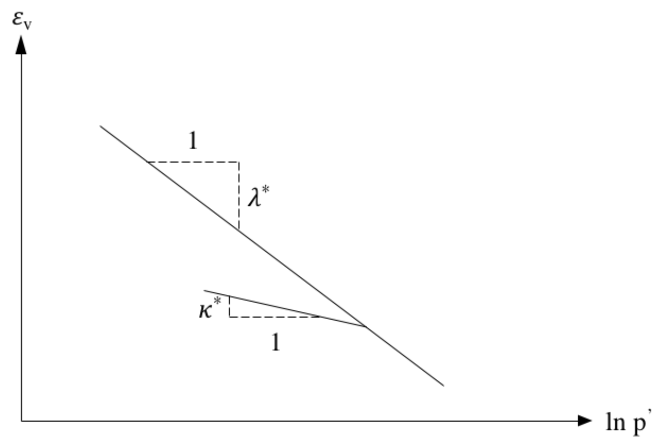

Figure 3.2: *Logarithmic relation between ε_v and p', giving the values for λ^* and κ^*.*

For the Thesis were μ^* retrieved from the *Design Base* and λ^* and κ^* was retrieved from IL Oedometer test performed for *Västlänken Station Centralen* on the depths of 8, 15, 19 and 45 metres. The resulting values of λ^* and κ^* were plotted against the depth creating an interpolation of the values between the test depths, these graphs can be seen in *Appendix A*, *Figure A.2* to *Figure A.6*.

3.3 Construction of Base Model in PLAXIS 2D

A Base Model was constructed with a plane strain model, 15-nodes and SS model. The chosen soil profile can be seen in *Figure 3.3*, where the first layer of fill consists of friction material and begins at level +2.5 metres, in the model. The second layer of fill consists of dredged material and starts at level +1.5 metres, following are five clay layers with different sets of model parameters and lastly a layer of friction material before the bedrock. There are two different geological deposits between clay layer 3 and 4 on a depth of 20.5 metres, where the model parameters differ significantly, especially with consideration to κ^*, λ^*, OCR, effective cohesion (c') and effective friction angle (ϕ'_c).

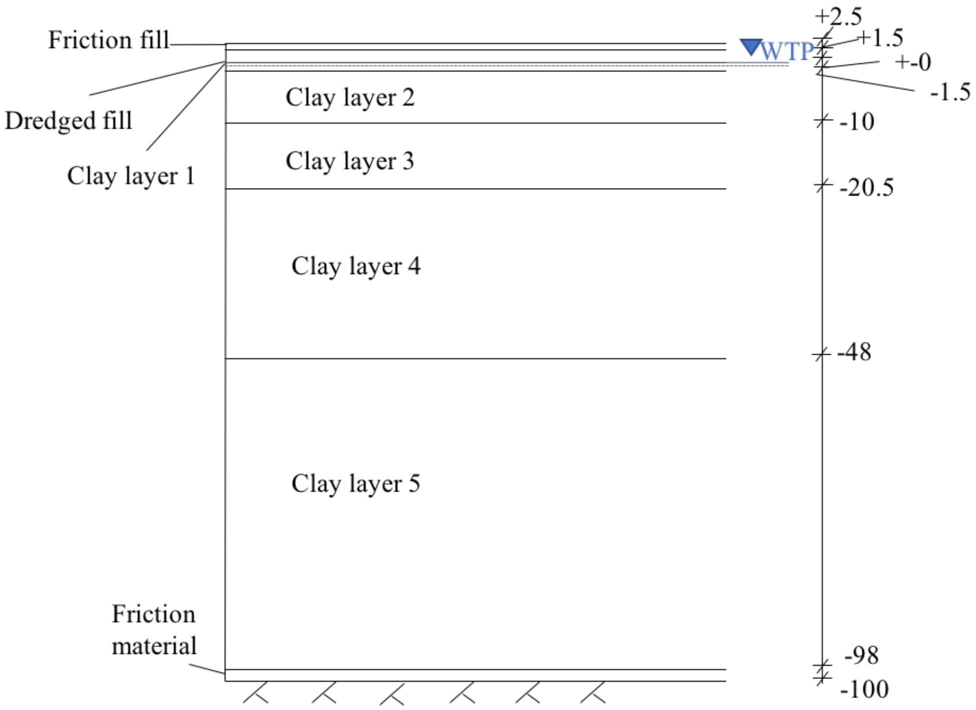

Figure 3.3: *Schematic illustration over the chosen soil profile in the Base Model.*

The Base Model contained a horizontal ground surface, and was 200 metres wide with the superpile structured in the centre, see *Figure 3.4*. The superpile was constructed as a soil cluster, on which the prescribed line displacement was added. The soil cluster had a width of one metre from the beginning. The prescribed line displacement was set to be prescribed in the horizontal direction and fixed in the vertical direction to prevent drag down. The pile was not included in the original Base Model due to how the superpile differed depending on the design of the piles. Both sides of the superpile was structured in the model, to be able to try different unsymmetrical cases. A borehole was structured in origo where the layers of fill, clay and friction material as well as the water table, was set. The water table was set to level ±0 in the model, the top of the first clay layer.

The horizontal boundaries (x_{min} and x_{max}) were set to be closed for ground water flow in the clay layers, but seepage was allowed in the friction material and fill. The minimum vertical boundary (y_{min}), was also set to be closed for groundwater flows. Whereas the maximum vertical boundary (y_{max}), was set to be open. The bedrock typically consists of some crushed or cracked areas, therefore not initially closed for groundwater flow as a closed y_{min} entails. However, as a friction material layer which allowed for groundwater flow was placed on top of the bedrock was this argued to be a valid assumption.

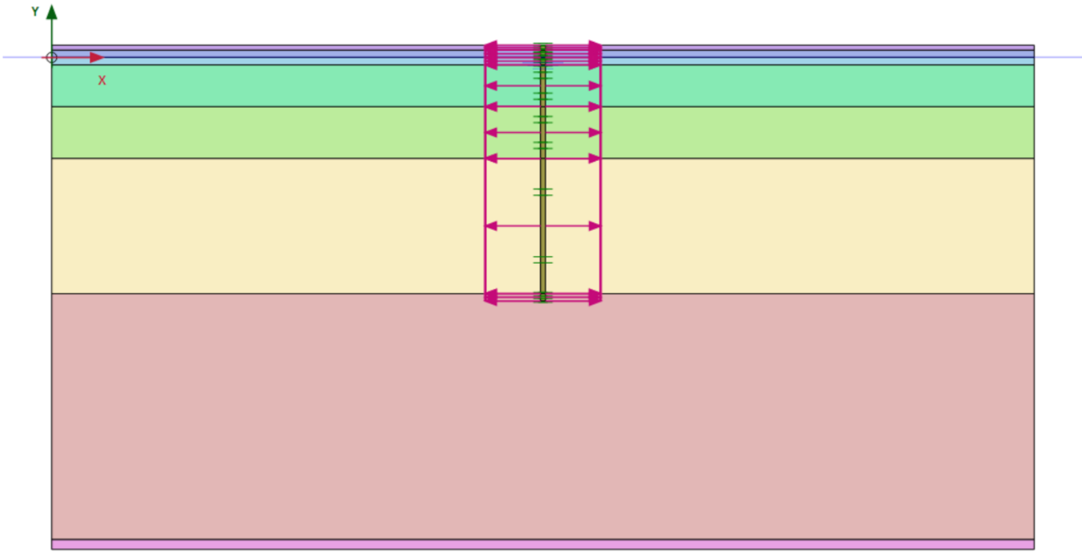

Figure 3.4: *The Base Model in PLAXIS 2D.*

The mesh of the Base Model was constructed through applying a coarseness factor of 0.5 to the model and refining the mesh. This gave a quality of the mesh where two elements had a size under 0.5 and 13 elements under 0.6. The result was symmetrical, without a too time consuming calculation time. Furthermore, the mesh could cope with the large strains that occurs when activating the prescribed line displacement. A finer mesh could lead to model collapse, as smaller deformations are allowed.

To investigate the models capacity, if it could cope with the deformations, stresses and strains due to mass displacement, the OCR was firstly set to 10 for all clay layers. Thus, making the the model behave falsely Linear Elasto-Plastic and see if the model could handle the deformations, before using the chosen OCR values in the model for SS and SSC.

3.3.1 Calculation of prescribed line displacement

The prescribed line displacement was calculated to correlate with the amount of piles installed. Where it was assumed that no volume change would occur in the soil when the piles were installed, due to the low permeability of the clay. Hence, the volume of piles installed were assumed to be the same volume as the mass displacement. The equation used considered the piling area, number of pile rows and number of piles among other things. The reason to calculate the cross sectional area, seen from above, of the piles and piling area, in contrary to the volume of the piles and piling area; were that the ratios were equal, as the depth and height of the pile and piling areas was the same. A schematic illustration of a general piling area, seen from above, can be viewed in *Figure 3.5*.

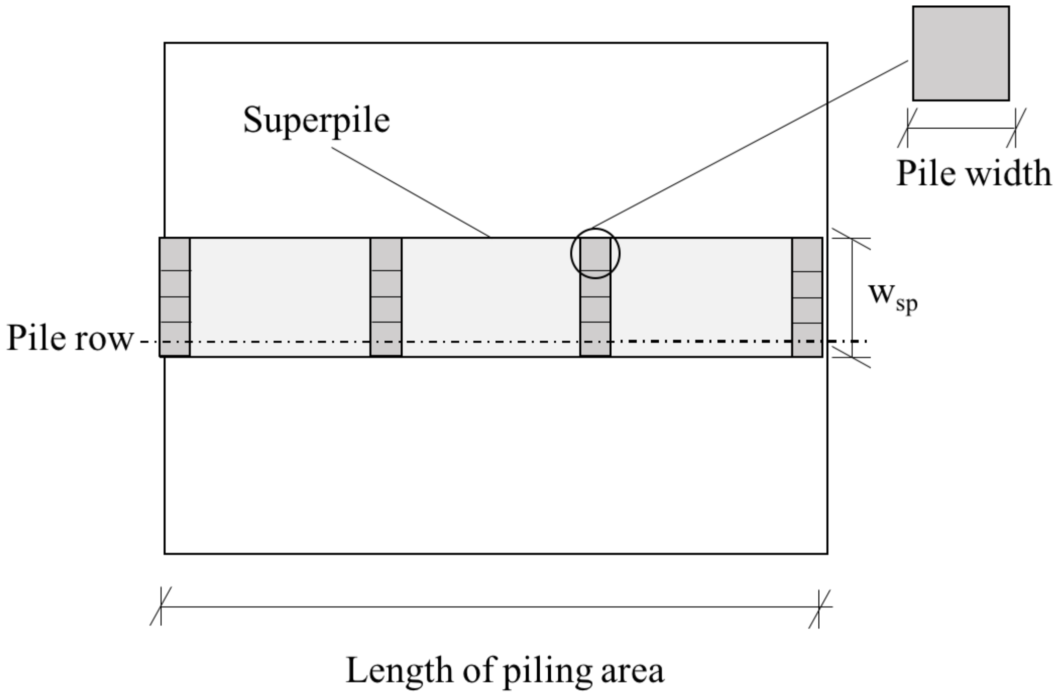

Figure 3.5: *Schematic illustration over a general piling area, seen from above.*

The equation used to calculate the prescribed line displacement can be seen in *Equation 3.1.*

$$Prescribed\ line\ displacement = \frac{(w_{sp} * \sqrt{(\frac{a_{sp}}{a_{pa}} + 1)} - w_{sp}}{2} \tag{3.1}$$

Where:
w_{sp} - width of superpile; $number\ of\ pile\ rows * pile\ width$
a_{sp} - area of superpile; $(pile\,diameter)^2 * number\ of\ piles$
a_{pa} - piling area; $w_{sp} * length\ of\ piling\ area$

The ratio between the area of the superpile to the area of the total piling area, soil included, was calculated. Hence, the percentage of piles with consideration to the total area. It was assumed that the area would increase the total percentage calculated. Furthermore, it was assumed that each pile would increase equally in all directions. As the Thesis investigates a two dimensional case, where the mass displacement only can occur in two directions was the percentage square rooted. Hence, the percentage each side of the pile was increased to get the total area increase. This was then multiplied with the width of the superpile, and then subtracted with the width of the superpile (the number of pile rows installed in that step) to get the total prescribed line displacement that should be applied in the model, in that step. As the prescribed line displacement were applied in two directions was the total prescribed line displacement divided by two.

3.3.2 Calculation phases

The Base Model were calculated through a number of calculation phases, in all phases were the pore pressure set to be phreatic, suction ignored and the mesh set to be updated. Furthermore, different structures were activated and deactivated in the different calculation phases, see *Table 3.1.* The plastic procedures can generally be viewed as the undrained response and calculation, and the consolidation phases as the drained calculation and response.

Table 3.1: *Calculation phases used in the Base Model.*

Calculation Phase	Procedure	Activated structures
Inital phase	K0	Generates the initial stresses, the two fill layers were deactivated. No structures were activated.
Phase 1	Plastic	Activation of the dredged fill.
Phase 2	Consolidation	Consolidation for 10 years, letting the excess pore pressure from the activation of the fill dissipate.
Phase 3	Plastic	Activation of the friction fill.
Phase 4	Consolidation	Consolidation for 10 years, letting the excess pore pressure from the activation of the fills dissipate.
Phase 5	Consolidation	Consolidation for 178 years, until present day, letting the excess pore pressure from the activation of the fills dissipate.
Phase 6	Plastic	No additional structures were activated, the displacements that had occured during the previous steps were reset to zero. The nil-step furthermore made the stress field be in equilibrium, and made the stresses obey the failure condition.
Phase 7	Consolidation	Consolidation for one year in order to be able to validate the excess pore pressure and settlements with values measured in the area.

The reason to model the previous soil history, although the model parameters are derived from the current soil, was to obtain the stress and strain state in the soil. Which is a consequence of the soil history. Furthermore, is the excess pore pressure also created through the modelling of the soil history. Whereas, directly after the Initial Phase no excess pore pressure is existing in the model. The nil-step only resets the displacements, hence the stresses, strains and pore pressures are still there.

To validate the Base Model before calculations were carried out, the excess pore pressures during the control year in the model and the occurring settlements in the field were compared. The settlements in the area around Gothenburg Central Station is as most two millimetres per year [Wood, 2014]. The model gave a vertical settlement of approximate 1.5 millimetres. Therefore, the settlement rate was valid, as the model captured the behaviour.

The excess pore pressure in the area, due to the placement of the fill, varies, see *Appendix A*, *Figure A.7*. In the Base Model the pore pressures simulated were compared to the ones measured in the field. The excess pore pressures occurring in the model at the control year can be viewed in *Figure 3.6*. When compared to the measurements in *Appendix A*, *Figure A.7* can it be seen that the maximum excess pore pressure in the Base Model occurs around level -30 to -42 metres, with a magnitude of 12 kPa, which correlates fairly well to the measured excess pore pressures on that depth in the area, see *Appendix A*, *Figure A.7*. This validation could not be done for the SSC model, as the model creates large pore pressures to simulate the creep. Hence, gave exorbitant excess pore pressures in the control year.

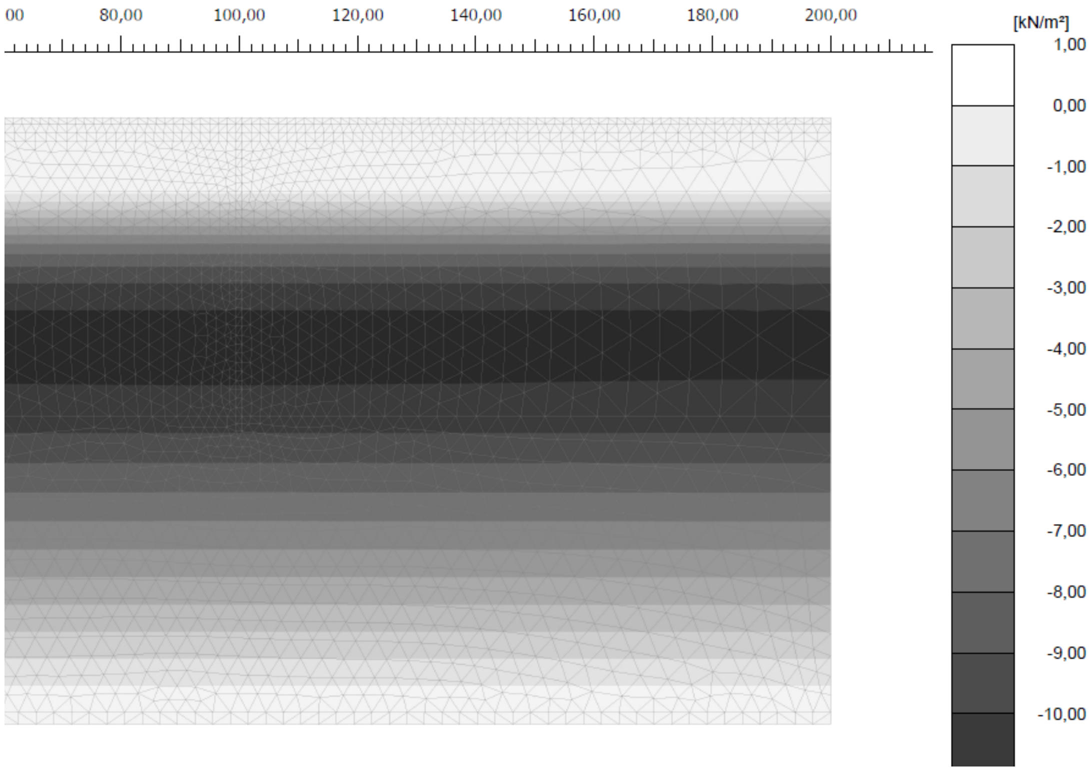

Figure 3.6: *Excess pore pressures in the Base Model during the control year.*

4

Validation of model and modelling technique

Field measurements were derived from two construction projects to verify chosen modelling technique, the Base Model and the equation for the prescribed line displacement. The projects investigated where the pile installation for one of the bridge support abutments of *Partihallsbron* and the pile installation in section 0/550 to 0/600 of the lowering of the highway *E45*, which stretches from Lilla Bommen to Marieholm. From now on in the Thesis the projects are referred to as *Partihallsbron* and *E45* respectively. The pile installation, and consequently mass displacement, for the project *Partihallsbron*, have been studied in technical reports such as the SBUF-report *Massundanträngning i samband med pålslagning i lera*, [Edstam, 2011]. Hence, the number of piles, pile installation order and field measurements are well documented in comparison to general construction projects. The soil profile for the two projects are nearly identical, as they are located in close proximity to each other, in typical Gothenburg clay. Further is *E45* located in the area from which the model parameters were derived, see *Figure 1.2*.

4.1 Field measurements and project information from *Partihallsbron* and *E45*

The vertical field measurements for *Partihallsbron* came from bellow hoses, which were placed from level ±0 to -45 metres. The horizontal field measurements came from inclinometers retrieving information between the same levels. The field measurements evaluated in the Thesis were derived from four locations adjacent to the piling area, see *Figure 4.1*. The measurements of the vertical mass displacement was derived on a distance of 12 and 20 metres from the piling areas centre, on the long side of the piling area. Hence, the distance to the superpile, the locations are marked with smooth rings in *Figure 4.1*. Whereas, the field measurements of the horizontal mass displacement were taken from the short side of the piling area, marked with dotted rings in *Figure 4.1*. Because, the location from where the vertical field measurements were retrieved, had faulty horizontal measurements. Thus, were instead measurements on the short side with roughly the same distance used, 14 respectively 24.5 metres. Although, from the edge of the piling area as the superpile stretches throughout it. Whilst, in PLAXIS the result is retrieved 12 and 20 metres from the superpile centre and from the long side of the piling area. Same as the result for the vertical mass displacement, due to the setup of the model. Thus, the horizontal field measurements is an approximate benchmark as the field measurements should be smaller further from the piling area, and on the short side.

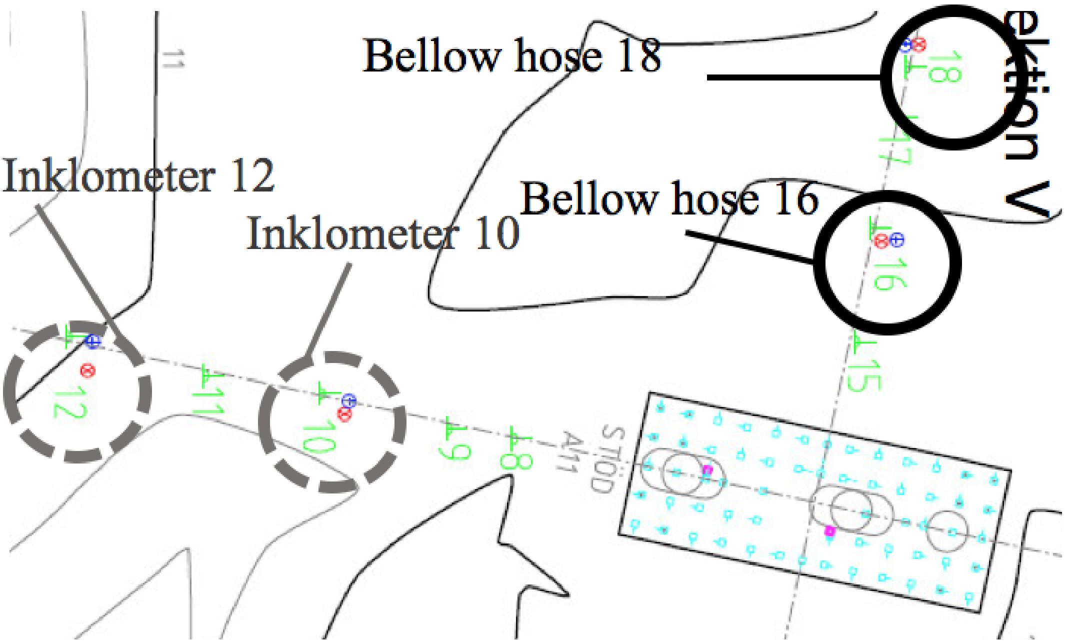

Figure 4.1: *Schematic illustration over the piling area for Partihallsbron and the location from where the field measurements were retrieved, modified from [Edstam, 2011].*

For *E45* the field measurements were retrieved from *Project Navet*, and settlement gauge plates measuring the vertical movement of the ground surface. A total of six points were evaluated in the Thesis. The points were located 20 (D), 38 (E), 50 (F), 60 (A), 65 (B) and 74 (C) metres from the centre of the piling area, hence superpile, see *Figure 4.2*. The distance was measured as a straight line from the superpile, and assumed to be on the same distance horizontally in the model.

One thing that differentiates the two projects with relevance to the Thesis and modelling, was the size of the piling area. The piling area in *Partihallsbron* was 16.2 metres long. Whereas, the length of the section investigated in *E45* was 50 metres. Hence, the piling area for *E45*, better corresponds to the plane strain assumption. However, where it fewer uncertainties around the geometry and field measurements from *Partihallsbron*. Thus, through modelling both projects the influence of plane strain and accurate model geometry could be evaluated.

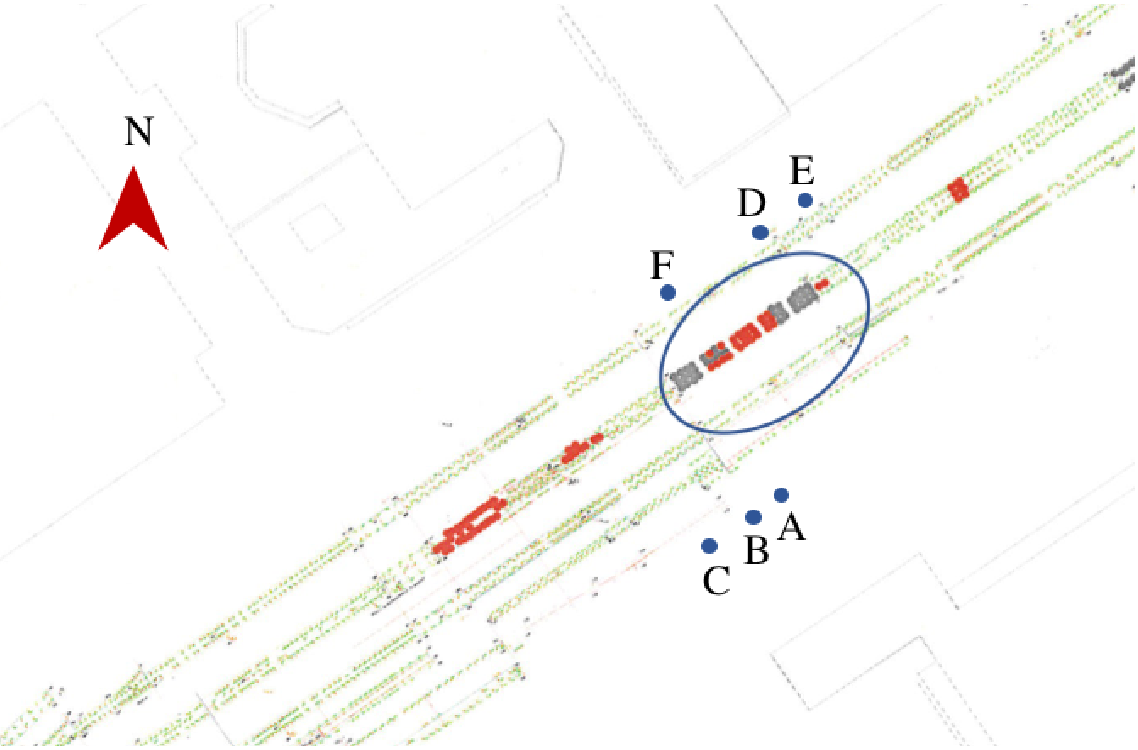

Figure 4.2: *Illustration over E45, where the dots inside the circle are installed piles. The circle marks the chosen section and the points A-F the location from where the field measurements were retrieved, modified from [Trafikverket, 2018].*

The piling area for *Partihallsbron* were horizontal, though the information was lacking on which level the pile installation occurred from. Hence, if the pile installation was performed from top of fill, or if the fill were partly excavated and replaced with a piling bed, made of i.e. gravel. This information was not retrieved from *E45* either, as the geometry of the area has differed during the project. Through, excavations of soil masses, placement of gravel beds, construction of slopes etcetera. Therefore, a horizontal model in PLAXIS was used. Through using field measurements from both sides of *E45* the results could be better evaluated as the geometries differs. The location of Point D, E, F were closer to existing buildings and slopes. Whereas, the location of Point A, B, C were located closer to another construction project which installed piles, *Regionens Hus* see *Figure 1.2*. As no information was retrieved on if the pile installation were performed from top of fill or if the fill were partly excavated and replaced with a piling bed. Three scenarios were modelled for both *Partihallsbron* and *E45*:

- **Scenario 1:** The pile installation was performed from top of fill.
- **Scenario 2:** The fill was excavated/removed and replaced with a 0.1 metre thick piling bed consisting of gravel, from where the pile installation then was performed.
- **Scenario 3:** The fill was excavated/removed and replaced with a 0.2 metre thick piling bed consisting of gravel, from where the pile installation then was performed.

4.2 Calculations of *Partihallsbron* and *E45*

The Base Model was used for both projects and from the nil-step were different phases added to simulate the different scenarios, parameter validation and validation of prescribed line displacement.

The pile installation for *Partihallsbron* was performed in three stages. The installed piles had a length of 52 metres and pile width of 275 millimetres. Number of piles and pile rows and the calculated prescribed line displacement can be seen in *Table 4.1*. The calculated prescribed line displacement from each calculation phase were added onto the previous. No information on the time span for the pile installation were available. Hence, the pile installation was simulated in three calculation phases which each lasted one day in PLAXIS, with no intermediate consolidation phase.

Table 4.1: *Prescribed line displacement for Partihallsbron.*

Phase	Number of piles	Pile rows	w_{sp} [mm]	a_{sp}/a_{pa}	Prescribed line displacement [mm]
1	9	1	0.275	0.15278	10.1303
2	22	2	0.550	0.18673	24.5769
3	29	2	0.550	0.24614	31.9845

The pile installation for *E45* was performed during two weeks, week 50 and 51 year 2016. Thus, the pile installation in PLAXIS were simulated in two calculation phases, each lasting five days. Intermediate consolidation phases, lasting two days, were included after each pile installation phase; to simulated the weekend since the work was assumed to only occur on weekdays. The chosen weeks and the section were somewhat isolated from other pile installation and construction work on *E45*. Due to the holidays no pile installation was performed during week 52. Thereof, could one week of consolidation in PLAXIS be compared with the field measurements for week 52 without concern for external disturbances. The installed piles had a length of 65 metres and a pile width of 275 millimetres. Number of piles and pile rows and the calculated prescribed line displacement can be seen in *Table 4.2*. Where, as in *Partihallsbron*, the prescribed line displacement for the second calculation phase was added onto the previous.

Table 4.2: *Prescribed line displacement for E45.*

Phase	Number of piles	Pile rows	w_{sp} [mm]	a_{sp}/a_{pa}	Prescribed line displacement [mm]
1	36	3	0.275	0.06600	13.3950
2	26	3	0.550	0.04767	9.7168

For the calculation phases for *Partihallsbron* see *Table 4.3*, and for *E45* see *Table 4.4*. Both projects were consolidated for 80 years after the final pile installation phase with SS and SSC model, to investigate the influence of creep. This was carried out for *Scenario 1.* Otherwise, was the result only derived from the models using SS model.

Table 4.3: *The calculation phases used in Partihallsbron, Scenario 1.*

Phase	Procedure	Activated structures
Phase 8	Plastic	First pile installation phase.
Phase 9	Plastic	Second pile installation phase.
Phase 10	Plastic	Third pile installation phase.
Phase 11 to Phase 17	Consolidation	Consolidated for 10 years in each phase until 80 years was reached.

Table 4.4: *The calculation phases used in E45, Scenario 1.*

Phase	Procedure	Activated structures
Phase 8	Plastic	First pile installation phase
Phase 9	Consolidation	Consolidated for two days.
Phase 10	Plastic	Second piling phase
Phase 11	Consolidation	Consolidated for two days.
Phase 12	Consolidation	Consolidated for seven days.
Phase 13	Consolidation	Consolidated for seven days.
Phase 14	Consolidation	Consolidated for 80 years.

For the calculations of *Scenario 2* and *Scenario 3* the material used as the piling bed was the friction material, used in the Base Model. When modelling the removal of fill were the fill layers deactivated after the nil-step and the piling bed activated. Following were consolidation phases with the purpose to dissipate most of the excess pore pressures generated when the bed was placed. The calculation phases for *Partihallsbron* can be seen in *Table 4.5*, and for *E45* in *Figure 4.6.* As before the phases do follow the nil-step. After one year of consolidation the maximum excess pore pressure was 32.16 kPa, thus within the range measured in the area, see *Appendix A.1*, *Figure A.7.* Furthermore, the model was consolidated for 1.5 and 2 years, the excess pore pressure did not decrease significantly. Thereof, was one year of consolidation considered to be sufficient.

Table 4.5: *Calculation phases used in Partihallsbron, for Scenario 2 and Scenario 3.*

Phase	Procedure	Activated structures
Phase 8	Plastic	Deactivation of the fill layers.
Phase 9	Consolidation	Consolidation for one year.
Phase 10	Plastic	Activation of piling bed, 0.1 or 0.2 meters.
Phase 11	Consolidation	Consolidation for one year.
Phase 12	Plastic	First pile installation phase.
Phase 13	Plastic	Second pile installation phase.
Phase 14	Plastic	Third pile installation phase.
Phase 15 to Phase 22	Consolidation	Consolidated for 10 years in each phase until 80 years was reached.

Table 4.6: *Calculation phases used in E45, for Scenario 2 and Scenario 3.*

Phase	Procedure	Activated structures
Phase 8	Plastic	Deactivation of the fill layers.
Phase 9	Consolidation	Consolidation for one year.
Phase 10	Plastic	Activation of piling bed, 0.1 or 0.2 meters.
Phase 11	Consolidation	Consolidation for one year.
Phase 12	Plastic	First pile installation phase
Phase 13	Consolidation	Consolidated for two days.
Phase 14	Plastic	Second piling phase
Phase 15	Consolidation	Consolidated for two days.
Phase 16	Consolidation	Consolidated for seven days.
Phase 17	Consolidation	Consolidated for seven days.
Phase 18	Consolidation	Consolidated for 80 years.

4.3 Validation of model parameters and prescribed line displacement

To evaluate the influence the prescribed line displacement and the model parameters κ^*, λ^* and v_{ur} had on the resulting mass displacement, a sensitivity analysis of the parameters was performed. Through, decreasing and increasing the calculated and derived values. This was done for *Partihallsbron* with *Scenario 1.* The sensitivity analysis was further validated against field measurements.

The prescribed line displacement was halved and doubled, with comparison to the original value, to determine the accuracy needed and validate the derived *Equation 3.1.* The result on the vertical mass displacement can be seen in *Figure 4.3*, along with the result for the original line displacement and field measurements. Through, halving the prescribed line displacement the result was underpredicted, and the doubled line displacement overpredicted the mass displacement. The same result was obtained for the horizontal mass displacement, see *Appendix B*, *Figure B.1.*

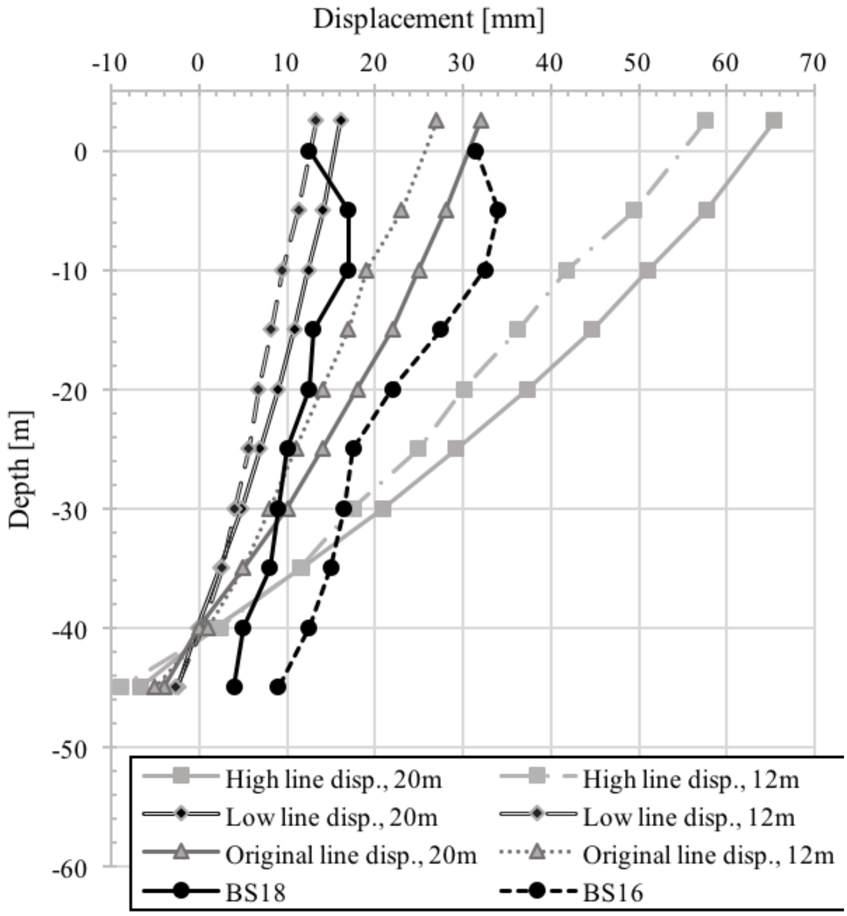

Figure 4.3: *Resulting vertical mass displacement for the high-, low- and original line displacement, and field measurements for Partihallsbron, Scenario 1.*

An overpredicted prescribed line displacement influenced the result more than an underpredicted. As the line displacement was halved or doubled can it be argued that the difference was no surprise. However, the prescribe line displacement was still relatively small as the final prescribed line displacement for the case with low line displacement were approximate 0.033 metres, the original line displacement approximate 0.067 metres and the large line displacement 0.13 metres. The result shows that the calculation for the prescribed line displacement may not be accurate to the extent that it captures the field measurements fully; which is probably due to other factors as well, such as model parameters, the SS model which fails to capture the hardening due to small strain stiffness, certain margin of errors in the field measurements etcetera. However, the calculation gives a prescribed line displacement that captures the mass displacement adequate without modifying the prescribed line displacement after the field measurements. Whereas, a calculation that would give larger or lower values would not capture the field measurements. Hence, it can be concluded that for this model the calculation for the prescribed line displacement was verified, giving resulting mass displacement close to the field measurements.

The model parameter v_{ur} was decreased from the chosen value of 0.15 to 0.1 and then increased to 0.2, the common span for the parameter. The result can be seen in *Appendix B Figure B.2*. The change of v_{ur} lead to minor differences of the horizontal mass displacement, maximum one millimetre. Whereas, the vertical mass displacement showed no difference. Due to the low impact of the model parameter it was concluded that the ratio had minor influence on the model, and no further parameter evaluation was performed on v_{ur}.

The model parameter λ^* was decreased through subtracting the original derived parameter value with 0.1 in each clay layer, and increased through adding 0.1 to the original derived parameter value. The increasing and decreasing of the model parameter had no influence on the resulting mass displacement, neither vertically or horizontally. Hence, the parameter was not investigated further in the Thesis.

The model parameter κ^* was decreased through subtracting the original derived parameter value with 0.005 in each clay layer, and increased through adding 0.02 to the original derived parameter value. The change of κ^* resulted in deviation from the curves obtained with the original derived model parameters, both for the vertical mass displacement, see *Appendix B*, *Figure B.3* and the horizontal mass displacement, see *Figure B.4*. The maximum deviation for the vertical mass displacement were approximate three millimetres for the measurements closer to the pile and two millimetres for the measurements farther from the pile. The deviation of the horizontal mass displacement was more unevenly distributed, as the result with the higher κ^* values followed the original result fairly well. Whereas, the use of the lower κ^* values resulted in lower horizontal mass displacement, with a maximum of four millimetres for the measurements closer to the pile and three millimetres from the measurements farther from the pile. As κ^* influenced the resulting mass displacement both vertically and horizontally the parameter was further evaluated with PLAXIS SoilTest.

Both IL Oedometer test and Triaxial compression tests were carried out with PLAXIS SoilTest and compared to laboratory tests. Where the laboratory IL Oedometer tests used for deriving κ^* was used. Thus, laboratory tests performed on samples from the depths 8, 15, 19 and 45 metres. For the Triaxial compression test laboratory tests were performed on samples from the depths 11, 20 and 30 metres used. The Triaxial compression tests were performed for the project *Västlänken Station Centralen*. In PLAXIS SoilTest the laboratory tests were mimicked with consideration to load step etcetera. The result for the IL Oedometer SoilTest and laboratory test on the sample from eight metres can be seen in *Figure 4.4*. As σ'_c had a large influence on the first compression line, and the σ'_c derived in the Thesis did not capture the behaviour observed in the laboratory, the curve was retrieved from PLAXIS SoilTest moved in the vertical direction to align with the unloading and reloading bulb from the laboratory test. As the parameter validation concerned the inclination of the unloading and reloading bulb which was not interfered with. The inclination of the unloading and reloading line derived from PLAXIS SoilTest matched well with the unloading and reloading bulb from the laboratory test. For the tests from the depths of 15, 19 and 45 metres see *Appendix B*, *Figure B.5* to *Figure B.7.* These tests showed similar results, where the inclination was adequate. Hence, the accuracy of the derived κ^* was validated with consideration to IL Oedometer test and the level of accuracy sought in the Thesis.

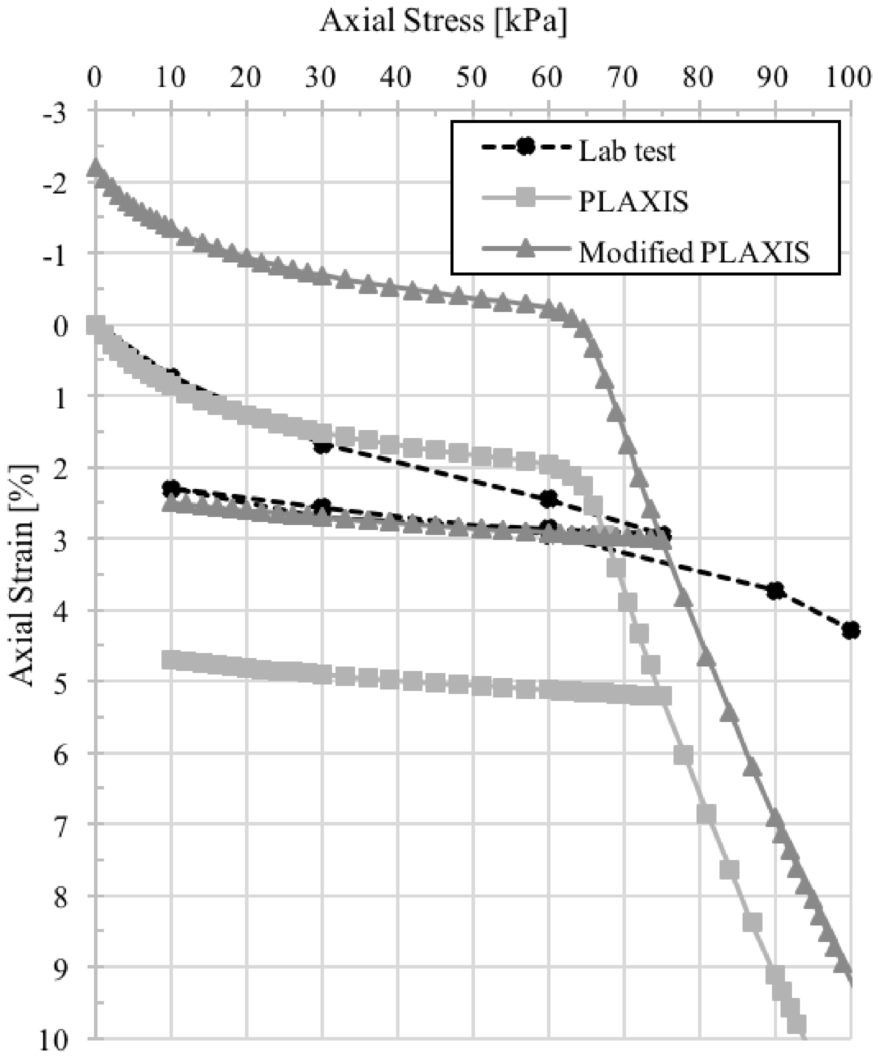

Figure 4.4: *Result from IL Oedometer test performed on a sample from 8 metres depth in laboratory and simulated in PLAXIS SoilTest.*

As the original κ^* values in the Thesis was derived from laboratory IL Oedometer test were the result from PLAXIS IL Oedometer SoilTest better fitted with these, in contrary to the comparison with Triaxial compression tests. Thus, was another κ^* evaluated, which made the PLAXIS Triaxial compression SoilTest better match the labratory Triaxial compression tests. The result for the test performed on a sample from 11 metres depth, and the PLAXIS SoilTest, can be seen in *Figure 4.5.* Where the original κ^* is referred to as κ_1^* and the new parameter value is referred to as κ_2^*.

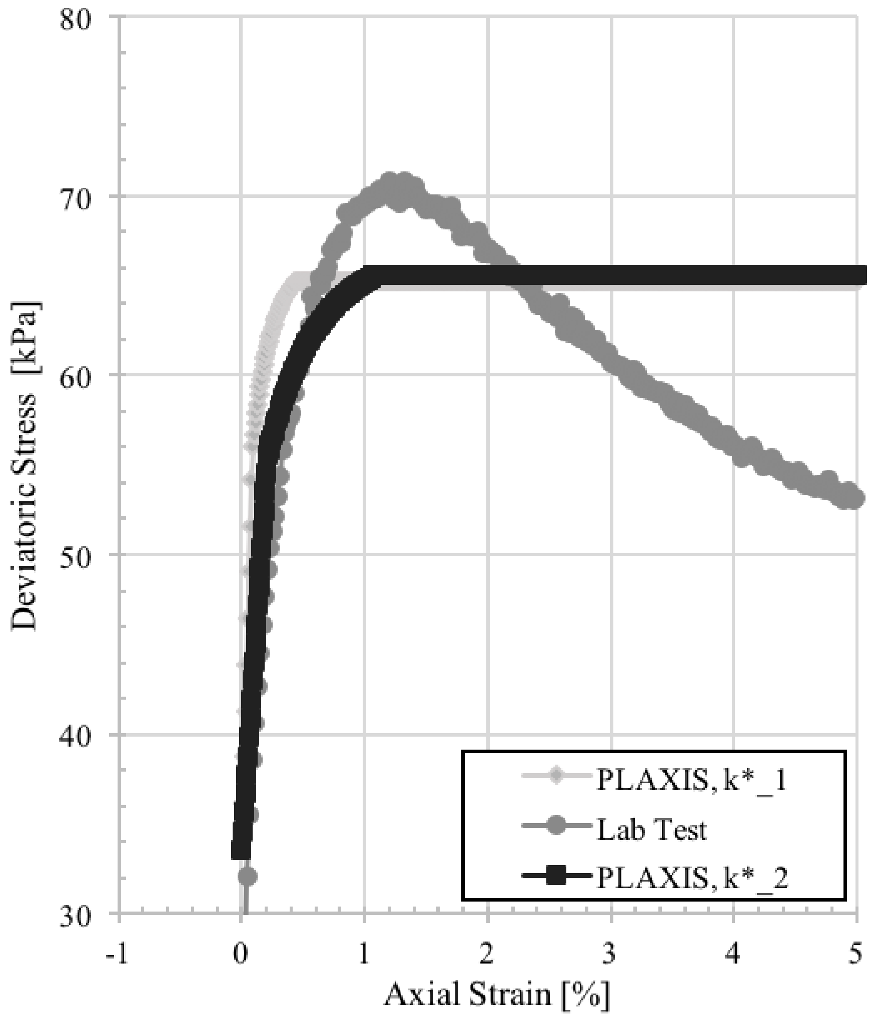

Figure 4.5: *Result from Triaxial compression test performed in laboratory on a sample from the depth 11 metres and simulated in PLAXIS SoilTest. With both the original κ^*, κ_1^*, and the new derived κ_2^*.*

The result when using κ_2^* better matched the initial part of the curve. As the original parameter, κ_1^*, gave a stiffer response of the soil than κ_2^*. The result for the tests performed on samples from the depths 20 and 30 metres can be seen in *Appendix B*, *Figure B.8* and *Figure B.9*. On 30 metres were there no need to evaluate a second κ^* as the curve matched well from the beginning, see *Figure B.9*. Hence, when referring to the result for κ_1^* and κ_2^* it is only the model parameter in clay layer three which differs, the remaining clay layers have the same parameter value as before. Both κ_1^* and κ_2^* were used in the modelling *Partihallsbron* and *E45*.

Furthermore, the model parameter κ^* was evaluated with the PLAXIS function *Sensitivity Analysis and Parameter Variation*. This was done for *E45* and for clay layers two, three and four. The range of the parameter where, as before, calculated through subtracting the original parameter value with 0.005 and then adding 0.02 to the original value. The criteria used were the influence on the vertical mass displacement of the ground surface, in the first pile installation phase. Resulting in a

SensiScore of 25 in clay layer two, 39 in clay layer three and 36 in clay layer four. Hence, the layer most sensitive to the parameter value was clay layer three and also the layer which two sets of κ^* were derived for, in the Triaxial compression test. The result further showed that clay layer four was almost as sensitive to the parameter value. However, as the original derived κ^* for clay layer four matched both the IL Oedometer curve and Triaxial compression curve was the parameter in this layer not evaluated further in the Thesis.

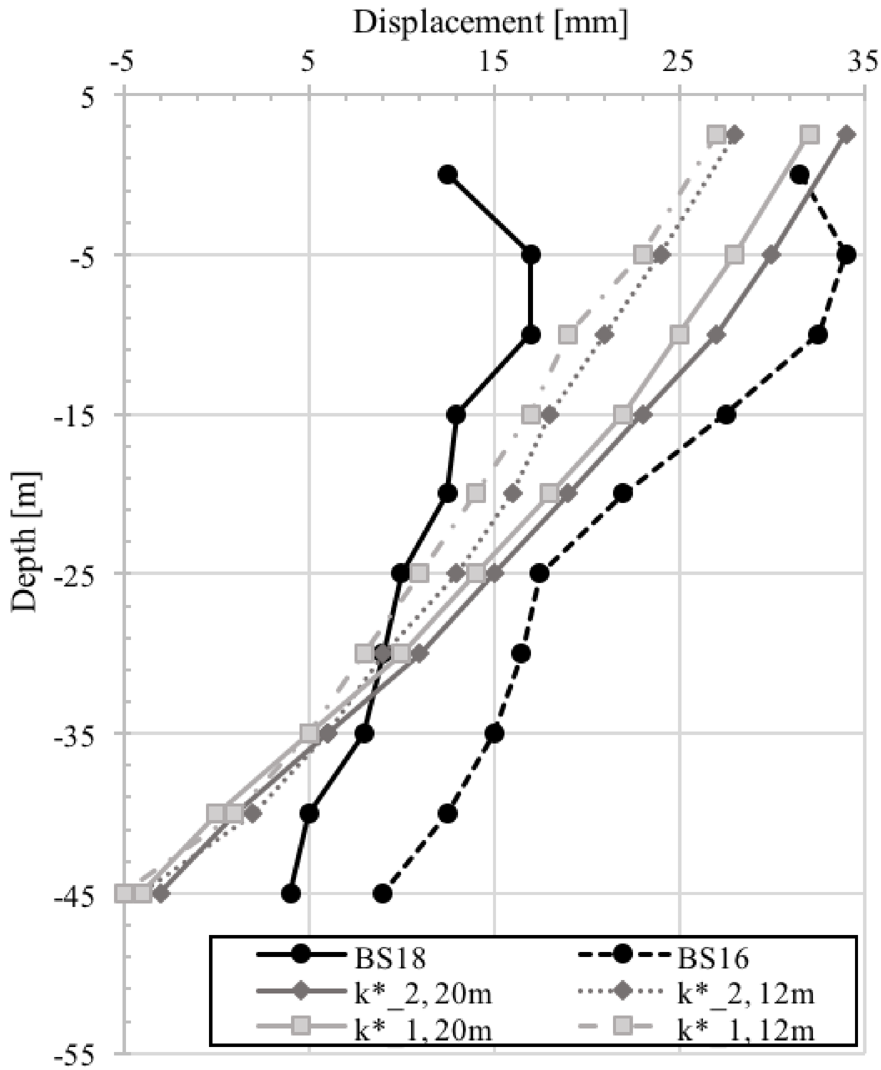

Figure 4.6: *Resulting vertical mass displacement for κ_1^*, κ_2^* and the field measurements for Partihallsbron, Scenario 1.*

The influence the model parameter κ_1^* versus κ_2^* had on the vertical mass displacement in *Partihallsbron* can be seen in *Figure 4.6*, and the horizontal in *Appendix B*, *Figure B.10*. The model with κ_1^* had lower vertical mass displacement compared to the model with κ_2^*. Both models underpredicted the mass displacement with comparison to the field measurements 12 metres from the pile. Whereas, 20 metres from the pile the models did better fit the field measurements. Although, the models first overpredicted the mass displacement down to approximate level -32 metres, then underestimate the mass displacement down to level -45 metres. Furthermore, the modelled vertical mass displacement on level -12 metres for *Partihallsbron* was smaller than the mass displacement on 20 metres which contradicts the field measurement and literature on the subject.

Whereas, the horizontal mass displacement for *Partihallsbron* in PLAXIS gave an expected outcome, as the horizontal displacement close to the pile were higher than the displacement farther from the pile. Though, the field measurements were not retrieved from the same location, as the vertical. The influence on the result from the different κ^*s were as most two millimetres. Down to approximate level -20 metres, was the mass displacement larger for the model with κ_2^*, and then became the smaller of the two.

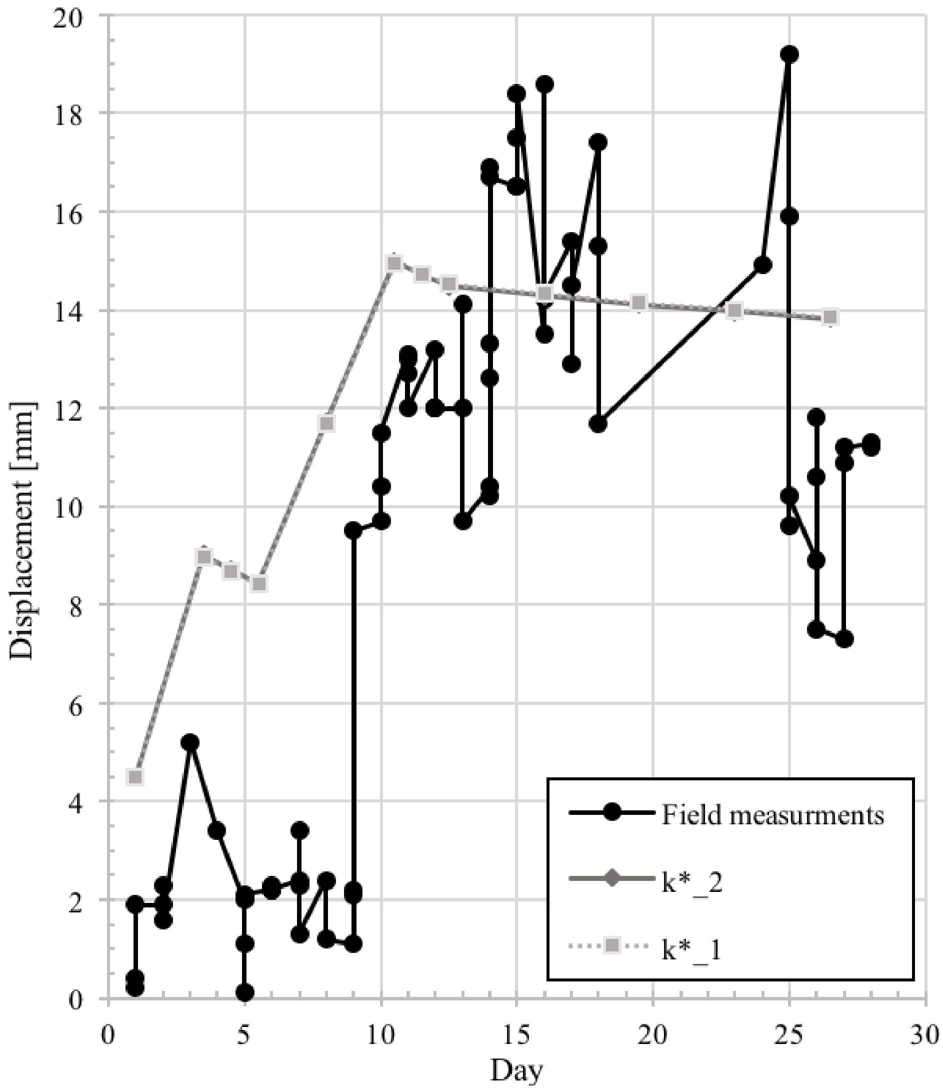

Figure 4.7: *Resulting vertical mass displacement on the ground surface with κ_1^* and κ_2^*, compared with the field measurements for E45 in Point F, Scenario 1.*

The difference in vertical mass displacement for *E45* when using κ_1^* versus κ_2^* in Point F, can be seen in *Figure 4.7*. The difference was minor for all points investigated. Whereof, only one result is presented in the Thesis. The model with κ_1^* showed slightly larger vertical mass displacement of the ground surface, approximate between 0-0.5 millimetres.

Minor differences in both the vertical and horizontal mass displacement could be seen in the two projects, all under five millimetres. An doubtful accuracy that this kind of 2D simulation can obtain, with the number of uncertain parameters and factors that comes with modelling soft soil. Therefore, was it argued to further on in the Thesis only use the original parameter value, κ_1^*, since the result from comparing κ_1^* and κ_2^* gave minor differences. However, the curves differ throughout the profile, especially the horizontal curves in *Partihallsbron*, see *Appendix B*, *Figure B.10*. Where the use of κ_1^* and κ_2^* results in curves which moves opposite to each other. Furthermore, was only the κ^* changed in clay layer three which had a thickness of 10.5 metres, but the effect was universal in the profile. Whereas, the vertical curves showed that a higher κ^* lead to higher vertical movements. Which was no surprise as a higher modified swelling index, should induce higher swelling in the soil. Therefore, it is important to evaluate the influence from the model parameter, which was done.

4.4 Validation of model behaviour with focus on strains

Model parameters never fully capture the soil behaviour as there derived from a handful of laboratory and field tests. Hence, parts of the model will underpredict the soils response, such as stiffness and shearing, whilst other parts will overpredict it. To ensure that the model does not overpredict the deviatoric strains (γ_s), that can be withstand before the soil reaches failure, the triaxial compression tests in *Chapter 4.3*, were further evaluated. Through, evaluating between which strains the model would capture the stress response, be conservative or underpredict the response. The axial strains (ε_1) in the Triaxial compression tests were converted to deviatoric strains with the use of *Equation 4.1*, with undrained $v_{ur} = 0.5$ [Knappett and Craig, 2012].

$$\gamma_s = 1.5 * \varepsilon_1 \tag{4.1}$$

Furthermore, as two κ^* was used in clay layer three, did the span for where the model underpredicted, matched and overpredicted the soil response vary, see *Figure 4.5* and *Appendix B*, *Figure B.8* and *Figure B.9*. Where κ_1^* gave a stiffer behaviour of the soil, than the laboratory tests and κ_2^*. Between the strain range of 0 to 0.6 percent, on 11 metres depth, did the curve with κ_1^* overpredict the stress response due to the γ_s. Whilst, between 0.6 to 2.25 percent did the curve with κ_1^* instead underpredict the response. The response with κ_2^* better matched the behaviour seen in the laboratory tests. Matching the curve up to 0.5 percent of strains. However, the soil stiffness was underpredicted between 0.5 to 2.25 percent, where it once again matched in one point, then started to overpredict the stiffness of the soil. The result was similar when comparing the PLAXIS SoilTest with the laboratory test performed on a sample from the depth 20 metres. Which were no surprise as both lays within clay layer three. Comparing the laboratory test performed on a sample from the depth 30 metres the result in PLAXIS SoilTest gave matching curves between 0 to 0.5 percent. Thus, almost no overprediction of the soil stiffness. After 0.5 to 2.6 percent the curve underpredicted the stiffness. Since the model mostly underpredicted the stiffness response, hence the strength of the soil, should it not collapse. However, as the curves did not completely match, the soil behaviour was not fully captured.

For *Partihallsbron*, directly after the pile installation, did the γ_s range between 0 to 0.3 percent, which does not exceed the strains from the SoilTest curve as it overpredicted the stiffness response of the soil. The γ_s was further evaluated for the model after 80 years of consolidation, giving a ranged between 0 to 1.5 percent. Hence, the model does not overpredict the soil strength. For *E45*, directly after the pile installation, did the γ_s range from 0 to 0.4 percent and after 80 years of consolidation from 0 to 1.8 percent. Thus, do not overpredict the soil strength.

Furthermore, there were some limitations made with the validation of the model. Large strains were created at the bottom of the pile and in the pile when the line displacement was activated. Both ε_v and total γ_s showed non plausible magnitudes. The excess pore pressure just beneath the pile toe exhibited large suction and then large pressure adjacent to the side of the pile toe. Caused as the soil cluster, acting as the superpile, increased and the mesh of the soil beneath the pile was dragged out reluctantly, deforming the mesh in an unnaturally manner. To counteract this behaviour additional modelling was carried out for *Partihallsbron* and *E45*. Firstly an interface was modelled from the middle of the pile toe down to the bedrock, both with a R_{inter} of the adjacent soil and with a R_{inter} of zero. The results showed no significant improvement and the idea were therefore left. Secondly an interface was applied to the bottom of the pile, with R_{inter} of the adjacent soil and with a R_{inter} of zero as in the previous trial. As before the strains and excess pore pressures were still unnatural. Thirdly both these two trials were used, so an interface below the pile and from the middle of the pile toe down to the bedrock. The strains were mostly the same, and the suction was somewhat improved. The result in both vertical and horizontal mass displacement were therefore compared for *Partihallsbron*. At the depths investigated, down to level -45 metres, seven metres above the pile toe, there was no difference in the result. Hence, the original Base Model were assumed to be valid with the limitation that the soil adjacent to the pile toe could not be investigated or validated.

4.5 *Partihallsbron* and *E45* - Result and analysis

The result for *E45* is illustrated in curves which were normalised with consideration to the vertical displacement occurring the day before the investigated piling started. Hence, ignoring the previous displacement which has occurred in the area from of other pile installation, excavation work, removal of fill and placement of piling beds etcetera. In PLAXIS this was done with the nil-step, and with the field measurements through subtracting the measured displacement occurring the day before the investigated pile installation started. All curves have their starting point on day one of pile installation and ends after two weeks of consolidation, except for the curves where 80 years of consolidation have been investigated. Furthermore, some field measurements were ignored, as they contained what were assumed to be faulty measurements, where the displacement peaked for day 14 in several points with additional 20 to 25 millimetres.

The result for the vertical mass displacement in *Partihallsbron* can be seen in *Figure 4.8*. For the horizontal mass displacement, see *Appendix B*, *Figure B.11*.

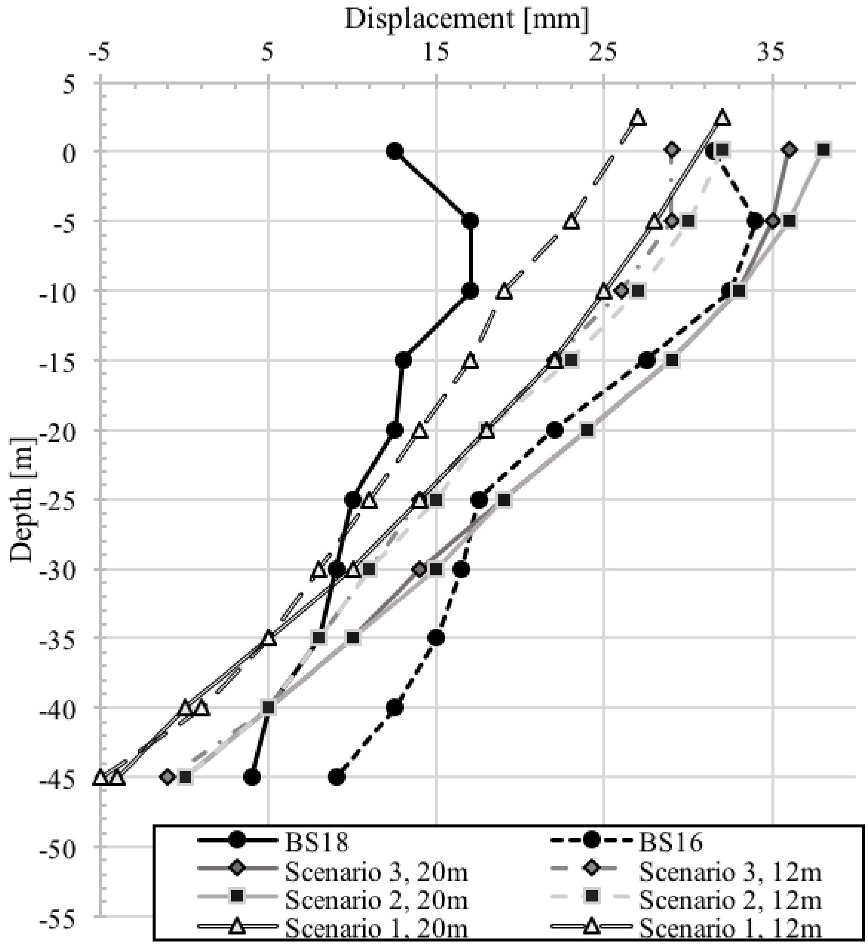

Figure 4.8: *The vertical mass displacement for the three scenarios, for Partihallsbron.*

Generally, the result from *Scenario 1* was smaller throughout the soil profile. However, for the horizontal movements the mass displacement were for the first 15 metres higher. Between level -25 to -45 metres was the mass displacement larger for *Scenario 2* and *Scenario 3*. Furthermore, there werenearly no difference in the horizontal movements for *Scenario 2* and *Scenario 3*, as opposed to the vertical mass displacement where the movement differs for the two scenarios.

The vertical mass displacement of the ground surface in *E45* for the three scenarios, in Point F, can be seen in *Figure 4.9*. The result for Point B and D can be seen in *Appendix B*, *Figure B.12* and *Figure B.13*. The other points showed similar results and trends due to close proximity, thus not included in the Thesis.*Scenario 3* had lower vertical movements during the pile installation and slower regression of the vertical displacement during the consolidation. Thus, resulting in that the vertical displacement was approximate the same after two weeks of consolidation. Except for the closest point, Point D, where *Scenario 1* had lower displacements.

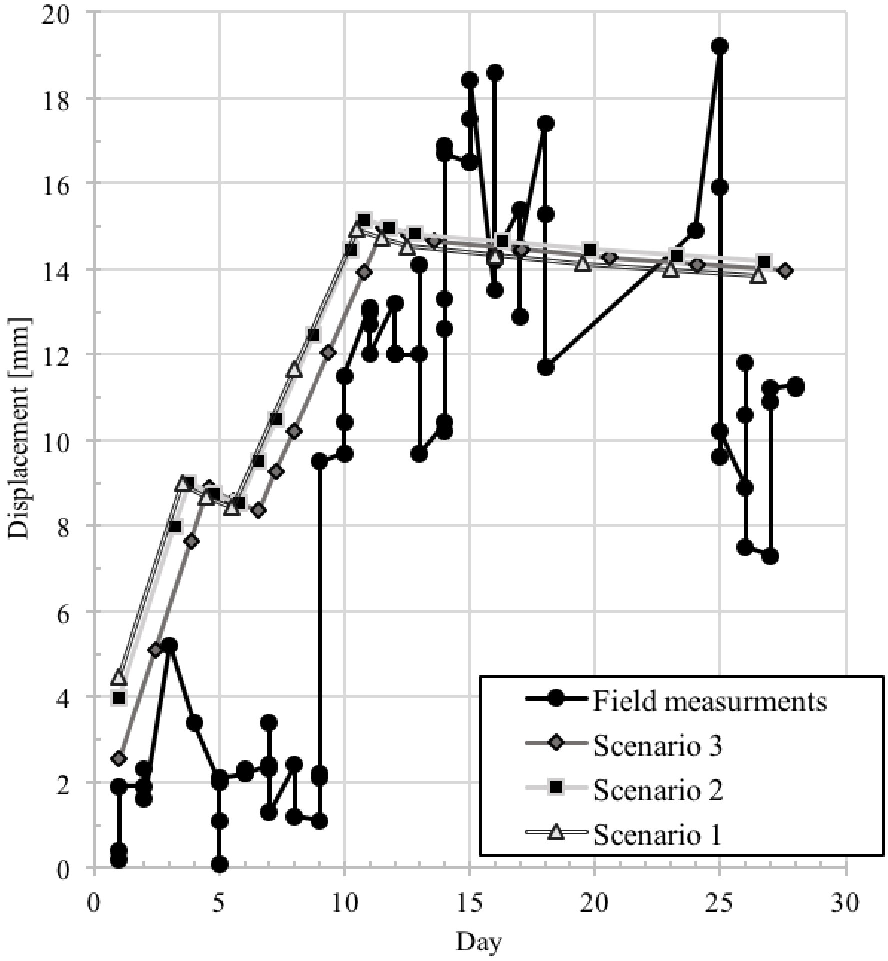

Figure 4.9: *The vertical mass displacement of the ground surface, for the three scenarios in Point F, E45.*

Furthermore, for the points closest to the piling area/superpile was the vertical displacement overpredicted in PLAXIS. Farther away, 60 metres and beyond, instead the mass displacements was underpredicted. The field measurements contradicted literature due to larger displacements farther from the piling area.

In *Partihallsbron* the resulting curves from *Scenario 2* and *Scenario 3* were similar to the field measurements. Which can be linked to the common use of piling beds. Implying that in the project were fill removed and a piling bed placed. However, the vertical mass displacement was better matched for the field measurements 12 metres from the piling area/superpile. Whereas *Scenario 2* and *Scenario 3* overpredicted the movements 20 metres from the superpile. The movements were larger than in *Scenario 1*, which can be linked to that a smaller load acted on the surface. Furthermore, all fill in the model for *Partihallsbron* was removed in *Scenario 2* and *Scenario 3*, which is not the case in the field. Where the fill is removed with a closer proximity to the piling area. When the fill was removed did the soil start to heave and then settle when the piling bed were placed. This caused rapid change in the excess pore pressure, thus it was consolidated. After the consolidation were the excess pore pressure still larger than before the fill was removed which also can be linked to the larger vertical movement of the soil. Although, the result of the horizontal movements showed no significant difference for the three scenarios.

For *E45* one vital difference between the field measurements and the result from PLAXIS were observed. The displacement in PLAXIS starts to subside directly after the pile installation had stopped and the consolidation starts. Whilst, in the field measurements for Point B can a trend of continuing soil displacement two weeks after the pile installation, be viewed. Though, for the first week of consolidation do the field measurements start to subside. Since additional piles were installed in the area during the second week of consolidation in the field, can it be argued that the increase was a consequence of this pile installation and not the pile installation modelled.

Generally, the models for *Partihallsbron* and *E45* did capture the vertical mass displacements compared to the projects field measurements fairly well with consideration to the magnitude of the vertical mass displacement. The main problem with the model was that the vertical mass displacement of the ground surface did not subside fast enough, leading to uniform vertical mass displacement, especially in *E45*. A result which is highly doubtful as the points differs on a span of 50 metres. Whereas, in *Partihallsbron* were the main problem, that the vertical mass displacement farther from the pile was larger than the one closer to the pile. This could be linked to the use of a SS model, as it does not consider hardening due to small strain stiffness and will not capture the decrease correct. However, it can be concluded that the calculated prescribed line displacement gave a reasonable vertical mass displacement which captures the behaviour between 12 and 74 metres from the superpile. With reservation that the behaviour is somewhat over and underpredicted with approximate ten millimetres. An accuracy which is not actually plausible to retrieve with numerical modelling with this number of uncertain variables.

Furthermore, the vertical field measurements showed less difference between the largest and smallest vertical movement for *Partihallsbron*. Thus, the curves had smaller inclination. Whereas, the curves retrieved from the PLAXIS models showed larger inclinations. This can be linked to the use of prescribed line displacement, where in the field the soil will not move to the same extent down at the pile toe as at the surface, due to the soils self weight and the stresses in the soil. Whereas, the prescribed line displacement in the model moves the soil the amount that is prescribed. What contradicts this is the movement further down in the soil, which becomes negative for the PLAXIS result, hence the soil moves downwards in the soil profile. This occurs at the bottom of the measurements close to the pile toe and can be due to the large strains created in PLAXIS when the soil cluster acting as the superpile extends whilst the soil beneath the pile is dragged out. Creating falsely high shear and volumetric strains, which do not occur in the field. Therefore, the measurements close to the pile toe should be ignored as stated before. Thus, it could be argued that the model captures the behaviour down to approximate ten metres above the pile toe.

When comparing the difference between the settlement after 80 years with either the SS or SSC model were there a significant difference. The SSC model resulted in a nine and six centimetres higher settlement for *Partihallsbron* and *E45* respectively, compared to the result from the SS model. For *Partihallsbron* were the maximum settlement in the SS model 12 centimetres and occurred 55 metres from the superpile and beyond to the boundaries in the horizontal direction. In the SSC model did the maximum settlement occur 70 metres from the superpile with a size of 21 centimetres. For *E45* did the SS model result in a maximum settlement of 11 centimetres and in the SSC model 17 centimetres. In both the SS model and SSC model did the maximum settlement occur 80 metres from the superpile and continued to the boundary in the horizontal direction as in *Partihallsbron*. The difference in the result was reasonable since the SSC model takes both consolidation and creep into consideration, whereas the SS model only considers the consolidation. Furthermore, the maximum settlements did occur on approximate 1 pile length to 1.5 pile lengths from the superpile and with the same rate of settlement for both the SS and the SSC model, as in their respective control year. Implying that an area of approximate 1 to 1.5 pile length from the superpile was influenced by the pile installation which is stated in empirical research and literature [Edstam, 2011].

Furthermore, the settlements with the SS models for both *Partihallsbron* and *E45* were nearly the same. However, there were a difference in the SSC model, which could imply that the SSC model and creep were more sensitive to the pile length and pile volume.

The excess pore pressure build up in the model for *Partihallsbron* directly after the pile installation on the levels -10, -20, -30 and -40 metres in the SS model, with consideration to distance, can be seen in *Figure 4.10*. Directly after the pile installation was the maximum excess pore pressure in direct connection to the superpile at level -40 metres. The excess pore pressure then decreased with distance. Whereas, for the levels -10 and -20 metres did the excess pore pressure increase a couple of metres before starting to decrease.

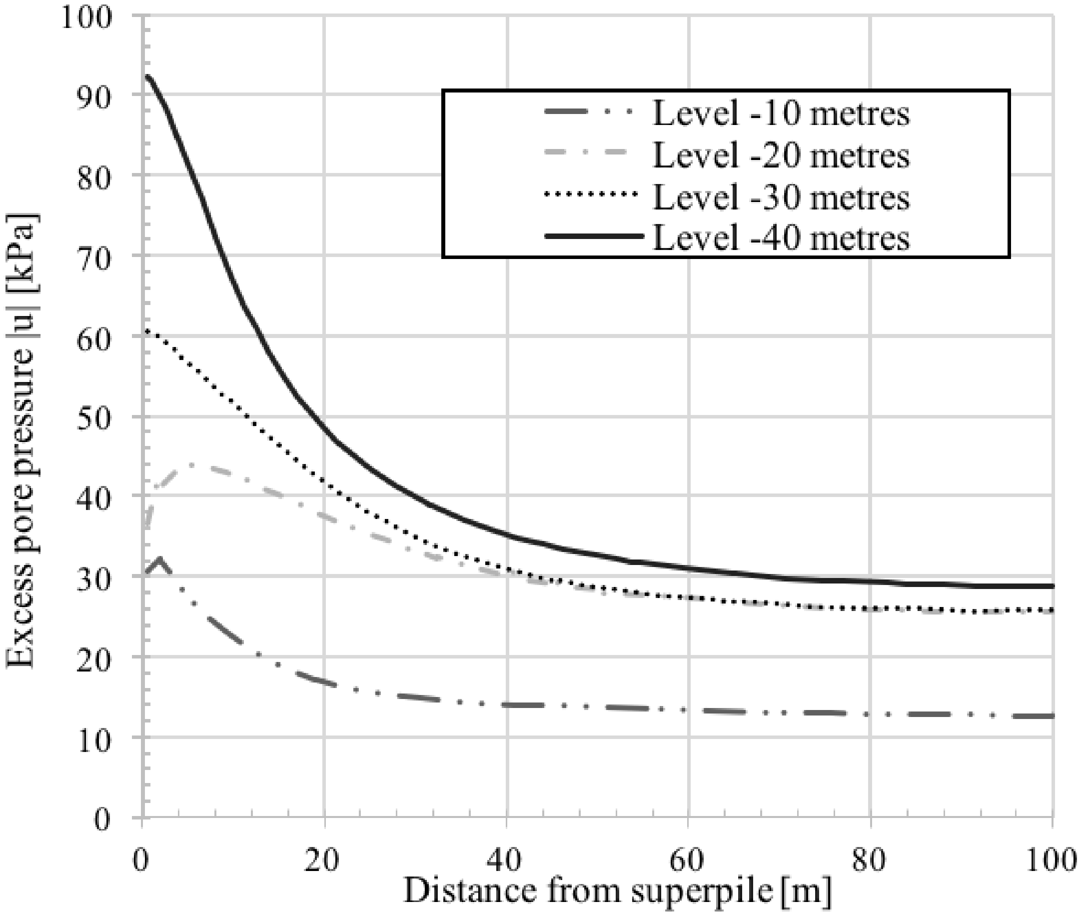

Figure 4.10: *Excess pore pressure distribution with distance from the superpile, with consideration to depth, directly after piling, for Partihallsbron, Scenario 1.*

Furthermore, the pore pressure distribution directly after the pile installation and during 80 years of consolidation was investigated for *Partihallsbron* with the SS model, see *Figure 4.11*. The excess pore pressure peaked during the pile installation, as expected, and then subside when the consolidation started and the excess pore pressure dissipated. During the first year had the dissipation the highest rate, generally decreased with 10 kPa. On level -5 metres in the model, had the excess pore pressure nearly fully dissipated after one year. A trend can be seen in *Figure 4.11*, were the excess pore pressure increases further down the pile as in *Figure 4.10*. However, on the depth of -40 and -45 metres were the excess pore pressure nearly identical as the maximum excess pore pressure in the soil profile had been reached. After approximate 15 years was the maximum excess pore pressure the same as in the control year when considering a distance of ten metres from the superpile, and after 20 years were the excess pore pressures for all depths lower than 10 kPa. Whilst, when considering the maximum excess pore pressure in the whole model were the time before reaching the level in the control year between 40 to 50 years. After 80 years of consolidation were the excess pore pressures approximate the same for all depths, ten metres from the superpile.

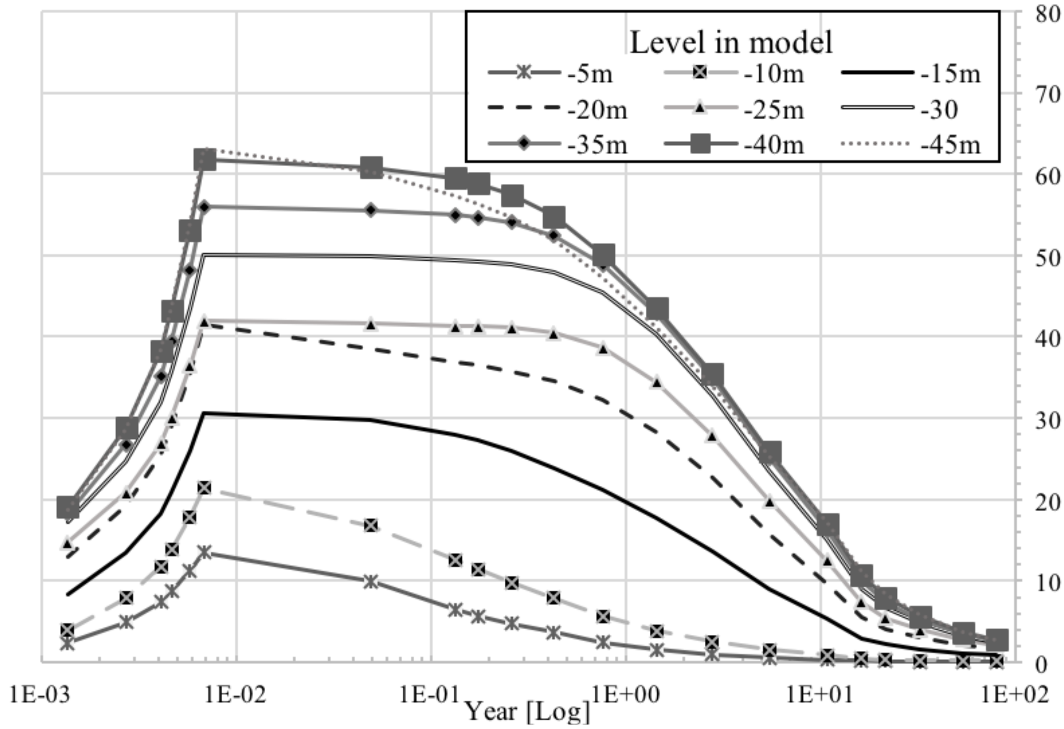

Figure 4.11: *Excess pore pressure distribution ten metres from the superpile in Partihallsbron, Scenario 1. On different levels with consideration to time.*

Evaluation on how the excess pore pressure varied, for *Partihallsbron*, with consideration to the distance from the superpile and during the 80 years of consolidation, were carried out with the SS model. The excess pore pressures were plotted against the distance, with steps of 10 years of consolidation, and through, measurement on the levels -5, -15 and -30 metres in the model, the result for -15 metres can be seen in *Figure 4.12*. The excess pore pressure increased with the distance for all years investigated. Where the most apparent difference, with consideration to distance, was after ten years of consolidation. The difference with distance gets less apparent with time, where 80 years of consolidation shows the lowest difference. Ten years of consolidation further goes against the other trends which can be seen, as the excess pore pressure peaked around 50 metres from the superpile before starting to subside. Whilst, the other curves showed the peak 100 metres from the superpile, hence the boundary in the horizontal directions. In the clay layers were the groundwater boundary set to closed for the horizontal boundaries. Hence, the excess pore pressure could not continue to move farther away from the pile which could be the reason for the pore pressure bulb to stop moving. On the level -15 metres did the excess pore pressure on the distance of 100 metres from the superpile vary with approximate 1 kPa for the last 50 years of consolidation. One reason for this could be the closed boundary, which prevents dissipation out from the model.

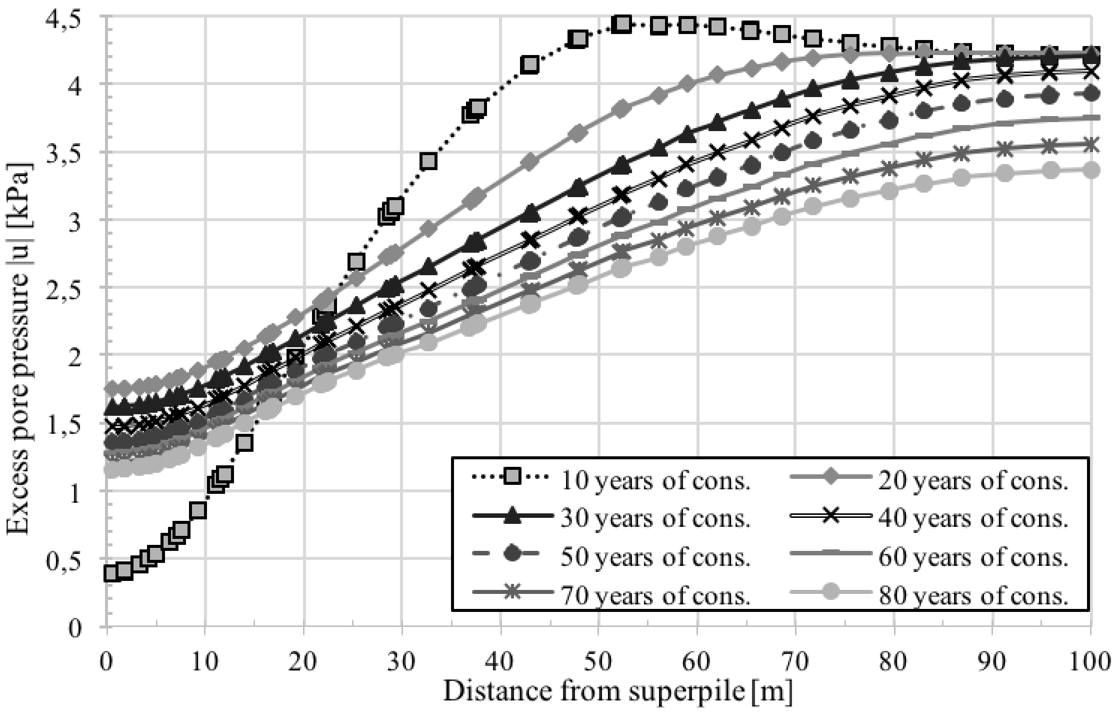

Figure 4.12: *The excess pore pressure distribution on the level of -15 metres in the model, with consideration to time and distance from superpile, for Partihallsbron Scenario 1.*

The maximum excess pore pressure occurred around level -30 to -40 metres, during the control year. Whereas, directly after pile installation did the maximum excess pore pressure occurs around level -40 to -45 metres. However, in the PLAXIS model can it be observed that the maximum excess pore pressure after a short time of consolidation once again occurs between the levels -30 to -40 metres. The cause for the large excess pore pressure between level -40 to -45 metres can be due to the faulty shearing and destruction of the soil below the pile toe as the prescribed line displacement was activated. The reason for the high excess pore pressure in the middle of the model is, except for the closed boundaries in the clay layers which prevents horizontal dissipation, the slow vertical dissipation due to the low permeability of clay. Whilst the clay close to the more permeable materials, friction fill and friction material can have a higher rate of dissipation in the vertical direction.

Furthermore, it is important to acknowledge how the water can flow. As the SS model is isotropic will the excess pore pressure dissipate equal in all directions. Whereas, soil actually is anisotropic. Thereof, the resulting dissipation in the models is a simplification resulting in that the behaviour observed is only predictions.

Further, the soil profile will influence the dissipation. The clay investigated is fairly homogeneous. However, some layering and non-homogeneous areas exist in the soil profile which will influence the rate of dissipation. If there is layering in the soil will the dissipation occur faster in these stratas. The soil around Gothenburg Central Station consist of two different geological deposits between clay layer three and four, level -20.5 metres in the model. Thus, the dissipation between these two layers should occur faster in the horizontal direction. In *Figure 4.11* can it be observed that the initial excess pore pressure accumulated directly after the pile installation for *Partihallsbron, Scenario 1,* for the levels -20 metres and -25 metres in the model are identical. The dissipation of excess pore water pressure on level -20 metres then occurs much more rapidly than on the level -25 metres. Which could be due to the closer proximity to the layering.

4.6 *Partihallsbron* and *E45* - Discussion

One assumption that could lead to secondary fault in the Thesis was from which level the field measurements for *Partihallsbron* starts. The level is not specified in the report *Massundanträngning vid pålning i lera* [Edstam, 2011]. Thereof, the level was assumed to be at ±0 meters in the models. If the assumption is inaccurate will it influence how the different curves correlate. However, would this not influence the comparison substantially, as the difference also could be linked to faulty field measurements or errors in the model. The importance of the comparison was to estimate if the model captures the behaviour in a reasonable way, which still could be done.

When it comes to the horizontal movements for *Partihallsbron* were the field measurements and the result from the PLAXIS model not compatible. Probably because the field measurements were taken from the short side of the piling area and on different distances. If the distance had been measured from the field measurement point to the centre of the piling area may the result matched the field measurements better. As the models now predicts larger movements than measured by the inclinometers. However, this can also lead to faulty predictions as the distance from the field measurement should be to the superpile, which technically ends at the short end of the piling area. Though, the model was simulated as a two-dimensional problem with a plane strain assumption, meaning that there would be no short end of the piling area as it continues for infinity. As the piling area, in this case, is short in comparison to problems better fitted for this type of calculation, e.g. road, can this also influence the outcome. To conclude should not the field measurements for the horizontal movement be a benchmark in the study of these movements, instead can the layout of the curve be studied and sought for. However, the horizontal result did show a larger movement closer to the superpile then farther away which correlates with the field measurements and literature.

Furthermore, the field measurements for *E45* showed a trend which contradicts literature and research project, which states that the vertical mass displacement of the ground surface is largest closest to the piling area and then subsides. Whereas, the field measurements showed an increase in the vertical mass displacement of the ground surface, farther from the piling area. The reason could be faulty field measurements or that several construction projects and different construction steps within the area had taken place and toke place during the time span the measurements were retrieved. Another reason could be that close to the piling area were heavier and thicker bed of agglomerated material placed, compared to further from the piling area. However, as the information around the geometry during those four weeks were scant was this not further investigated or modelled. Another problem connected with the geometry, were that excavations in the area had occurred in several steps, as well as placement of soil masses. Creating slopes, slip surfaces, excess pore pressure and suction etcetera. Which influence the result, but has not been considered in the PLAXIS model due to lack of both information and time. The points A, B and C are located on the side of *E45* which is flatter. However, the side closer to the project *Regionens Hus* were a large amount of piles had already been installed before the installation considered in the Thesis. How the installation from these piles influenced the area was not investigated, and therefore was it hard to pin point which movements are due to the installation of piles for E45, and which movements that can be linked to the pile installation for *Regionens Hus*. Whereas, the points D, E and F is on a side with several existing buildings and slopes which influence how the soil moves.

A further insecurity and assumption, that influenced the result, was the location of the field measuring points for *E45*. As theses points were scattered over the area and not located in the manner assumed in PLAXIS. Hence, the field measurements will not match the simulation. It is faulty to compare the field measurements in the way that has been done, as they are approximately the same length from the piling area in the horizontal direction. As in *Partihallsbron* was the problem that some of the field measuring points were closer to the short side of the piling area compared to the long side, which would mean that the PLAXIS model should overpredicts the result. However, as the field measuring points are scattered besides *E45* can it be seen that both Point B and Point C, see *Figure 4.2*, were located in such a way that it could be influenced by pile installation occurring further up and down the road construction. That could be one reason why the model underpredicts the field measurements.

In retrospect, could only one side of *Partihallsbron* and *E45* been modelled as no unsymmetrical modelling was carried out. This could further have decreased the unnatrual behaviour of the soil under the pile toe.

5
Case study - *Västlänken Station Centralen*

To further investigate the consequences from pile installation was a case study of the construction project *Västlänken Station Centralen* performed. This with focus on how the mass displacement and excess pore pressure differed in the model when performing the pile installation from different levels, and with different pile installation techniques. The cross section investigated was 475+480, which is part of the *Västlänken Station Centralen*, see *Figure 1.2*. Thus, constructed in the area from which the model parameters were derived, [Wood, 2017]. The information of number of piles, size of piling area etcetera, were retrieved from tender documents as the construction had not initiated when the Thesis was written. A blue print over *Västlänken Station Centralen* can be seen in *Figure 5.1*, with the modelled section marked with a rectangle. The section is located at the end of the railway station. Thus, before the tunnel starts to taper and thereof one of the widest sections of the tunnel. In the Thesis were the connected entrance and exit shafts ignored, see *Figure 5.1*. One reason for this was the plane strain assumption, which better matched the long uniform section of the tunnel.

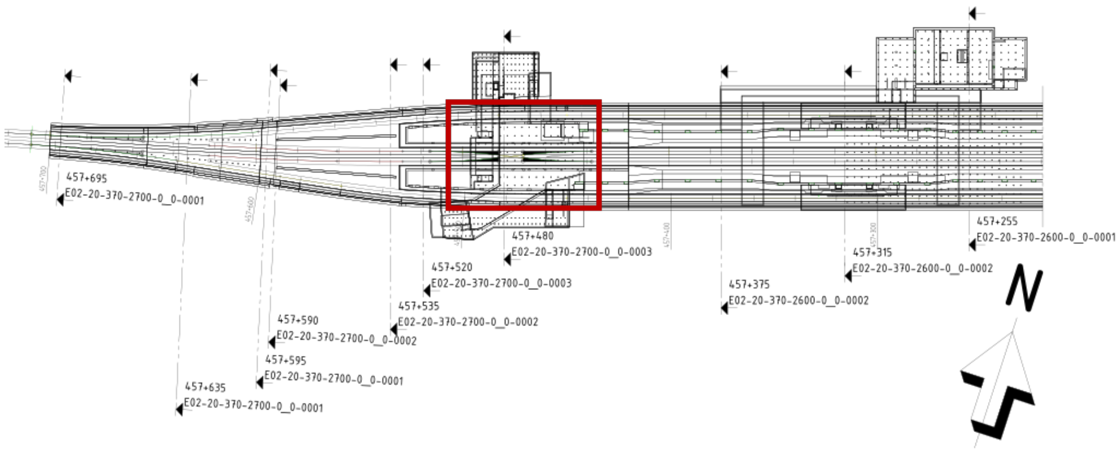

Figure 5.1: *Blue print over a part of Västlänken Station Centralen, retrieved from tender documents. The section investigated is marked with a rectangle, modified from [Andersson, 2018a].*

The cross section modelled can be seen in *Figure 5.2*, also retrieved from tender documents. The cross sectional blue print gave information on pile length, the excavation depth etcetera. The part modelled is marked with a rectangle in *Figure 5.2*. In PLAXIS were not the internal constructions of the station modelled, only the external, such as the support structures and a load corresponding to the weight of the tunnel. As the Thesis investigated the influence of pile installation on adjacent areas, and not the construction of the tunnel.

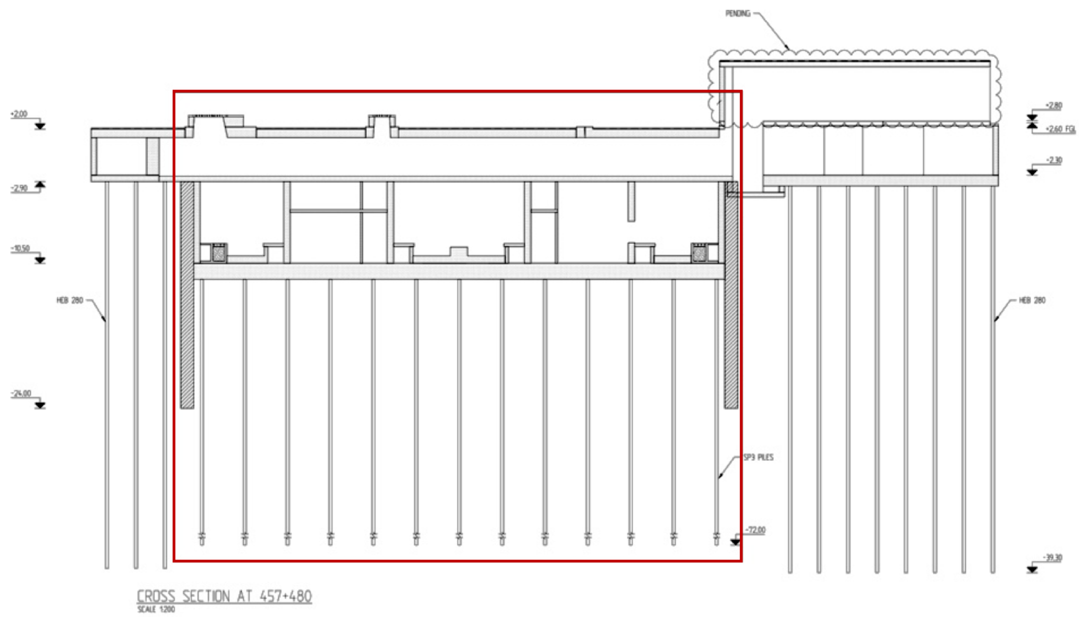

Figure 5.2: *Blue print over the cross section 475+480, retrieved from tender documents. The section investigated is marked with a rectangle, modified from [Andersson, 2018b].*

The size of the piling area was derived from the blue print in *Figure 5.2*, where the piling area was assumed to be the width of the railway tunnel, excluding the entrance and exit shafts. Thus, a width of 50 metres. The length of the investigated area was also 50 metres. The piles to be used is SP3, as the diameter then can be 270 or 275 millimetres were a pile width of 275 millimetres was chosen. The piles were to be driven to a depth of 72 metres from level ±0 metres, see *Figure 5.2*. The excavation was modelled down to level -12 metres in the models, hence the bottom of the concrete plate in *Figure 5.2*.

As the construction of the chosen section had not started during the Thesis were no field measurements available. Thereof, the result from the calculated models were only evaluated and discussed in comparison to each other and the result from *Partihallbron* and *E45*, see *Chapter* 4. The aim of the case study was to investigate if the mass displacement differed depending on if the piles were installed from the excavation bottom or before the excavation were carried out, and then with or without pile block/pre-augering.

5.1 *Västlänken* - Calculations

For the calculations were the Base Model used, but with several modifications, as additional structures and an excavation was modelled. A significant difference from the previously constructed Base Model, was that the global groundwater table was set to level +0.5 metres in the model, instead of ±0. However, this did not influence how the calculation phases were constructed. Thus, the additional phases were used in the calculation of *Västlänken Station Centralen* added onto the nil-step as in the previous models, see *Table 3.1*. The setup of the model can be seen in *Figure 5.3*. Three scenarios were modelled, for which the phases differed.

- **Model 1:** The excavation was carried out before the pile installation. Hence, the pile installation were carried out from the excavation bottom.
- **Model 2:** The pile installation occurred from top of clay, on level ±0 metres, in the model, as the fill was excavated adjacent to the deep excavation before the pile installation. This with and without a load activated on the excavation bottom, mimicking the weight of the tunnel acting under the foundation plate, 165 kPa/m [Wood, 2017].
- **Model 3:** The pile installation occurred from top of clay, on level ±0 metres, in the model, as the fill was excavated adjacent to the deep excavation before the pile installation. The piles were simulated to be installed with pre-auger or pile-block.

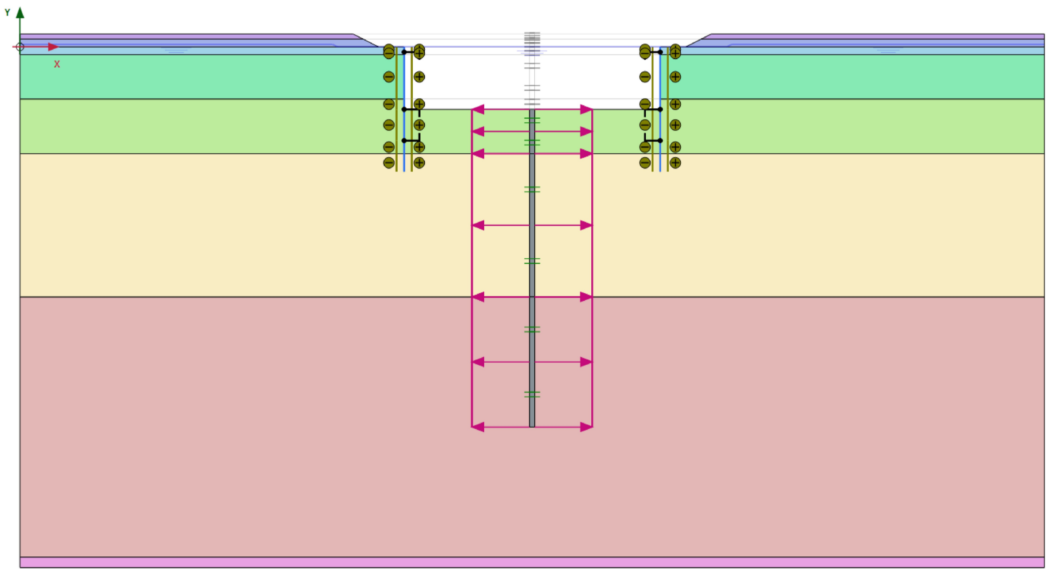

Figure 5.3: *Model in PLAXIS after the excavation was carried out.*

The calculation phases used for the three models can be seen in *Table 5.1.* Where an area of fill around the deep excavation was removed. Hence, it was necessary to locally lower the ground water table to level ±0 metres, in the model. This was done in the same phase as the deactivation of fill over and adjacent to the deep excavation. The support structures were activated before the pile installation started, for all three models. The support structures were constructed as plates, mimicking concrete diaphragm walls, with the material parameters listed in *Appendix C*, *Table C.1.* Interfaces were activated on the walls at the same time as the walls were activated, with the R_{inter} set to adjacent to soil. In the excavation phases were stamps activated on the support structures, with the material parameters listed in *Appendix C*, *Table C.2.* The interfaces were deactivated when the consolidation started to enable the model to consolidate for 80 years, to prevent model collapse.

Table 5.1: *Calculation phases used in the case study, Västlänken Station Centralen.*

Phase	Procedure	Activated structures
		Model 1
Phase 8	Plastic	Deactivation of fill and local lowering of the groundwater table.
Phase 9	Plastic	Activation of support structure.
Phase 10	Plastic	Excavation and activation of stamps.
Phase 11	Plastic	First pile installation phase.
Phase 12	Plastic	Second pile installation phase.
Phase 13	Plastic	Third pile installation phase.
Phase 14	Consolidation	Consolidate for one week. Interfaces deactivated.
Phase 15	Consolidation	Consolidate for 80 years.
		Model 2 and *Model 3*
Phase 8	Plastic	Deactivation of fill and local lowering of the groundwater table.
Phase 9	Plastic	Activation of support structures.
Phase 10	Plastic	First pile installation phase.
Phase 11	Plastic	Second pile installation stage.
Phase 12	Plastic	Third pile installation stage.
Phase 13	Plastic	Excavation and activation of stamps. Activation of the line load of 165 kPa/m.*
Phase 14	Consolidation	Consolidate for one week. Interfaces deactivated.
Phase 15	Consolidation	Consolidate for 80 years.

**Only for model 2*

The excavation was carried out through deactivating the soil clusters within the support structures, down to the chosen excavation bottom, see *Figure 5.3*. The excavation was then set to act as a dry cluster. As the construction of *Västlänken Station Centralen* had not started when the Thesis was written could no information on the pile order and number of piles in each step be retrieved. Hence, either could all piles be modelled to be installed in the same phase or a pile order be chosen. The latter was done in the Thesis, where the chosen pile installation occurred in three calculation phases. The number of piles, pile rows and prescribe line displacement can, among other things, be seen in *Table 5.2*. The calculation phases for the pile installation was assumed to occur directly after each other, without any intermediate consolidation. Each pile installation phase was set to one day in PLAXIS. The length of the piles installed differed between *Model 1*, *Model 2* and *Model 3*. For *Model 1* was the superpile constructed below the excavation bottom with a length of 60 metres, down to the level -72 metres in the model. The prescribed line displacement were then activated on the whole length of the superpile. For *Model 2*, was the superpile constructed from level ±0 metre in the model, with a length of 72 metres. The prescribed line displacement was activated on the whole length of the superpile. For *Model 3* was the superpile constructed from level ±0 metre in the model, with a length of 72 metres as in *Model 2*. The prescribed line displacement were then activated for the lower 60 metres. Thus, only under the excavation bottom, simulating pile installation with pre-auger or pile-block.

Table 5.2: *Prescribed line displacement for Västlänken Station Centralen.*

Phase	Number of piles	Pile rows	w_{sp} [mm]	a_{sp}/a_{pa}	Prescribed line displacement [mm]
1	60	4	1.1	0.0825	22.2379
2	60	4	1.1	0.0825	22.2379
3	60	4	1.1	0.0825	22.2379

5.2 *Västlänken* - Result and analysis

The maximum vertical mass displacement directly after the last pile installation phase, differed for the three models. For *Model 1* was the maximum vertical mass displacement approximate 16.5 centimetres, see *Figure 5.4*. The maximum vertical mass displacement for *Model 2* and *Model 3* was approximate seven centimetres, where the latter had an eight millimetres lower vertical mass displacement. An accuracy which is not plausible to obtain. The result for *Model 2* and *Model 3* can be seen in *Appendix C Figure C.1* and *Figure C.2* respectively. For all models did the maximum vertical mass displacement occurs within the support structures, either on the excavation bottom, as for *Model 1*, or at level ±0 metre in *Model 2* and *Model 3*. Directly after the excavation was carried out for *Model 2* and *Model 3* was an increase of approximate seven centimetres observed for the maximal vertical mass displacement. Which was linked to the bottom heave occurring in the excavation when the soil was removed.

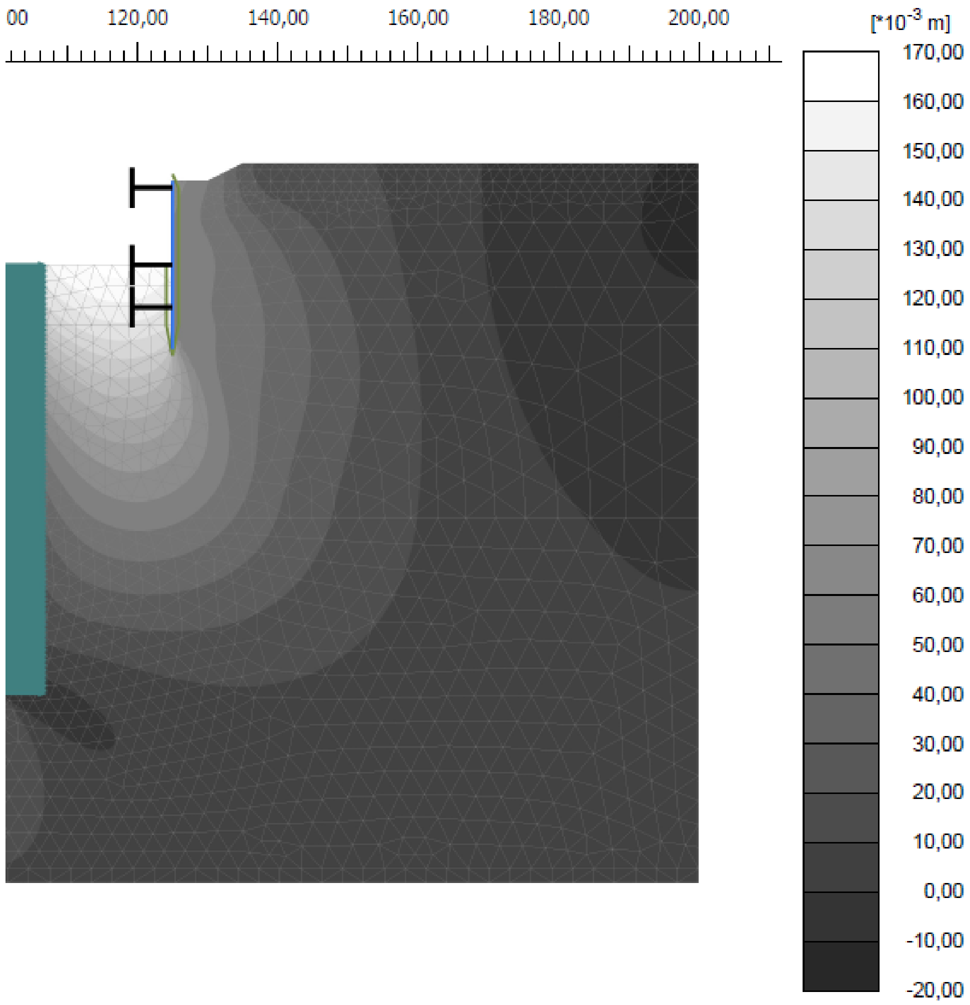

Figure 5.4: *Vertical mass displacement directly after the last pile installation phase for Västlänken, Model 1.*

The maximum vertical mass displacement, during the pile installation from the excavation bottom, were approximate six centimetres higher then when the pile installation occurred before the excavation. Which can be linked to that in *Model 1* was less load present within the support structures, and the fact that bottom heave of the excavation bottom already had started to occur due to the unloading.

Furthermore, the vertical mass displacement for *Model 1* were on the excavation bottom, evenly distributed between the supporting structures. Whilst, for *Model 2* and *Model 3* did the maximum vertical displacement occur adjacent to the support structures and were lower closer to the superpile, on the level ±0 metre. Which could be a consequence of that in *Model 1* were the stamps on the support structures activated, forcing the it to stay fixed and the distribution of the vertical mass displacement to occur within them. Whilst, for *Model 2* and *Model 3* is only the support structures activated, leading to that they can curve during the pile installation phases.

The distribution of the vertical mass displacement differed distinctly between *Model 1*, *Model 2* and *Model 3*. Where, *Model 2* and *Model 3* had nearly identical distributions. *Model 1* resulted in a distribution of the vertical mass displacement which faster subsided towards the boundaries in the horizontal direction. Whilst, *Model 2* and *Model 3* results in a distribution which were initial lower than the vertical mass displacement in *Model 1*, but subsided slower. Thus, for *Model 1* was the vertical mass displacement higher close to the piling area, but had a smaller impact area.

The maximum horizontal mass displacement was basically the same for all three models directly after the last pile installation phase, approximate seven centimetres. For the result from *Model 1* see *Figure 5.5*, and for *Model 2* and *Model 3* see *Appendix C, Figure C.3* and *Figure C.4* respectively. The maximum horizontal mass displacement occurred for all models adjacent to the superpile, approximate on level -50 metres. For *Model 2* and *Model 3* did the maximum horizontal mass displacement occurred between level -30 to -60 metres in the model. For *Model 1* did the maximum horizontal mass displacement occur a bit further down at the superpile and continued down to the same level, -60 metres. The distribution of horizontal mass displacement throughout the soil varied between *Model 1* and the two other models, which nearly were identical. Except for within the support structures, where *Model 2* had horizontal mass displacement up to level ±0 metre in the model. Whereas the horizontal mass displacement within the support structures at level ±0 was negligible for *Model 3*, as the prescribed line displacement only acted under the excavation bottom.

The distribution of the horizontal mass displacement differed for *Model 1*, *Model 2* and *Model 3*. The distribution for the two latter were nearly identical, where the main difference was between the support structures. For these models were the horizontal mass displacement more uniform for the superpile under the excavation bottom. Whilst for *Model 1*, were the horizontal mass displacement more unevenly distributed, where the impact area was largest at the pile toe.

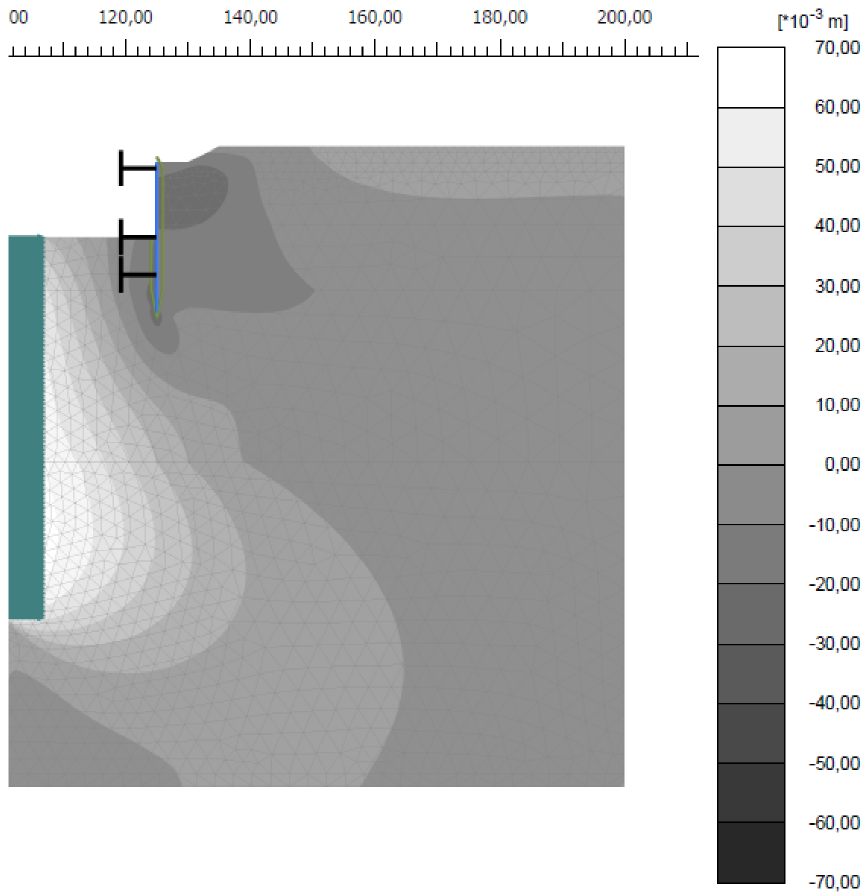

Figure 5.5: *Horizontal mass displacement directly after the last pile installation phase for Västlänken, Model 1.*

In *Model 1* did horizontal mass displacement occur towards the superpile from outside the excavation, hence negative displacement in *Figure 5.5*. This was a consequence of the support structures bending due to the large horizontal mass displacements, positive in *Figure 5.5*, occurring within the support under the excavation bottom, thus curving them. Hence, the support structures were deformed due to the mass displacement. Close to the pile toe did the horizontal mass displacement move towards the pile, which could be due to the large strains and deformed mesh created.

The excess pore pressure directly after the last pile installation phase in *Model 1* can be seen in *Figure 5.6*. Unrealistic pore pressures that occurred at the pile toe was neglected in the different models, due to the statement in *Chapter 4.3*. For the following figures is the suction defined as positive and the pressure as negative, due to how PLAXIS defines tension and pressure. Whereas, in the rest of the Thesis, figures and text, is pressure defined as positive and tension/suction as negative.

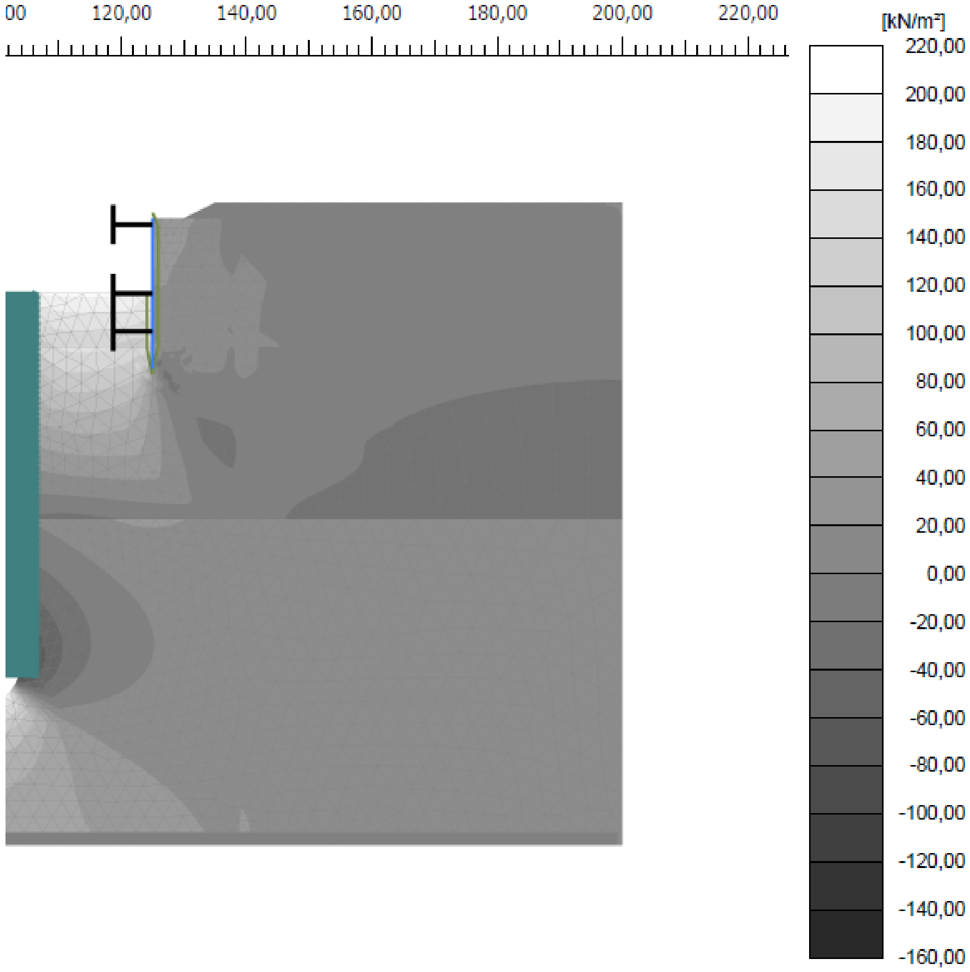

Figure 5.6: *Excess pore pressure directly after the last pile installation phase for Västlänken, Model 1.*

The largest excess pore pressures, directly after the last pile installation phase, occurred adjacent to the superpile for all three models. However, as in *Partihallsbron*, do the excess pore pressures wander away from the superpile and could after 80 years be found at the boundaries in the horizontal direction, see *Figure 5.7*. The excess pore pressures decrease significantly due to the consolidation. Whereas, the suction decreases fairly little. The suction is largest around the pile toe and in the excavation bottom directly after the piling, and at the excavation bottom after 80 years of consolidation, for all three models.

The result for the excess pore pressure in *Model 2* directly after the pile installation can be seen in *Appendix C*, *Figure C.5*. The suction between the support structures was approximate half the magnitude of the ones in *Model 1*. The same could be observed for *Model 3*, see *Appendix C*, *Figure C.7*. The distribution of the excess pore pressure was nearly identical for *Model 2* and *Model 3* directly after the pile installation.

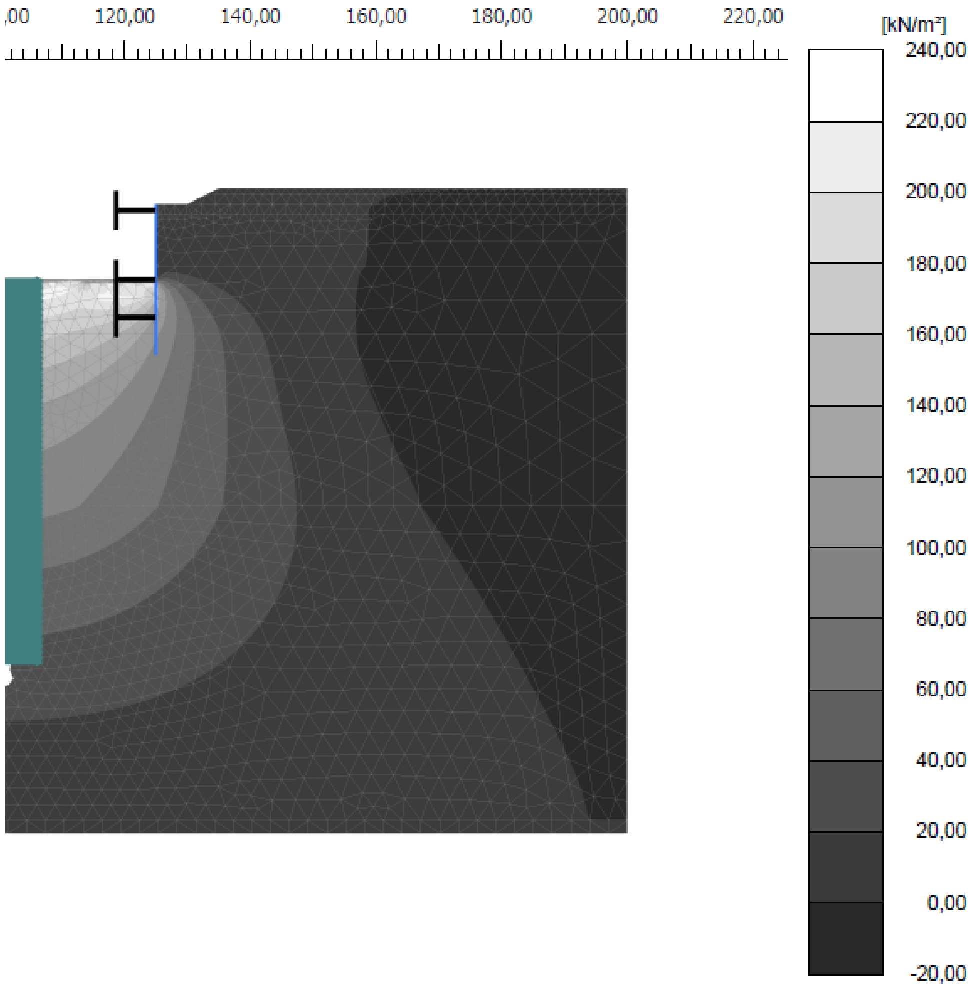

Figure 5.7: *Excess pore pressure after 80 years of consolidation for Västlänken, Model 1.*

The result for the excess pore pressure after 80 years of consolidation for *Model 2* and *Model 3* can be seen in *Appendix C, Figure C.6* and *Figure C.8* respectively.

Furthermore, the suction at the excavation bottom after 80 years of consolidation were not relevant for the real case as the excavation would not be open for that long; as a tunnel would be constructed in the excavation. Hence, as a load act on the excavation bottom and counteract the suction and bottom heave. Thereof, a line load was constructed and activated on the excavation bottom directly after the excavation phase in *Model 2*. Resulting in that the suction at the excavation bottom became close to zero after 80 years of consolidation, see *Figure 5.8*. A much more plausible outcome, and with an excess pore pressure distribution which were similar to the result for *Partihallsbron*. The maximum excess pore pressure occurred around level -30 metres in the model, at the boundaries in the horizontal direction. The magnitude of the maximum excess pore pressure after 80 years of consolidation, in *Model 2* with the line load, was approximate 2 kPa larger than the excess pore pressure in *Partihallsbron* after 80 years of consolidation, when on the level -15 metres. As the prescribed line displacements for the two projects were nearly identical could this difference be linked to the other processes occurring in *Model 2*. In the model for *Västlänken Station Centralen* was additional structures constructed and processes occurring, such as the support structures, excavation and local lowering of the groundwater table. Whilst, for *Partihallsbron*, *Scenario 1*, was only the pile installation carried out, since the the pile installation occurred from top of fill. After 16.5 years of consolidation was the excess pore pressure in the model the same as in the control year, meaning that the excess pore pressure due to the pile installation had dissipated.

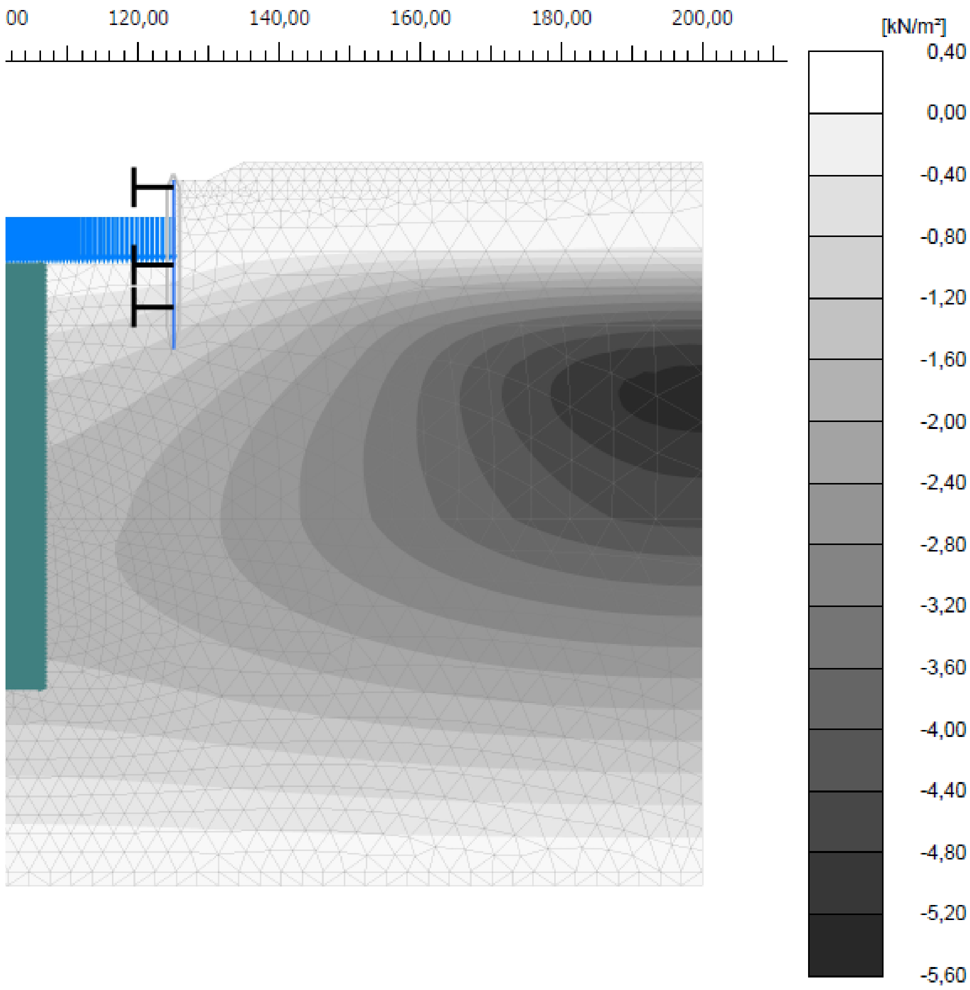

Figure 5.8: *Excess pore pressure after 80 years of consolidation with a load acting on the excavation bottom, for Västlänken, Model 2.*

The deviatoric strains for *Västlänken Station Centralen*, *Model 1*, was directly after the pile installation at most 2 percent. Thus, within the limit before the model starts to overpredict the soil strength, see *Chapter 4.3*. The maximum γ_s occurred at the bottom of the support structures. For *Model 2* and *Model 3* were the maximum γ_s 1 percent directly after the pile installation. Thus, the models did not overpredict the soil strength. Furthermore, the γ_s was generally 0.4 percent in all three models directly after the pile installation. Hence, within the range where the derived model parameters captured the soil behaviour accurate with consideration to the stress strain relationship evaluated in *Chapter 4.3*. After 80 years of consolidation was large γ_s occurring in the excavation bottom when no load was placed, this was the case for all three models. *Model 2* with the line load acting on the excavation bottom was the maximum γ_s 0.1 percent, thus within the range where the model captured the stress strain relationship evaluated in *Chapter 4.3*.

6 Conclusion and further investigations

The aim of the Thesis was to investigate the influence of installation of precast concrete displacement piles on adjacent areas, with a focus on the soil mass displacements and generation of excess pore water pressures. The main study area was Central Station in the Västlänken project. A numerical plane strain cavity expansion approach is adopted using a 2D Finite Element code with a suitable constitutive model for soft soils (soft soil and soft soil creep) that was extensively calibrated against laboratory data before being validated against field measurements. Nearby projects, i.e., a support of the *Partihallsbron* and a project on the lowering of the highway *E45* between Lilla Bommen and Marieholm were used for the validation process. In the final analyses for the Västlänken project time effects and the effect of construction sequence was studied in more detail.

The main conclusion is that it is possible to obtain reasonable short-term predictions of mass displacements from piling works using the proposed method given that the pile group can be approximated as a 2D cavity and the magnitude of the prescribed displacement on the cavity wall is derived using the newly proposed equation:

$$\text{Prescribed line displacement} = \frac{(w_{sp} * \sqrt{(\frac{a_{sp}}{a_{pa}} + 1)} - w_{sp}}{2}$$

As can be expected the modelling results are most sensitive for the stiffness of the soil, especially the unloading/reloading stiffness κ^*. At large distances, where only small changes in stress and strain are expected, the models used (SS and SSC) overpredict the mass transfer as the models are not incorporating a small-strain formulation of, in this case, κ^*. As a result for one of the validation cases the results are best matched at a distance ranging from 12 to 74 metres from the pile group (cavity), where the maximum margin of error was approximately 10 millimetres.

Unfortunately, the quality and completeness of the obtained monitoring data was insufficient to further refine the modelling approach, as for example in the *E45* case additional piling works compromise the measurement data. Furthermore, data on horizontal displacements is scarce and somewhat unreliable.

The Västlänken Central Station case study indicated that the largest magnitudes for the mass displacements would occur in a confined building pit, i.e. piling after construction of the support structures and excavation, as opposed to piling before constructing the building pit. Furthermore, the processes are faster due to a smaller affected volume with shorter drainage lengths and larger local pore pressures generated. Therefore, the pile installation should be carried out from the excavation bottom if a small impact area is sought, but large magnitudes of the vertical mass displacement are permissible close to the piling. Whereas, the magnitudes of the vertical displacement close to the piling area can be significantly reduced by smearing those out over a larger area by commencing piling works before installation of the support structures and excavation. The latter requires the use of a pile-block or pre-augering to enable trouble free excavation after pile installation.

The dissipation of excess pore pressures from construction (consolidation) and creep have a significant effect on the development of additional settlements over time. The predicted settlements nearly doubled when incorporating creep in the analyses. The creep rate was also more sensitive to the pile length, compared to the consolidation rate. It was further concluded that the long-term influence from the pile installation reached between 1 to 1.5 pile lengths from the piling area in both *Partihallsbron* and *E45* this agrees well with the distance found for the generation of excess pore pressures. The build up of excess pore pressure, due to pile installation, was largest adjacent to the pile directly after the pile installation, undrained response. During the dissipation the front of maximum excess pore pressure moved outward towards the boundaries. The excess pore pressure dissipated in 16 years for the Västlänken case and had the excess pore pressure dissipate to the same level as in the control year, 40 to 50 years for the *Partihallsbron*. This implies that the excavation will have a large influence on the dissipation rate. Only after 80 years of consolidation the maximum pore pressures reduced to those in the control year for both projects.

Finally, the mass displacement and stresses generated in the soil during pile installation will lead to deformation of adjacent constructions such as support structures (in this case a diaphragm wall). This will have an effect on additional deformations behind the wall.

Further investigations should investigate the validity of the the derived equation for the prescribed line displacement, in combination with an improved constitutive model that better captures the anisotropic and small-strain behaviour of the soil. Furthermore, it would be of interest to better evaluate the excess pore pressure with consideration to the generation and dissipation as function of the homogeneity in the soil.

Finally, in this research the reference point used to compare the predicted and measured vertical displacements was chosen at the centre of the cavity (pile group). Prior research refers to the distance of the edge of the pile group. It would, therefore, be interesting to investigate if the discrepancy between predictions and measurements in prior research is related to this arbitrary offset.

Bibliography

[Abu-Farsakh et al., 2015] Abu-Farsakh, M., Rosti, F., and Souri, A. (2015). Evaluating pile installation and subsequent thixotropic and consolidation effects on setup by numerical simulation for full-scale pile load tests. *Canadian Geotechnical Journal*, 52(11):1734–1746.

[Andersson, 2018a] Andersson, R. (2018a). E02-20-110-2000-0_0-0002.

[Andersson, 2018b] Andersson, R. (2018b). E02-20-370-2700-0_0-0003.

[Augustesen et al., 2006] Augustesen, A. H., Andersen, L., and Sørensen, C. S. (2006). *Assessment of time functions for piles driven in clay.* Citeseer.

[Bishop et al., 1945] Bishop, R. F., Hill, R., and Mott, N. F. (1945). The theory of indentation and hardness tests. *Proceedings of the Physical Society*, 57(3):147–159.

[Castro and Karstunen, 2010] Castro, J. and Karstunen, M. (2010). Numerical simulations of stone column installation. *Canadian Geotechnical Journal*, 47(10):1127–1138.

[Desai and Gioda, 1990] Desai, C. S. and Gioda, G. (1990). *Numerical methods and constitutive modelling in geomechanics*, volume 311. Springer.

[Edstam, 2011] Edstam, T. (2011). Massundanträngning i samband med pålslagning i lera. Technical report, Skanska, SBUF.

[Fellenius, 1972] Fellenius, B. H. (1972). Down-drag on piles in clay due to negative skin friction. *Canadian Geotechnical Journal*, 9(4):323–337.

[Fleming et al., 2008] Fleming, K., Weltman, A., Randolph, M., and Elson, K. (2008). *Piling engineering.* CRC press.

[Google Maps, 2018] Google Maps (2018). Kartdata ©2018 google. https://www.google.se/maps/@57.7128355,11.972913,15z. Online: accessed 2018-06-05.

[Hintze et al., 1997] Hintze, S., Liedberg, S., Massarsch, R., Hanson, M., Elvhammar, H., Lundahl, B., and Rehnman, S.-E. (1997). *Omgivningspåverkan vid pål- och spontslagning.* Pålkommissionen.

[Karstunen and Amavasai, 2017] Karstunen, M. and Amavasai, A. (2017). Best soil: Soft soil modelling and parameter determination. Technical report, Chalmers University of Technology, Department of Architecture and Civil Engineering.

[Knappett and Craig, 2012] Knappett, J. A. and Craig, R. F. (2012). *Craig's Soil Mechanics.* Spon Press, Abingdon, Oxon, United Kingdom.

[Lade, 2005] Lade, P. V. (2005). Overview of constitutive models for soils. In *Soil constitutive models: Evaluation, selection, and calibration*, pages 1–34. ASCE.

[Massarsch and Wersäll, 2013] Massarsch, K. R. and Wersäll, C. (2013). Cumulative lateral soil displacement due to pile driving in soft clay. In *Sound Geotechnical Research to Practice: Honoring Robert D. Holtz II*, pages 462–479. ASCE.

[Olsson and Holm, 1993] Olsson, C. and Holm, G. (1993). *Pålgrundläggning*. Svensk byggtjänst.

[Olsson, 2013] Olsson, M. (2013). *On rate-dependency of Gothenburg clay*. Chalmers University of Technology Gothenburg.

[Ottolini et al., 2014] Ottolini, M., Dijkstra, J., and van Tol, F. (2014). Immediate and long-term installation effects adjacent to an open-ended pile in a layered clay. *Canadian Geotechnical Journal*, 52(7):982–991.

[Ottosen and Petersson, 1992] Ottosen, N. S. and Petersson, H. (1992). *Introduction to the finite element method*. Prentice-Hall.

[PLAXIS, 2017a] PLAXIS (2017a). Material models manual.

[PLAXIS, 2017b] PLAXIS (2017b). Plaxis 2D reference manual.

[PLAXIS, 2018a] PLAXIS (2018a). Plaxis 2D reference manual 2018.

[PLAXIS, 2018b] PLAXIS (2018b). PLAXIS 2D Tutorial Manual.

[Ramböll AB et al., 2015] Ramböll AB, EGA Architects, and Lijewall Arkitekter (2015). Förstudie gullbergsvass.

[Randolph et al., 2011] Randolph, M., Gourvenec, S., White, D., and Cassidy, M. (2011). *Offshore geotechnical engineering*, volume 2. Spon Press New York.

[Sabattini and Wallgren, 2018] Sabattini, M. and Wallgren, J. (2018). Trehundratusen meter pålar i diket. In *Grundläggningsdagen 15 Mars 2018*, pages 249–251. Svenska Geotekniska Föreningen.

[Sagaseta and Whittle, 2001] Sagaseta, C. and Whittle, A. J. (2001). Prediction of ground movements due to pile driving in clay. *Journal of Geotechnical and Geoenvironmental Engineering*, 127(1):55–66.

[Trafikverket, 2014] Trafikverket (2014). Så här ska västlänken byggas. https://www.trafikverket.se/nara-dig/Vastra-gotaland/projekt-i-vastra-gotalands-lan/Vastlanken—smidigare-pendling-och-effektivare-trafik/Nyheter/2014/2014-04/Sa-har-ska-Vastlanken-byggas/. Online: accessed 2018-03-05.

[Trafikverket, 2018] Trafikverket (2018). Projekt E45, Lilla Bommen - Marieholm.

[Västsvenska paketet, nda] Västsvenska paketet (n.da). Paketet. http://www.vastsvenskapaketet.se/paketet/. Online: accessed 2018-03-05.

[Västsvenska paketet, ndb] Västsvenska paketet (n.db). Västlänken. http://www.vastsvenskapaketet.se/projekt/vastlanken/. Online: accessed 2018-03-05.

[Västsvenska paketet, ndc] Västsvenska paketet (n.dc). Centralenområdet. http://www.vastsvenskapaketet.se/projekt/centralenomradet-hjartat-i-goteborg-och-regionen/. Online: accessed 2018-03-05.

[Viggiani et al., 2014] Viggiani, C., Mandolini, A., and Russo, G. (2014). *Piles and pile foundations*. CRC Press.

[Wood, 2014] Wood, T. (2014). Phase 3 – Site Characterization and Sensitivity Analysis RegionCity. Technical report, Chalmers University of Technology.

[Wood, 2017] Wood, T. (2017). E02 – 15 – 013 – 2000 – 0_0 – 0001 – 6.6.5 TB Bilaga 4 Design Base - Geoteknik. Technical report, NCC.

[Yu, 2013] Yu, H.-S. (2013). *Cavity expansion methods in geomechanics*. Springer Science & Business Media.

A

Derived model parameters

Table A.1: *Model parameters derived and used in the modelling of fill and moraine.*

Mohr Coulomb model with drained conditions				
Parameter	**Friction fill**	**Dredged fill**	**Moraine**	**Unit**
γ_{unsat}	18	17	18	kN/m^3
γ_{sat}	21	21	18	kN/m^3
e_{init}	0.5	0.5	0.5	-
E'	$4.5e^4$	$2.0e^4$	$1.2e^4$	kN/m^2
G	17580	7692	5000	kN/m^2
E'_{oed}	57530	26920	$1.33e^4$	kN/m^2
c_{ref}	3	3	0	-
ϕ'	38	35	32	°
ψ	5	2	0	°
v'	0.28	0.3	0.2	-
$k_x = k_y$	0.6	0.6	7.65	m/day
R_{inter}	1	1	1	-

Table A.2: *Model parameters derived and used in the modelling of the clay.*

Soft Soil model and Soft Soil creep model with undrained conditions						
Parameter	**Layer 1**	**Layer 2**	**Layer 3**	**Layer 4**	**Layer 5**	**Unit**
γ_{unsat}	16.5	15.5	16.3	16.4	16.9	kN/m^3
γ_{sat}	16.5	15.5	16.3	16.4	16.9	kN/m^3
e_{init}	0.5	0.5	0.5	0.5	0.5	-
λ^*	0.21085	0.213	0.2225	0.337	0.361	-
κ_1^*	0.005865	0.006172	**0.00679**	0.011	0.0201	-
κ_2^*	0.005865	0.006172	**0.01679**	0.011	0.0201	-
μ^*	0.0032	0.003	0.003	0.0021	0.0034	-
c'	1	1	1	1	1	-
ϕ'	32	32	32	30.5	30.5	°
ψ	0	0	0	0	0	°
v'_{ur}	0.15	0.15	0.15	0.15	0.15	-
$k_{0,nc}$	0.53	0.53	0.53	0.53	0.53	-
$k_x = k_y$	0.01	0.00035	$4e^{-5}$	$5e^{-5}$	$2e^{-5}$	m/day
OCR	2	1.37	1.32	1.14	1.25	-
R_{inter}	1	1	1	1	1	-

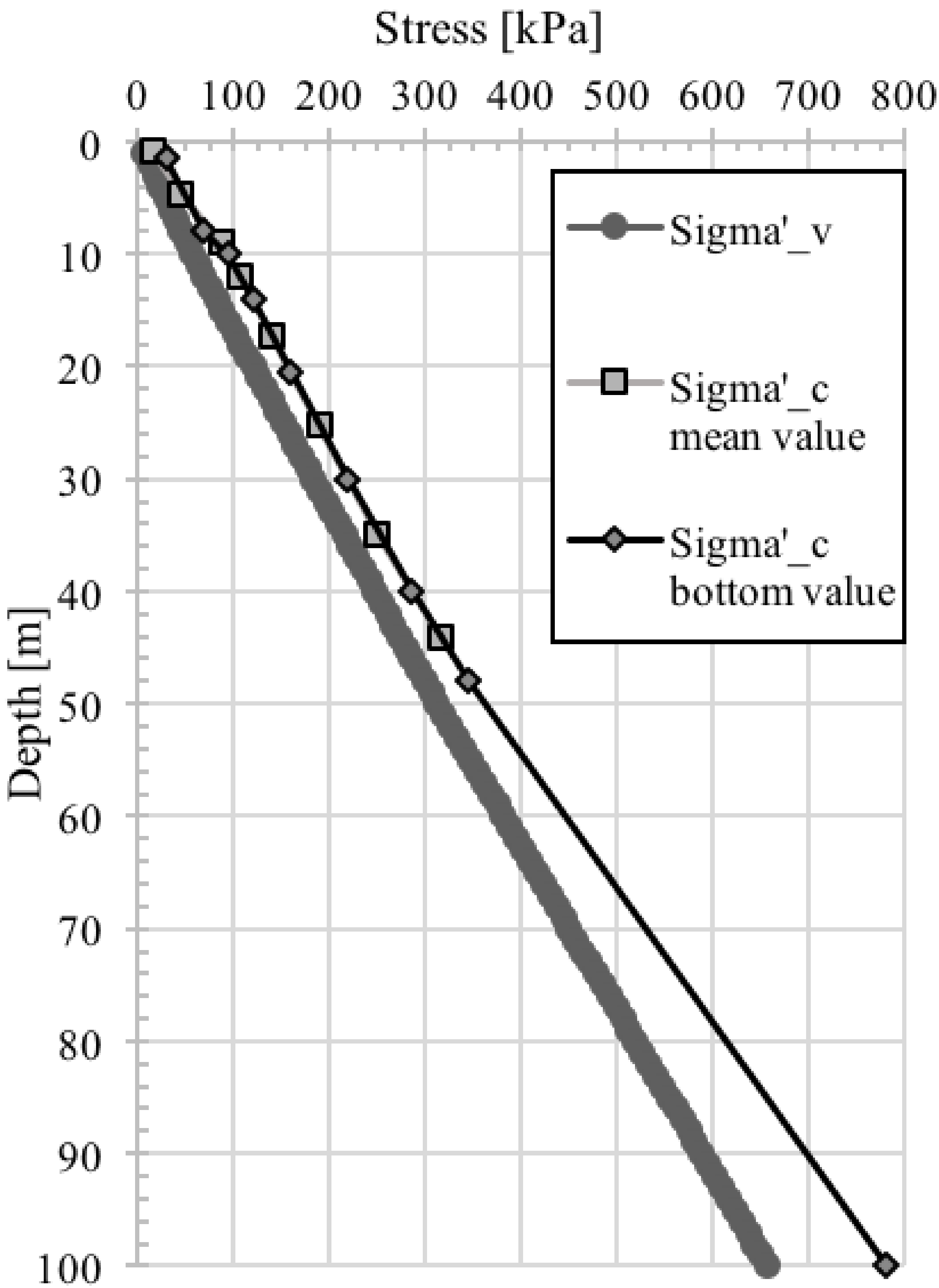

Figure A.1: *Plot of effective vertical stress and pre-consolidation pressure.*

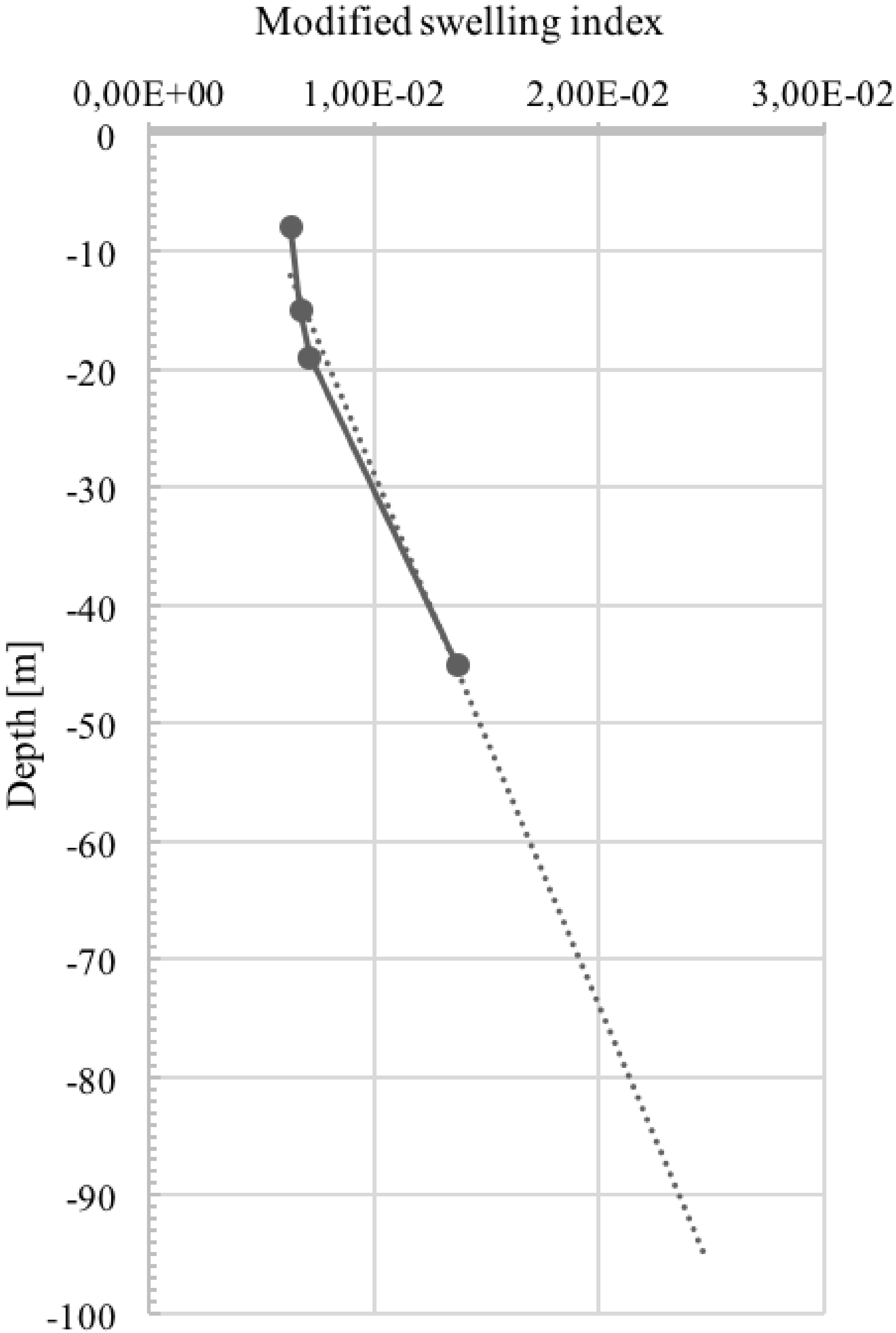

Figure A.2: *Interpolation of κ^* from IL Oedometer test samples on the depths 8, 15, 19 and 45 metres.*

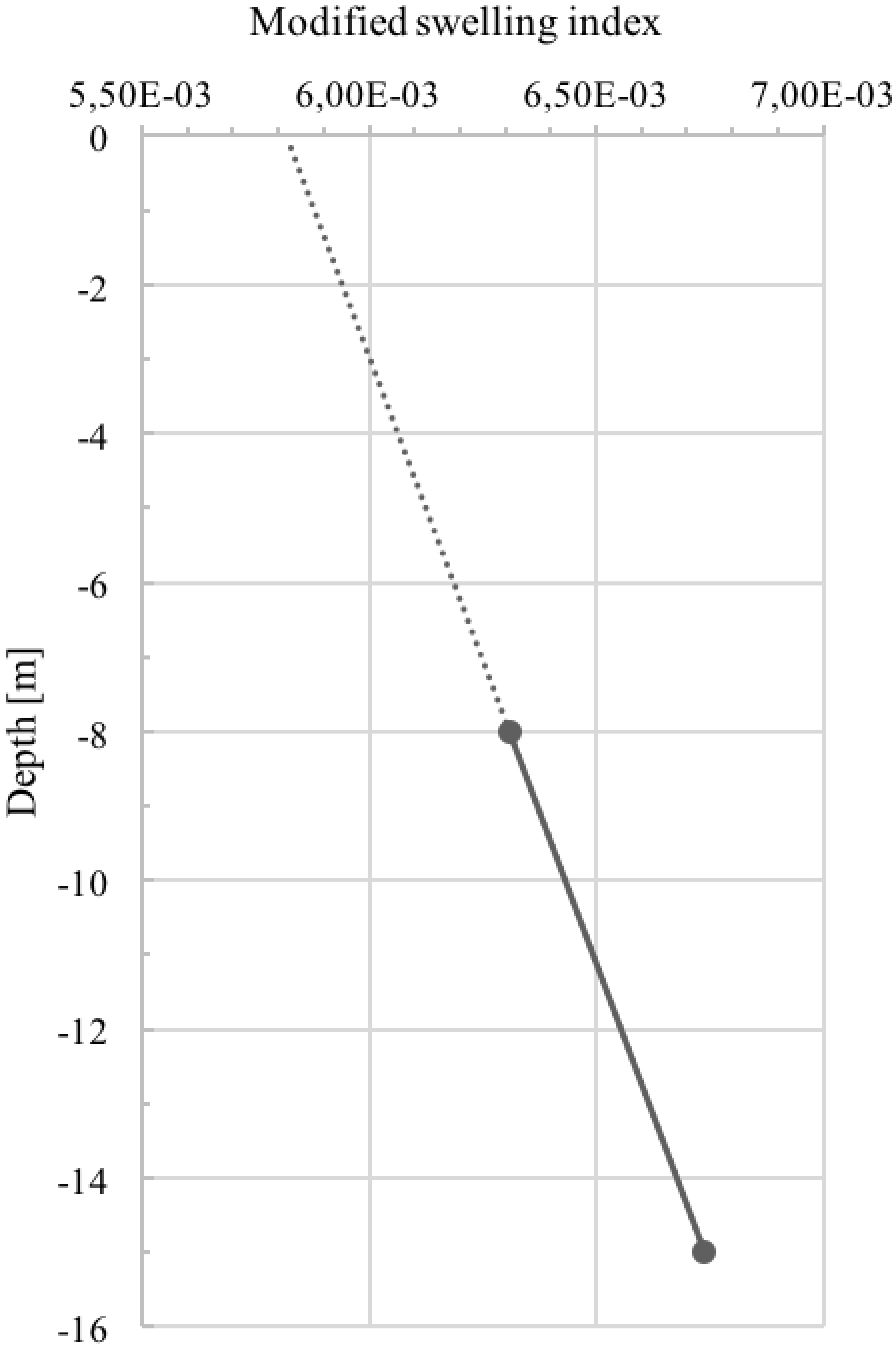

Figure A.3: *Interpolation of κ^* from IL Oedometer test samples on the depths 8, 15, 19 and 45 metres, for the first 10 metres.*

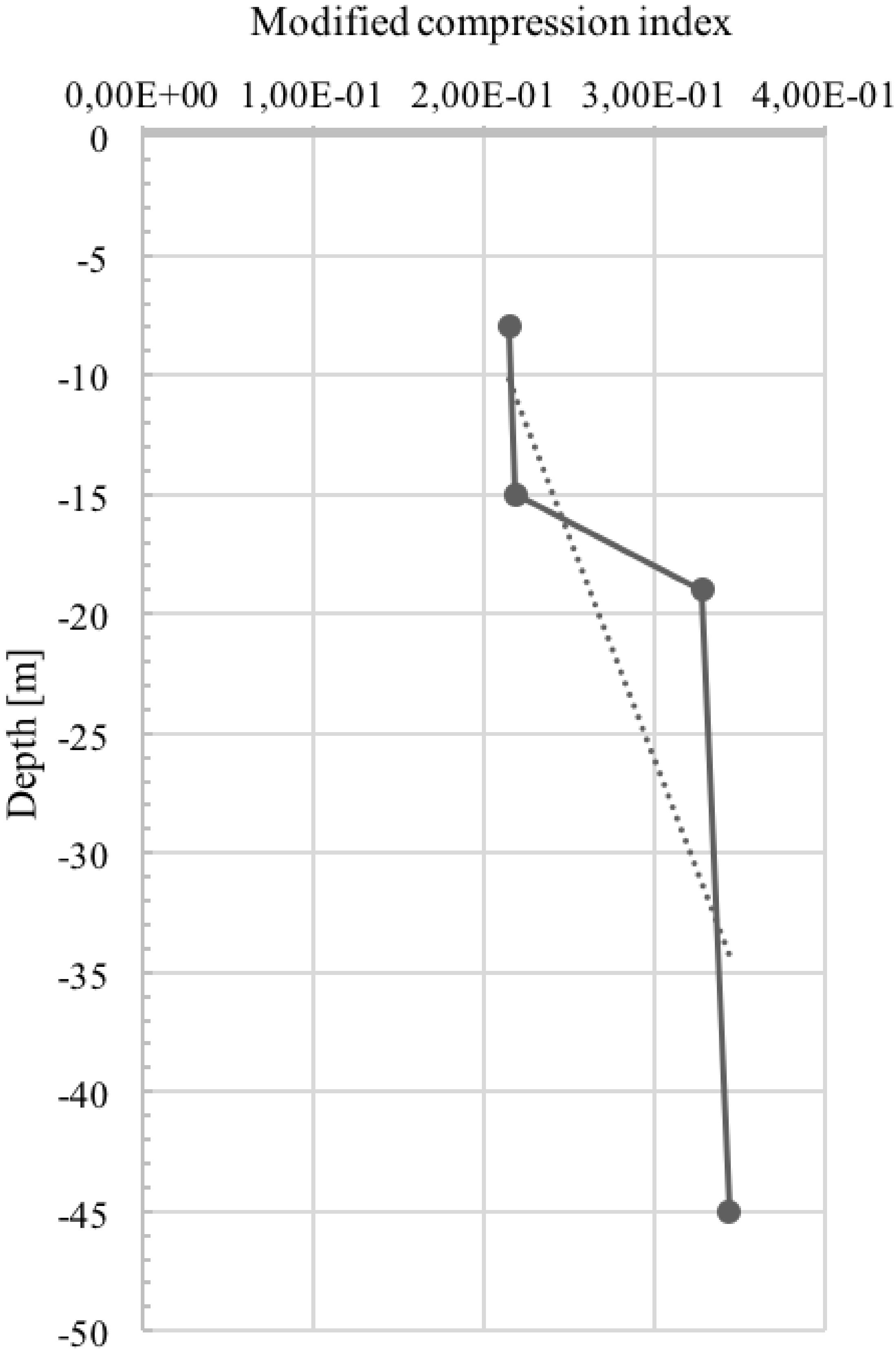

Figure A.4: *Interpolation of λ^* from IL Oedometer test samples on the depths 8, 15, 19 and 45 metres*

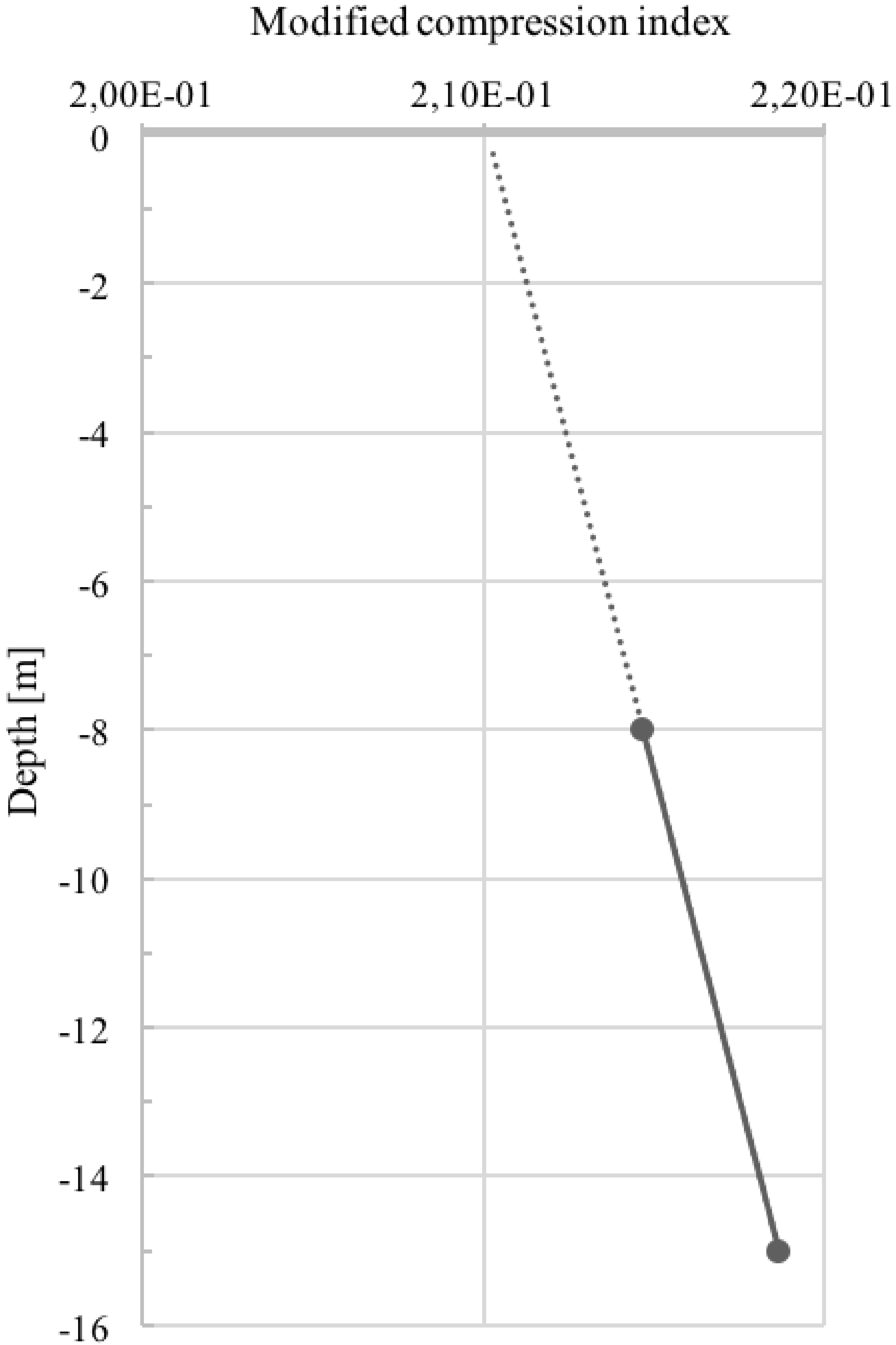

Figure A.5: *Interpolation of λ^* from IL Oedometer test samples on the depths 8, 15, 19 and 45 metres, for the first 10 metres.*

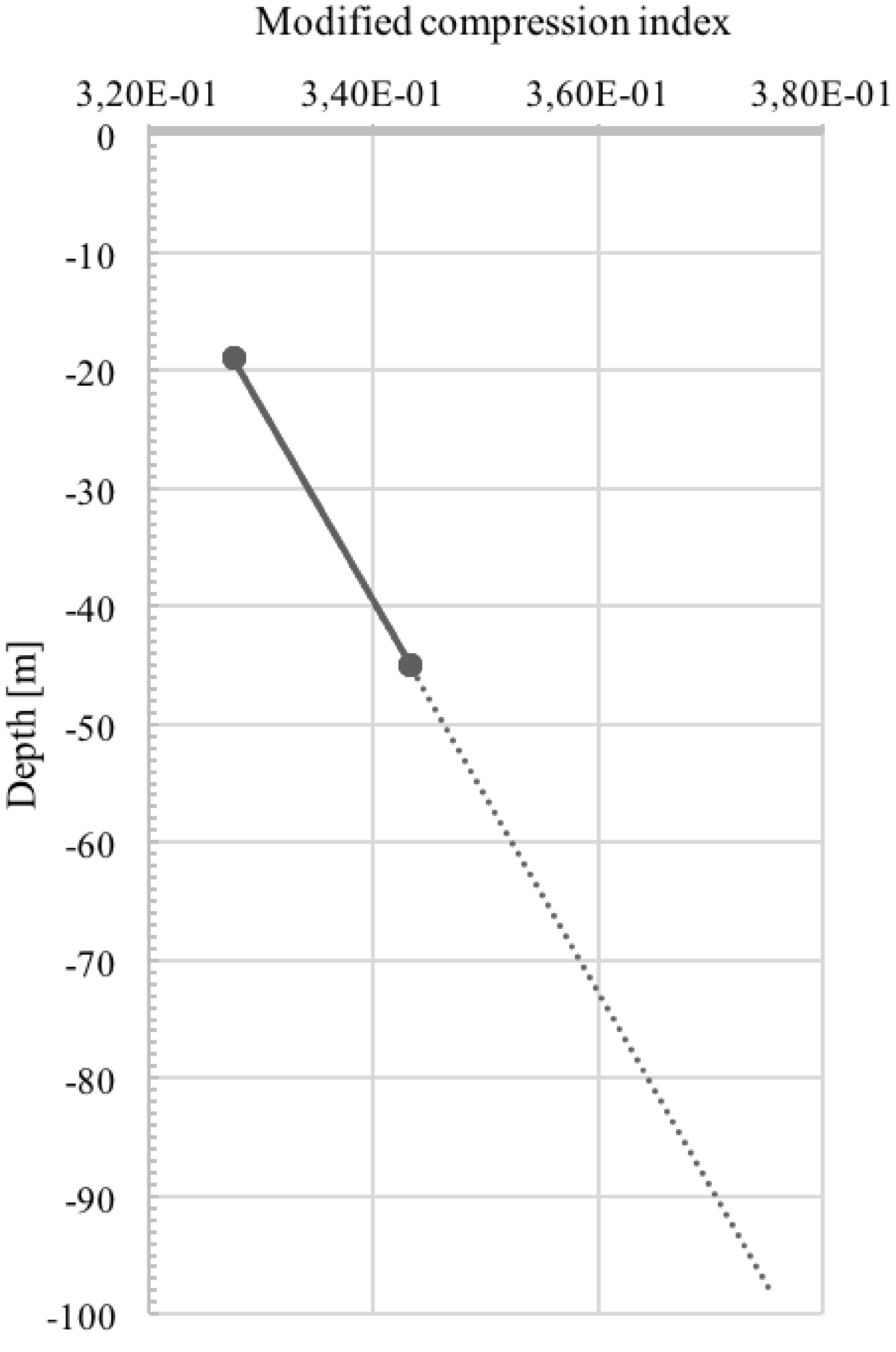

Figure A.6: *Interpolation of λ^* from IL Oedometer test samples on the depths 8, 15, 19 and 45 metres, for the last 79.5 metres.*

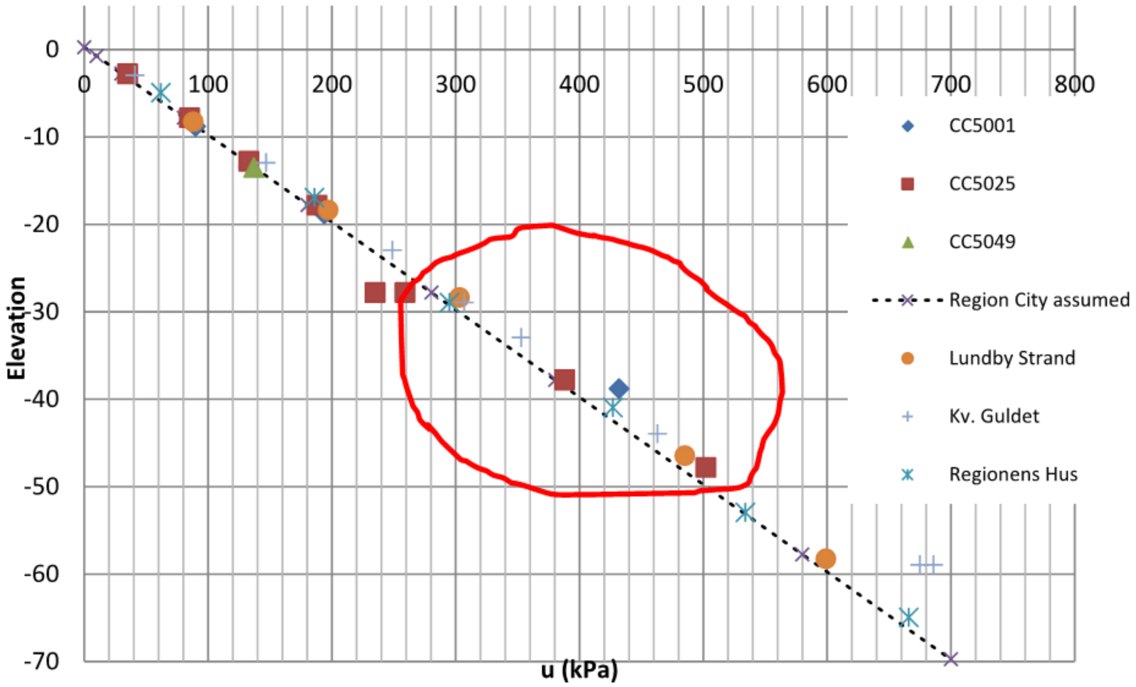

Figure A.7: *Pore pressure distribution in the area around Gothenburg Central Station.*

B

Validation of model and modelling technique

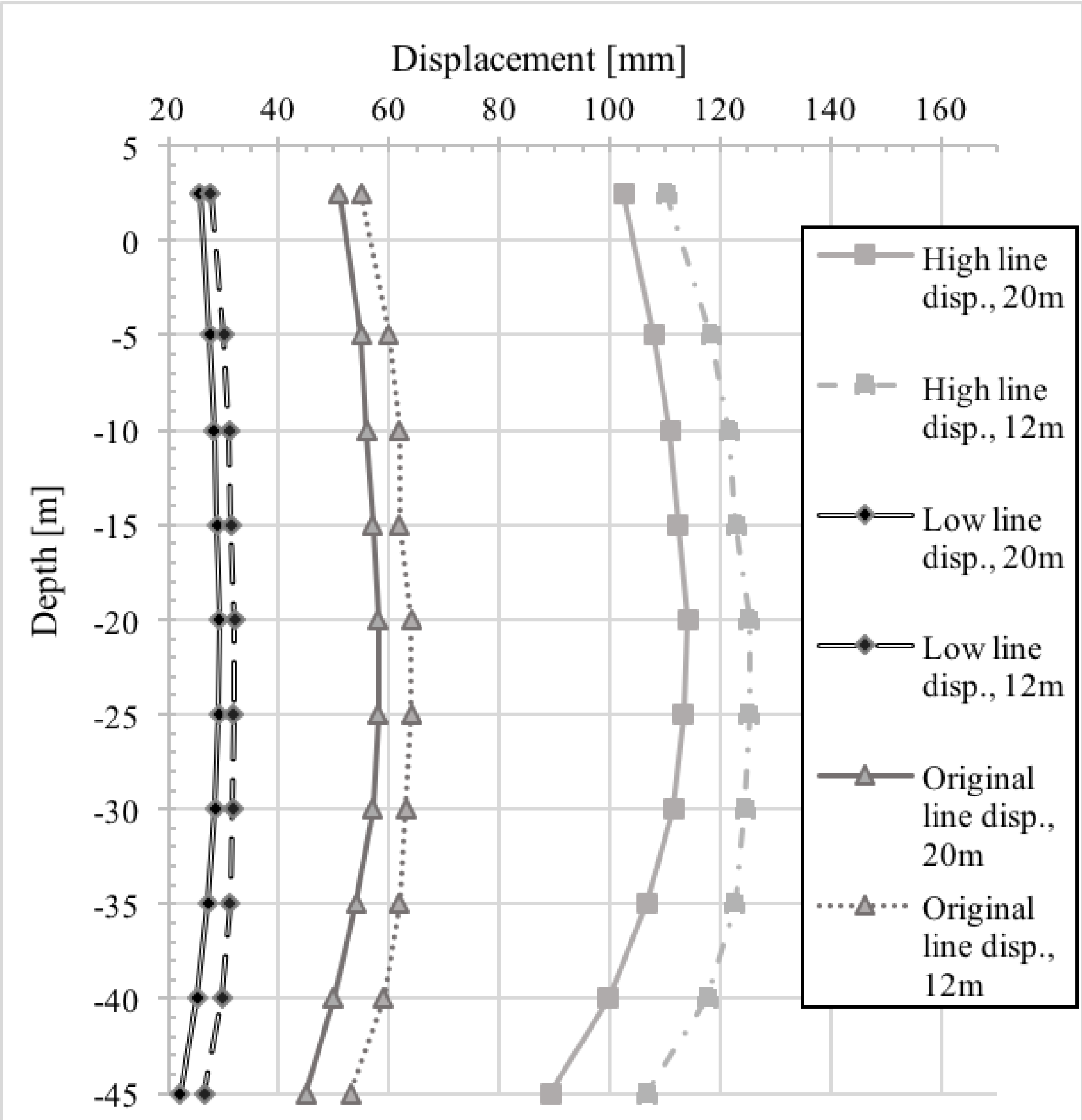

Figure B.1: *Evaluation of the prescribed line displacements influence on the horizontal mass displacement, in the project Partihallsbron, Scenario 1.*

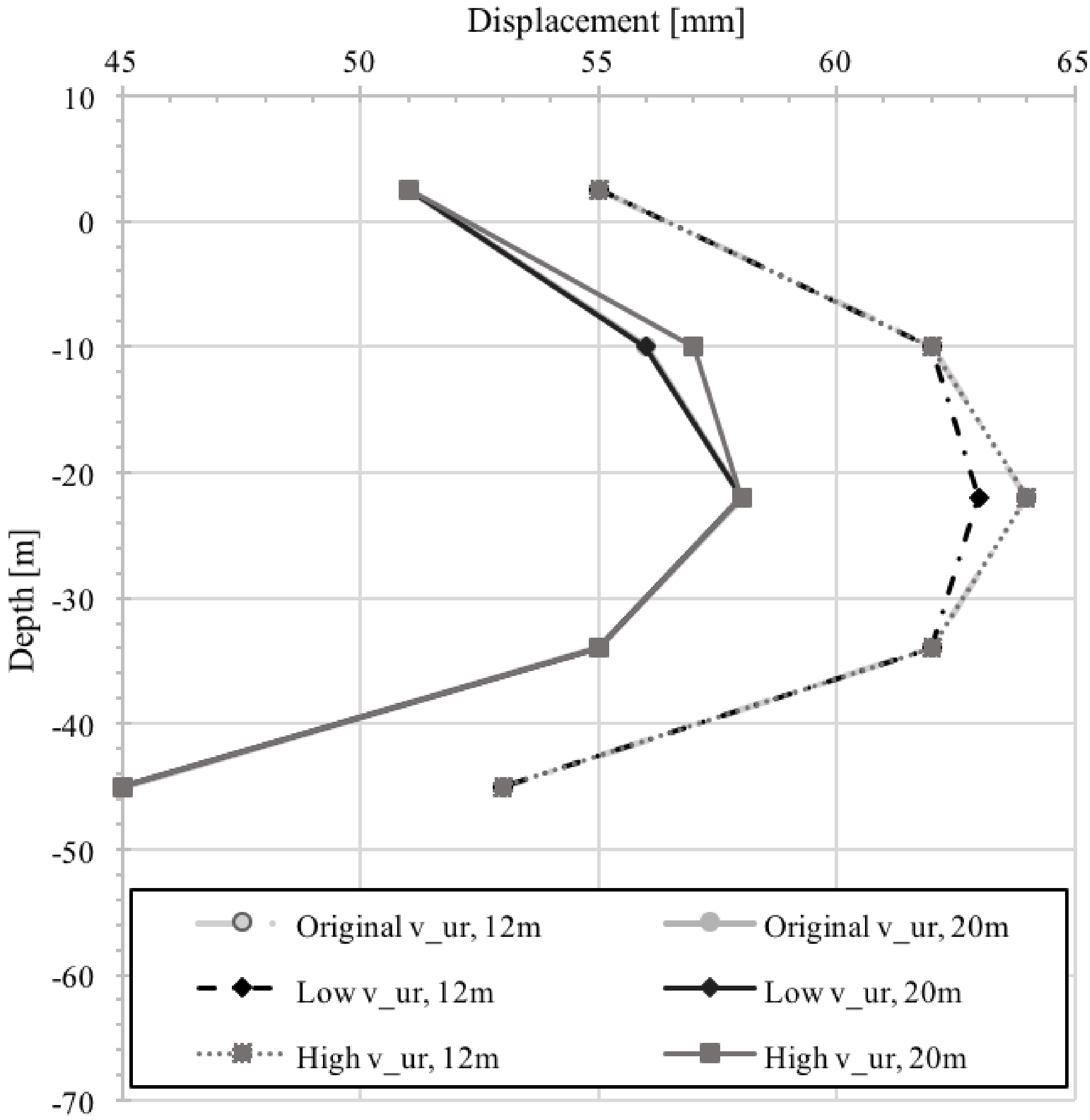

Figure B.2: *Parameter evaluation of v_{ur} on the horizontal mass displacement in the project Partihallsbron, Scenario 1.*

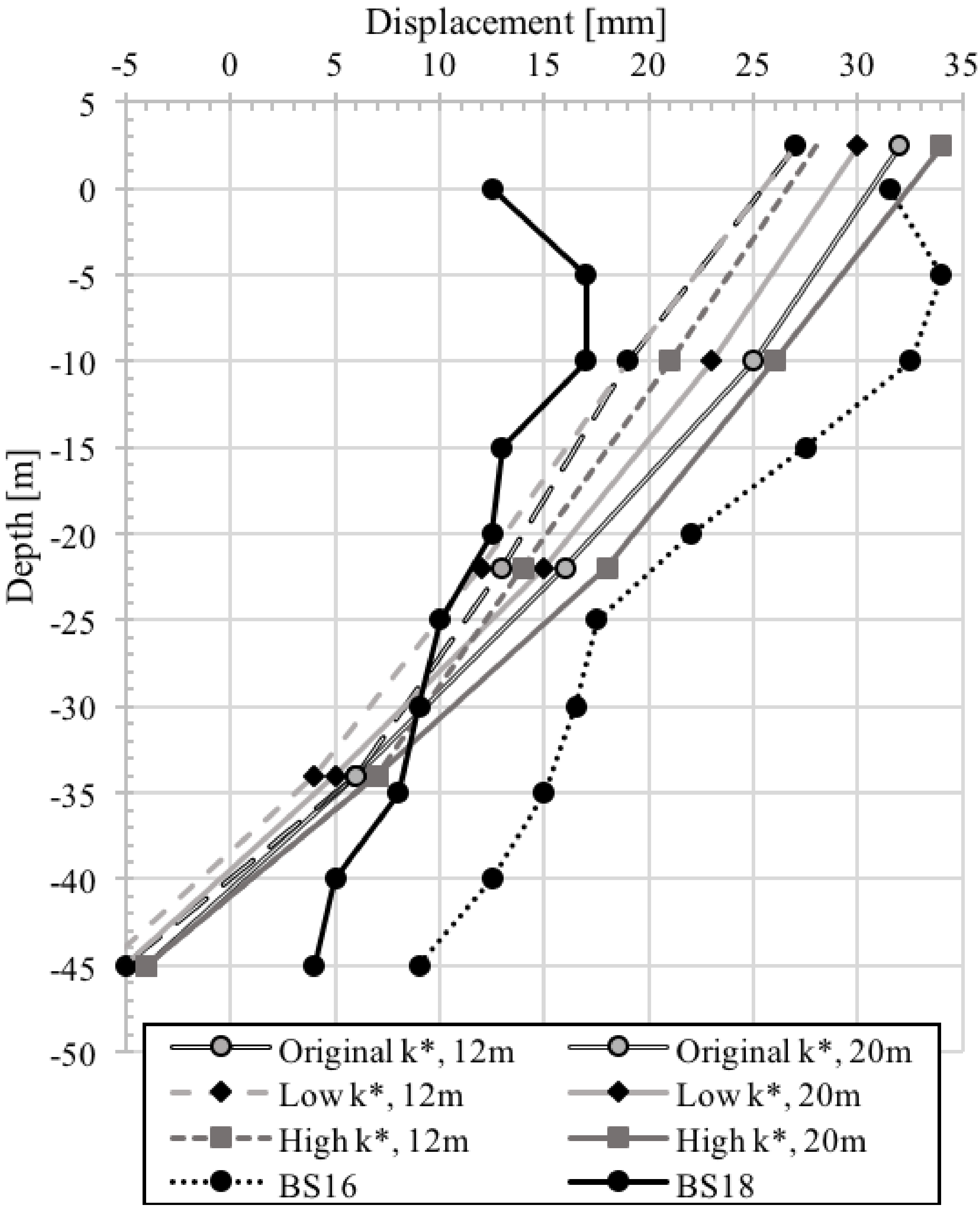

Figure B.3: *Parameter evaluation of κ^* on the vertical mass displacement in the project Partihallsbron, Scenario 1.*

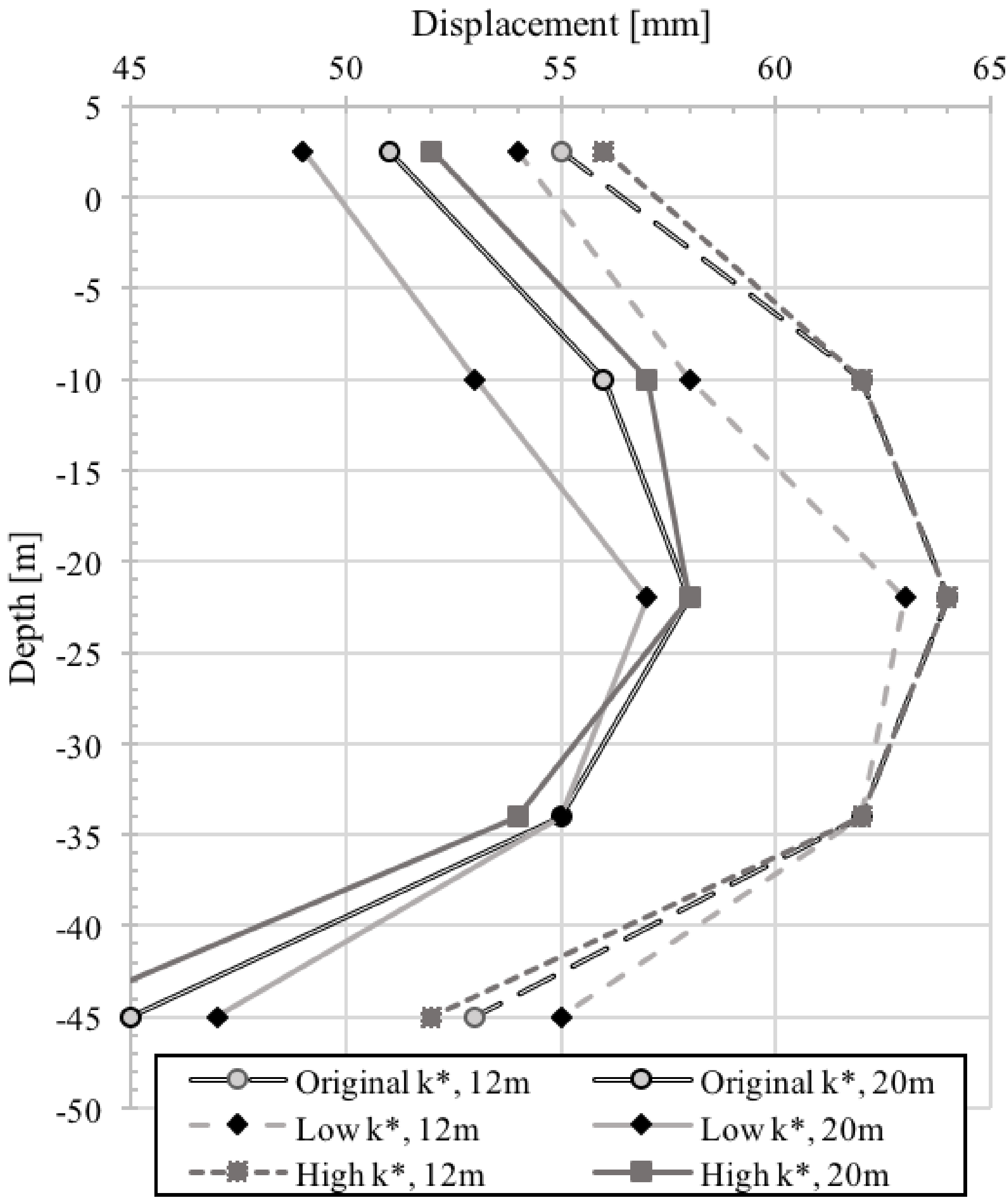

Figure B.4: *Parameter evaluation of κ^* on the horizontal mass displacement in the project Partihallsbron, Scenario 1.*

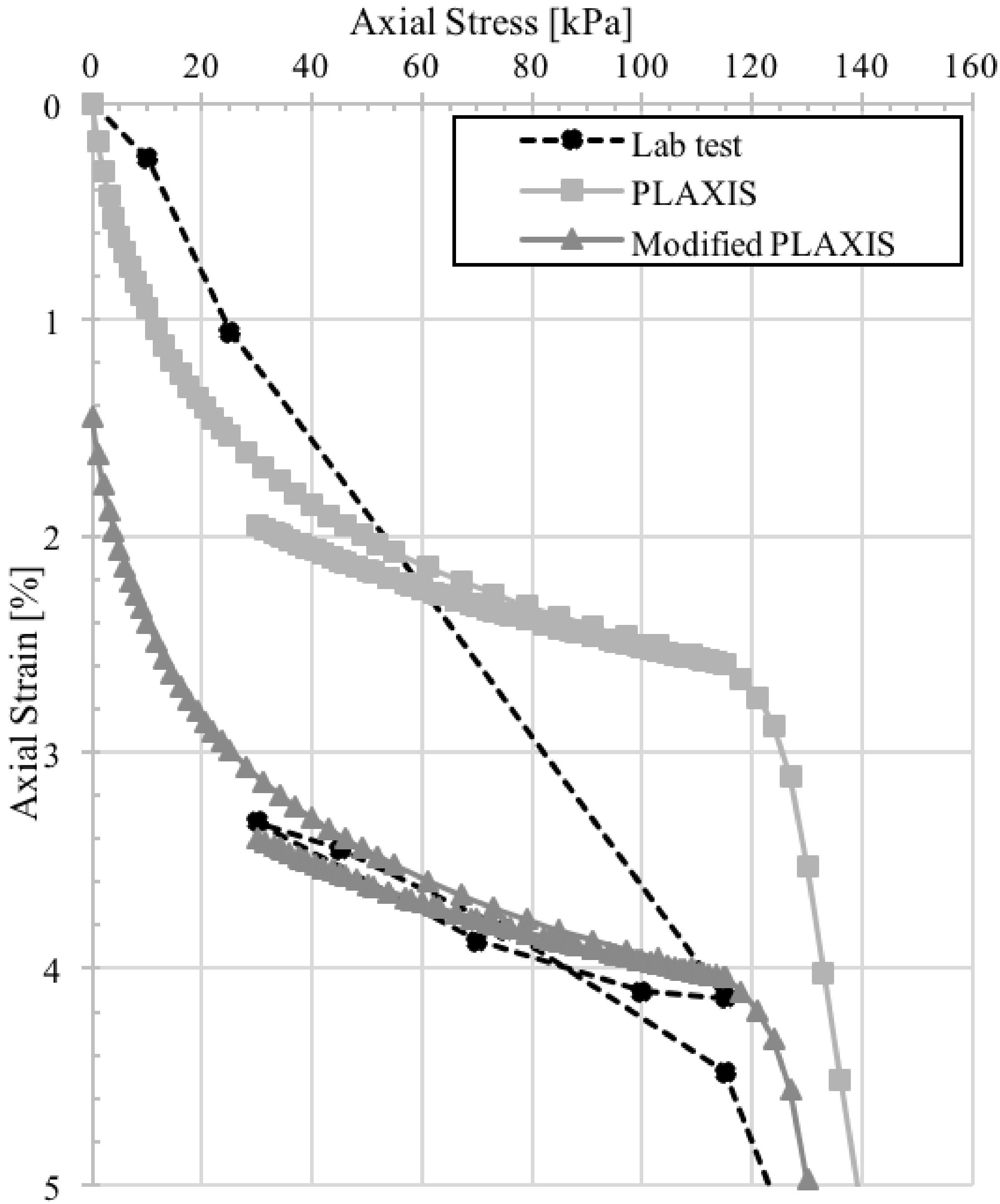

Figure B.5: *Result from IL Oedometer test performed on a sample from 15 metres depth in laboratory and simulated in PLAXIS SoilTest.*

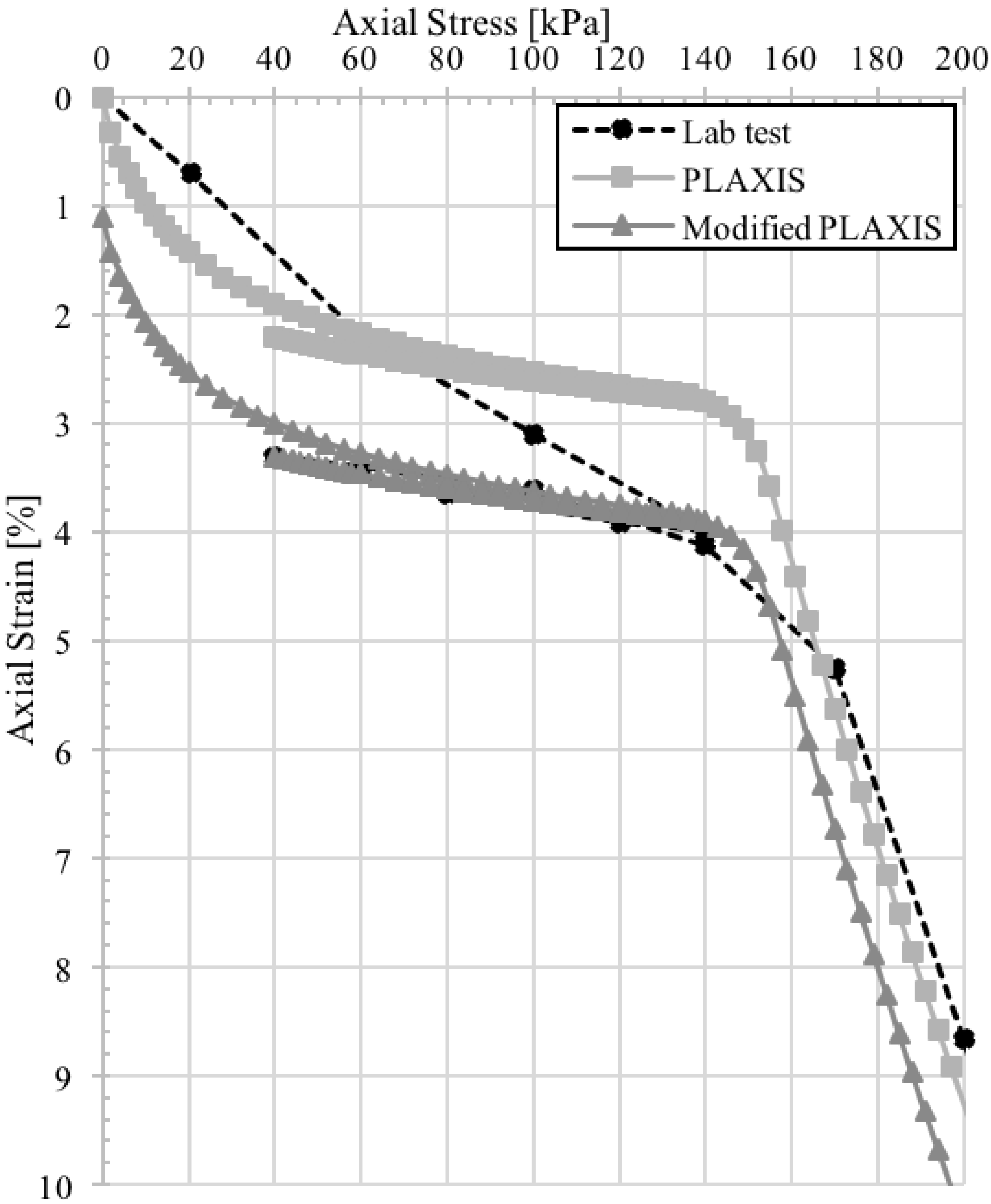

Figure B.6: *Result from IL Oedometer test performed in laboratory on a sample from 19 metres depth and simulated in PLAXIS SoilTest.*

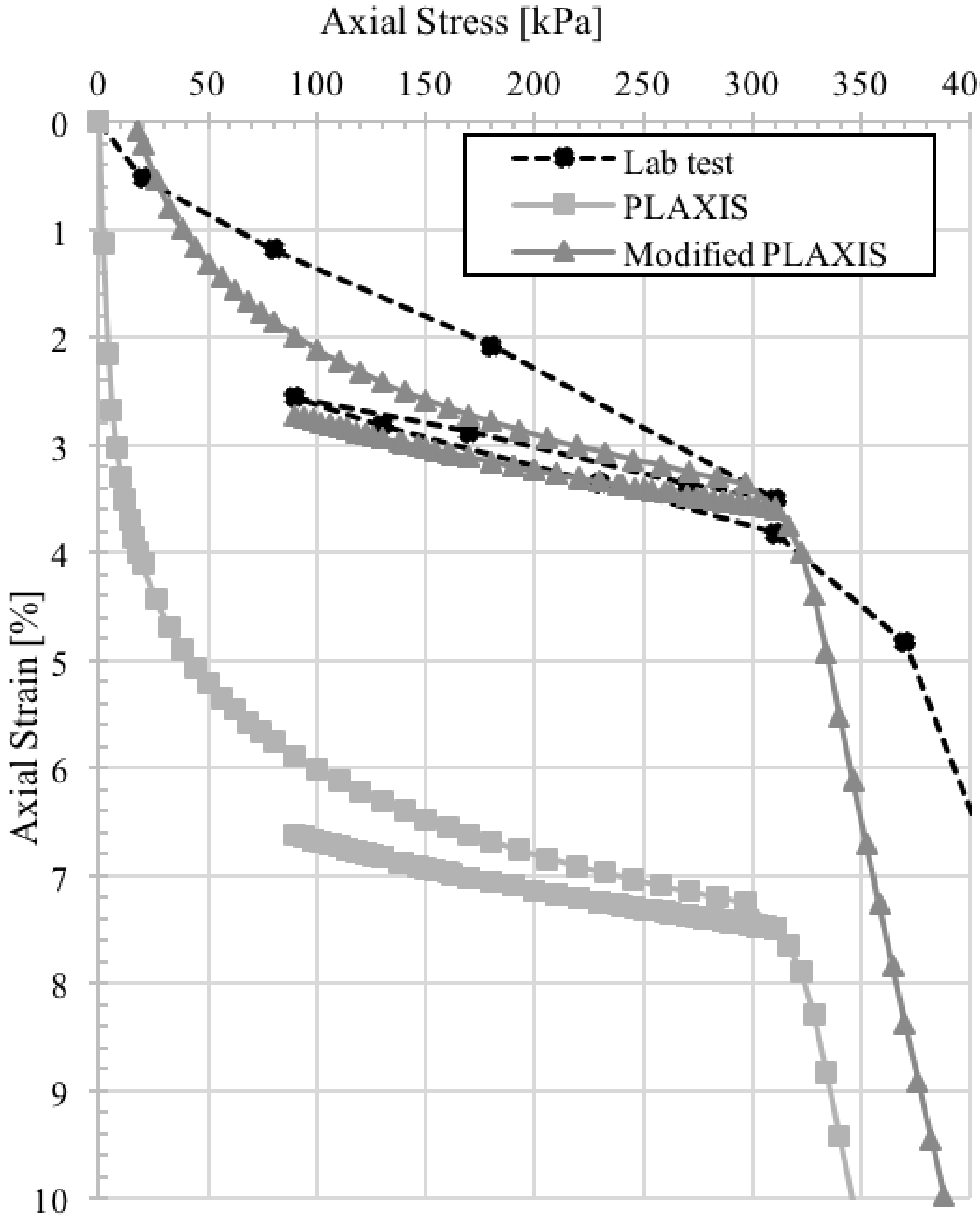

Figure B.7: *Result from IL Oedometer test performed on a sample from 45 metres depth in laboratory and simulated in PLAXIS SoilTest.*

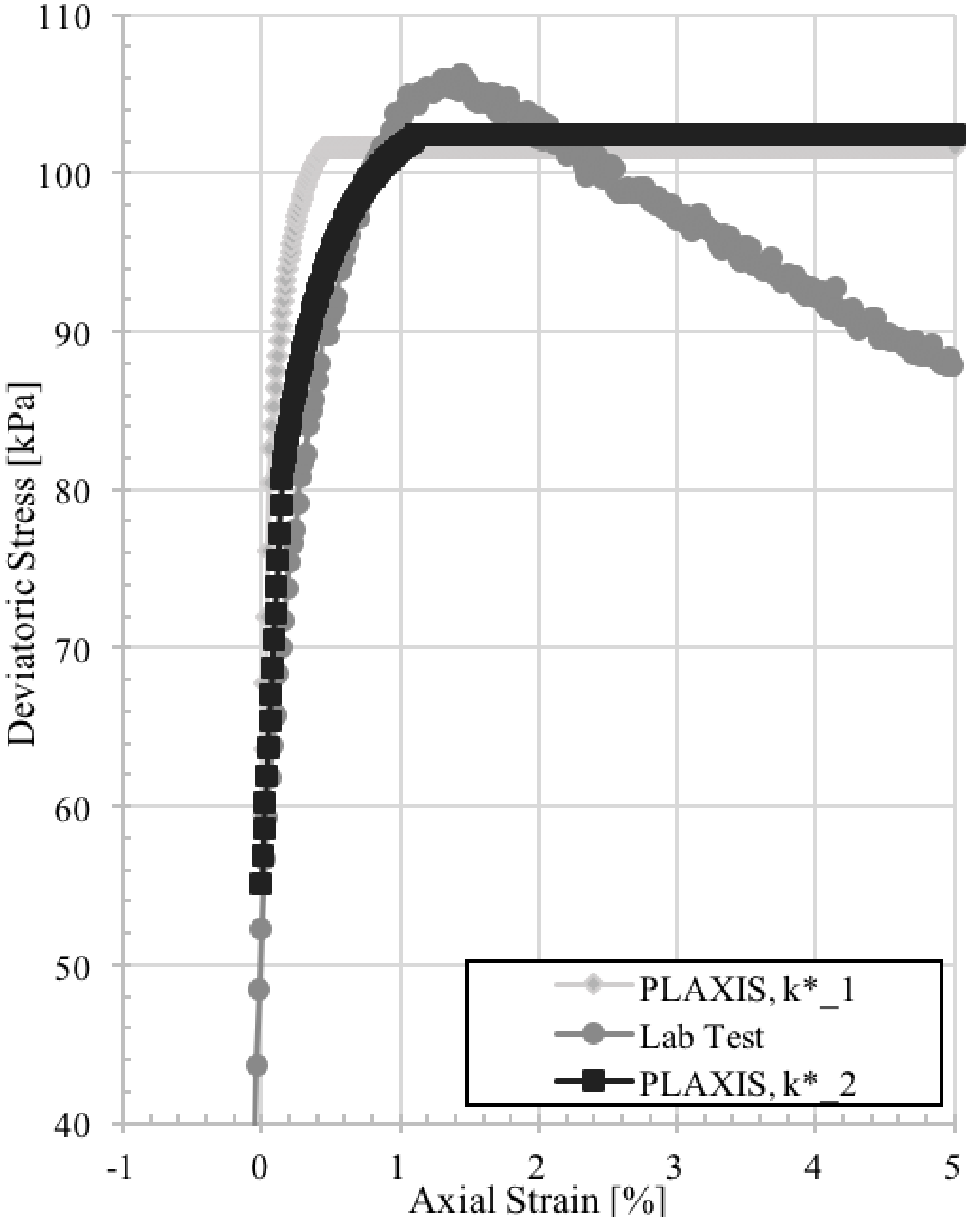

Figure B.8: *Result from Triaxial compression test performed in laboratory and simulated in PLAXIS SoilTest. With both κ_1^* and κ_2^*.*

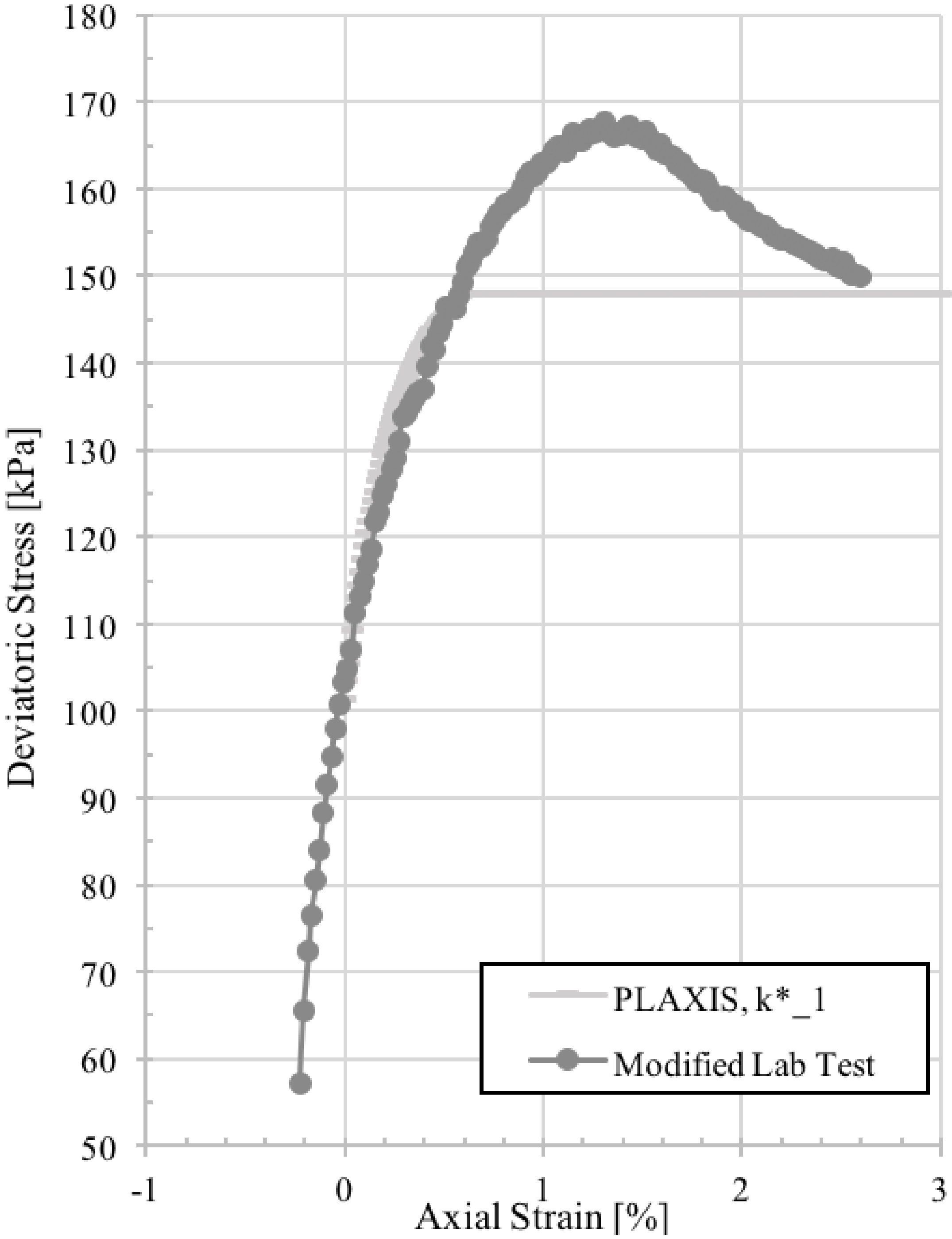

Figure B.9: *Result from Triaxial compression test performed in laboratory and simulated in PLAXIS SoilTest, with only κ_1^*.*

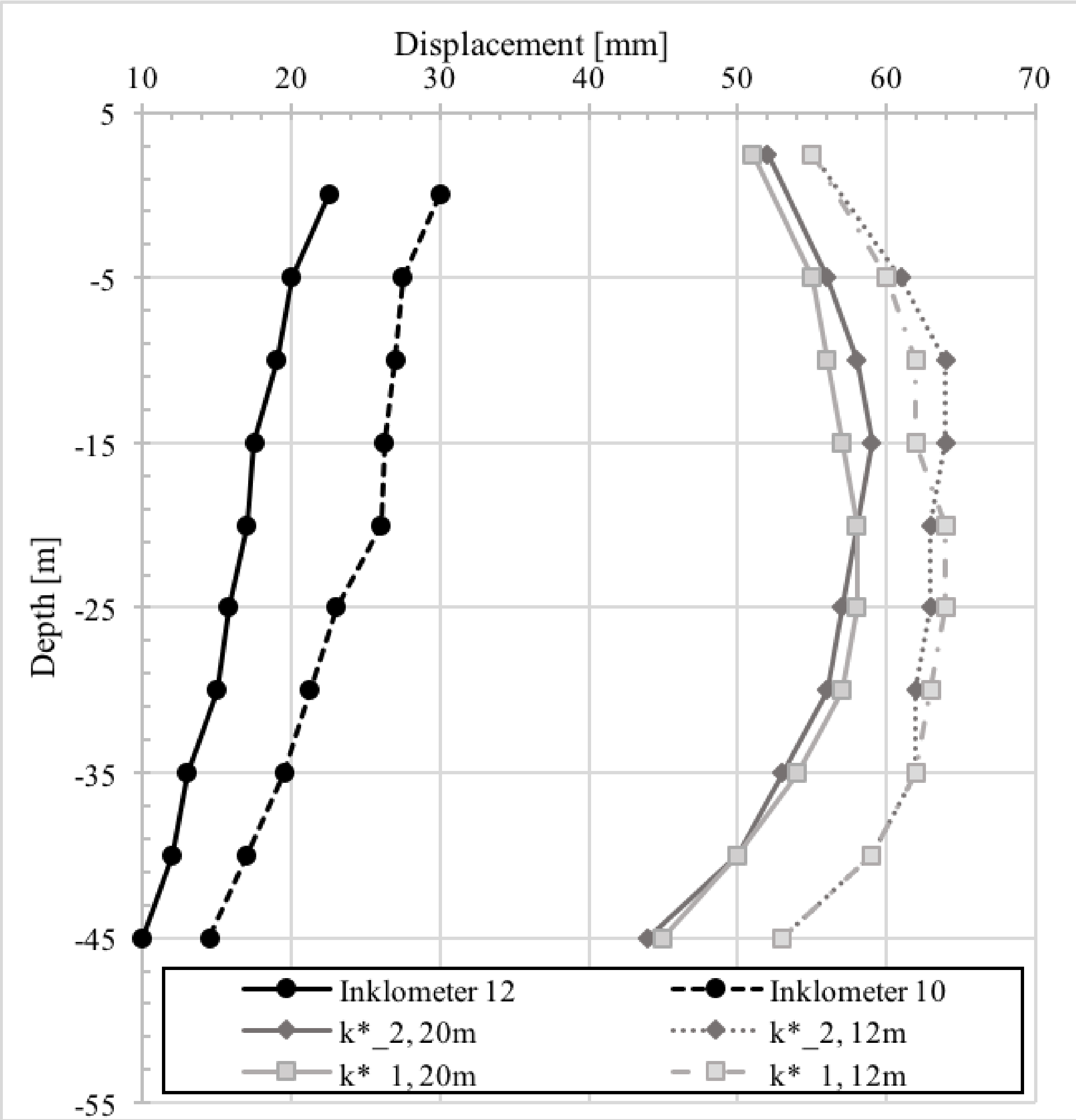

Figure B.10: *Resulting horizontal mass displacement for κ_1^*, κ_2^* and the field measurements in the project Partihallsbron.*

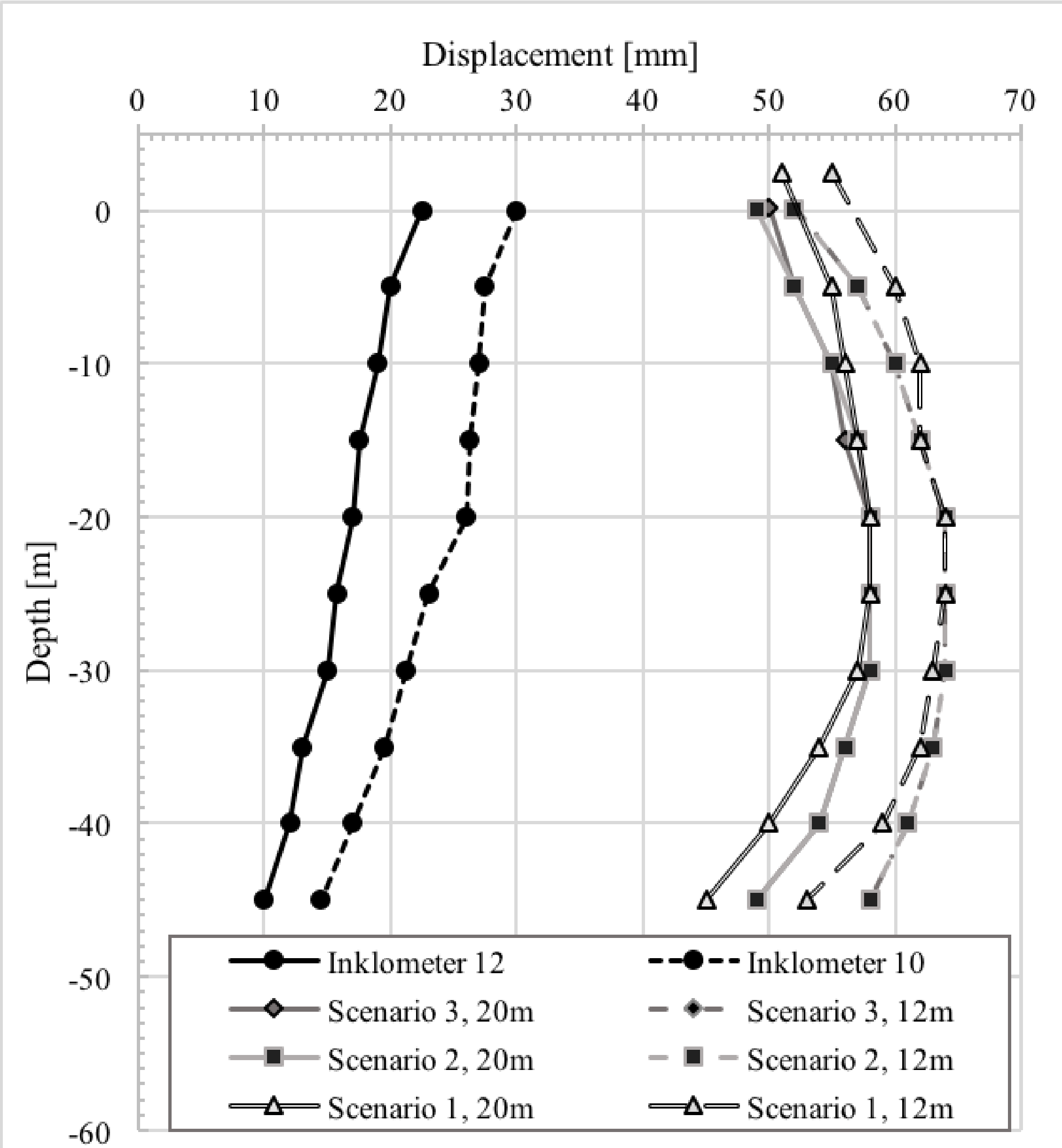

Figure B.11: *The horizontal mass displacement for Scenario 1, Scenario 2, Scenario 3 and field measurements, Partihallsbron.*

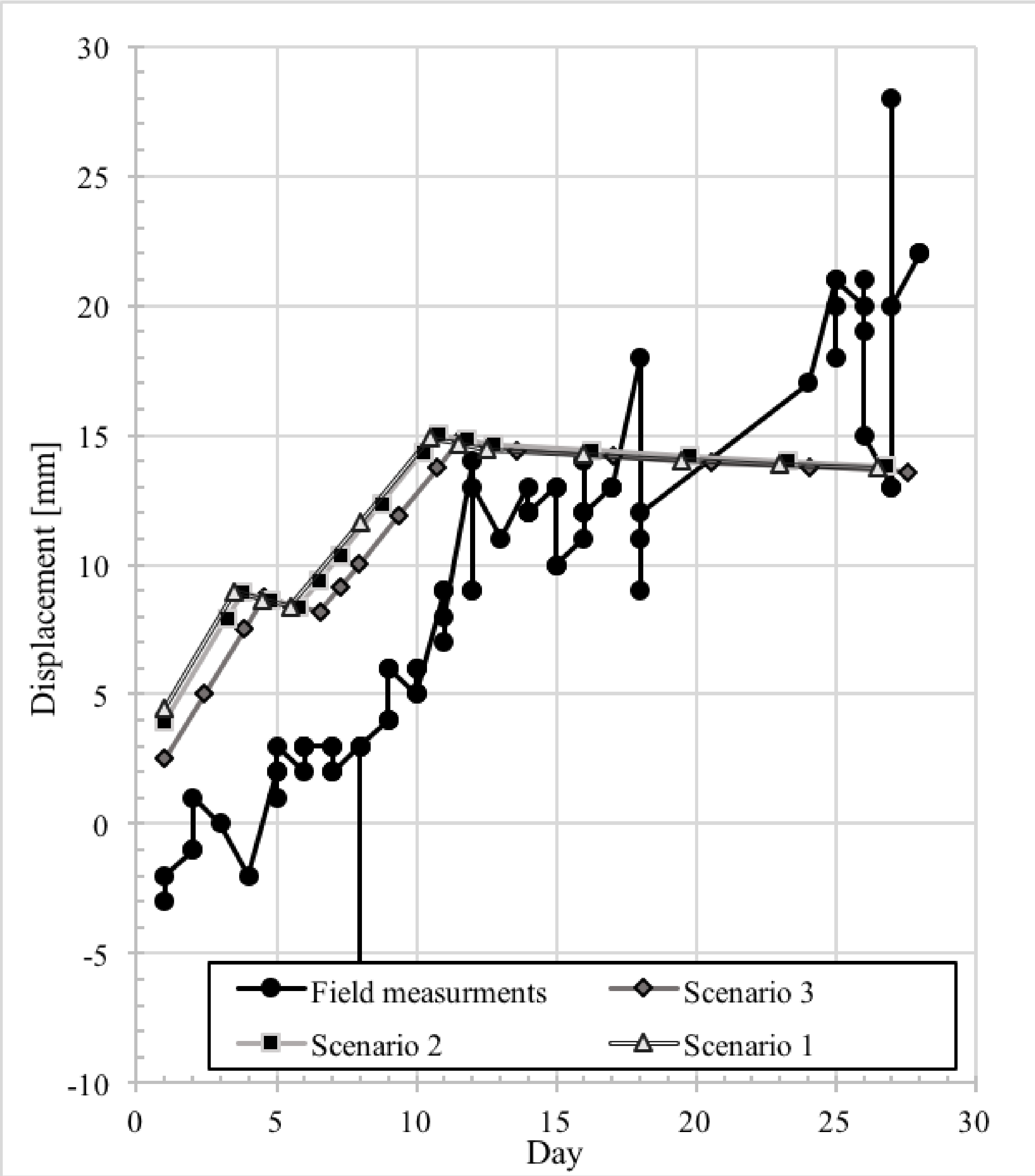

Figure B.12: *The vertical mass displacement of the ground surface in Point B, for the project E45.*

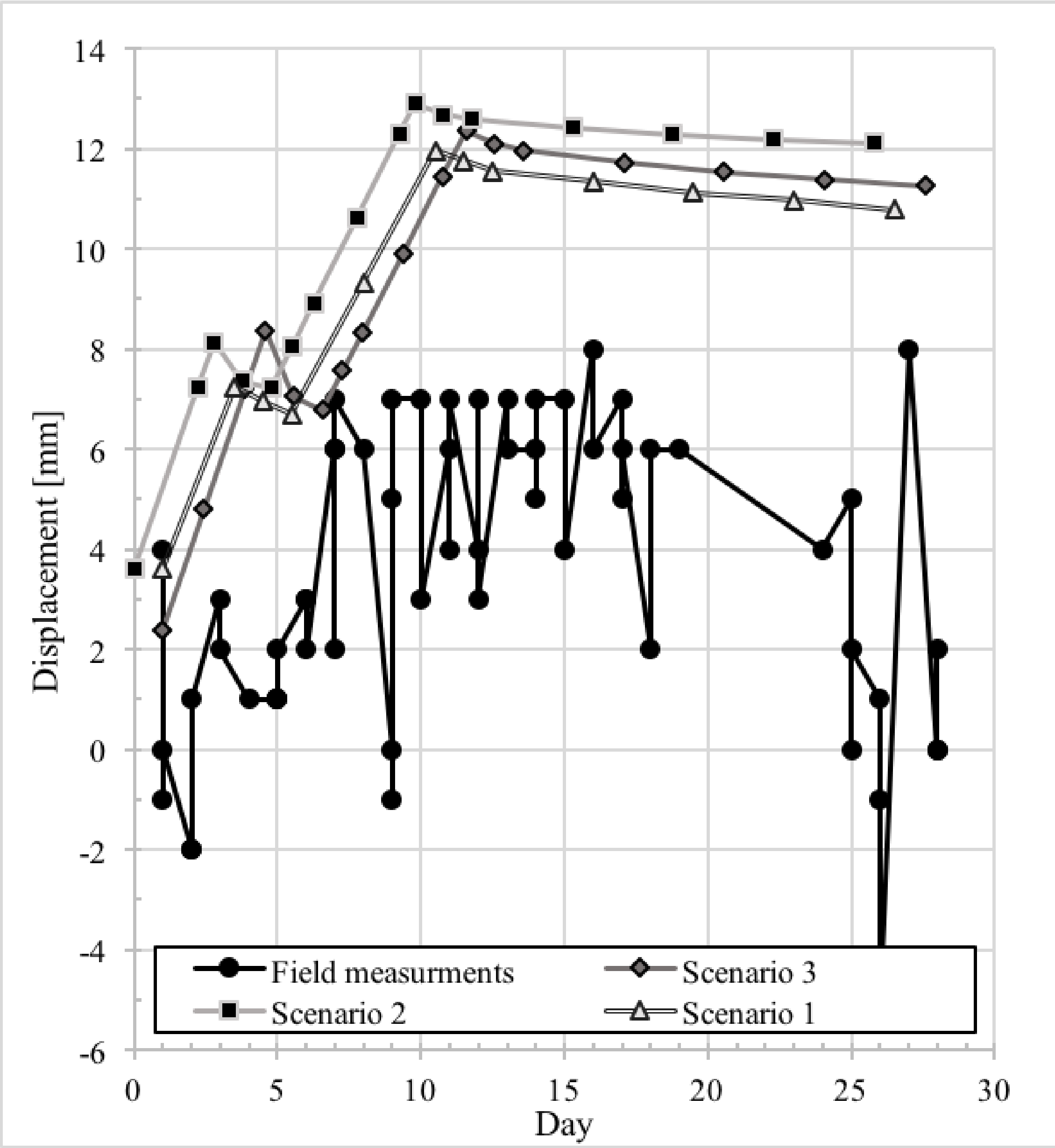

Figure B.13: *The vertical mass displacement of the ground surface in Point D, for the project E45.*

C

Case study - *Västlänken* Central Station

Table C.1: *Model properties for the support structures used for Västlänken [Wood, 2017].*

Parameter	**Diaphragm wall**	**Unit**
EA_1	$6.657e^6$	kN/m
EA_2	$6.657e^6$	kN/m
EI	$522.9e^3$	kNm^2/m
d	0.9709	m
w	2.5	$kN/m/m$
v (nu)	0.2	-
Rayleigh α	0	-
Rayleigh β	0	-
Isotropic	Yes	
End bearing	No	
Material type	Elastic	

Table C.2: *Model properties for the stamps used for Västlänken [Wood, 2017].*

Parameter	**Stamp**	**Unit**
EA	$13.15e^6$	kN
$L_{spacing}$	10	m
d	0.9709	m
$F_{max,tens}$	$22.22e^6$	kN
$F_{max,comp}$	$19.05e^6$	kN
Material type	Elastoplastic	

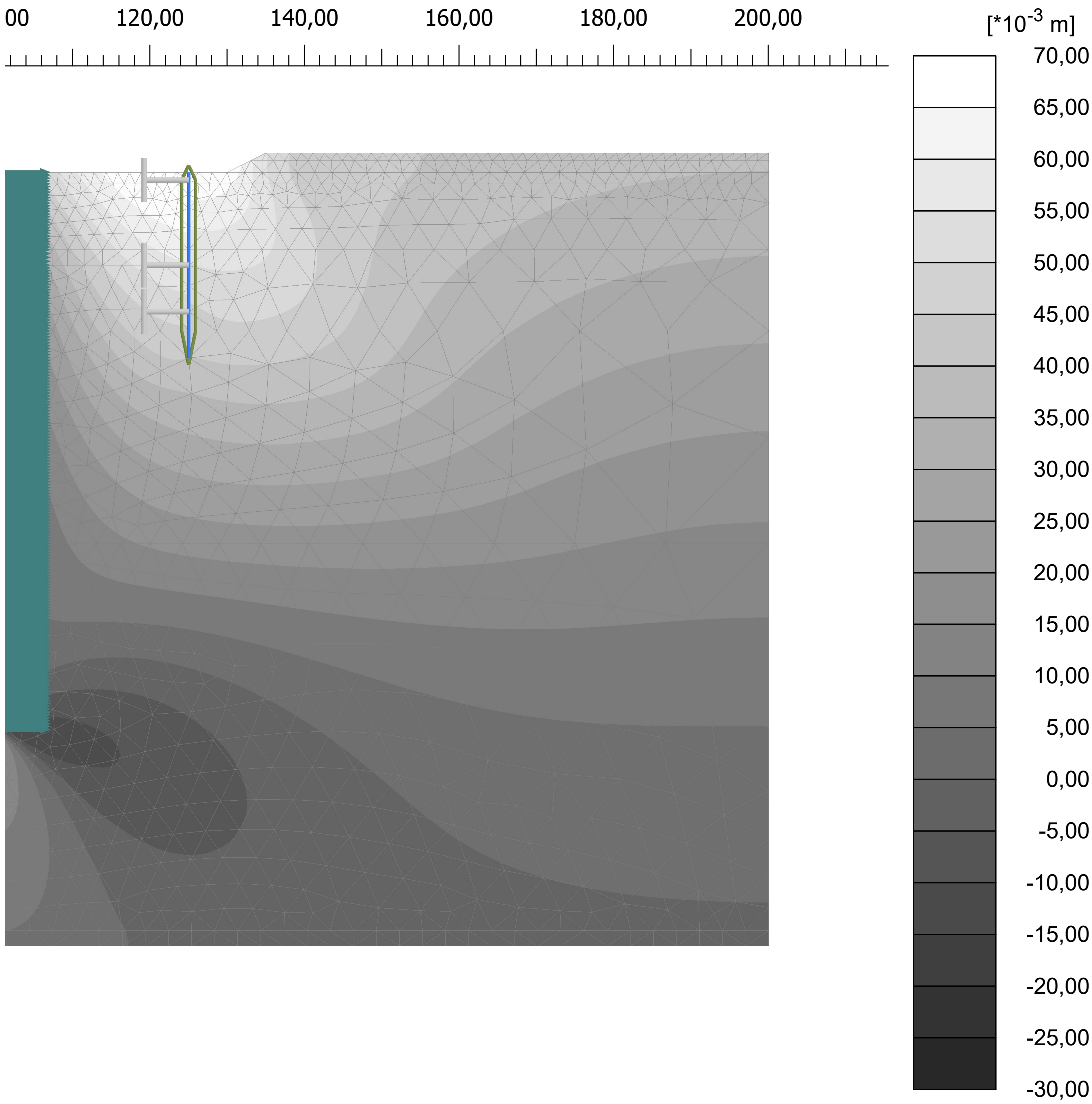

Figure C.1: *Vertical mass displacement directly after the last piling phase for Västlänken, Model 2.*

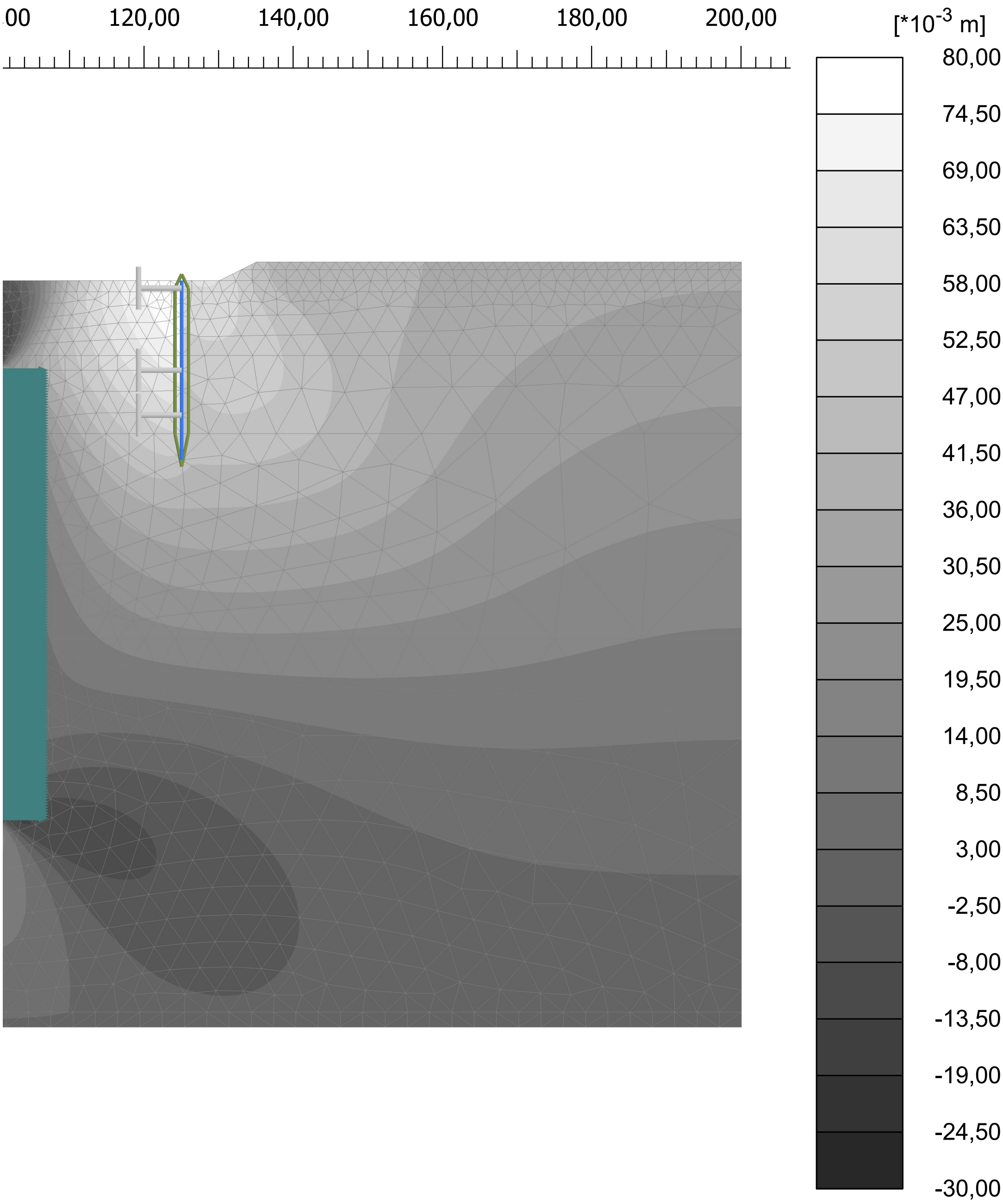

Figure C.2: *Vertical mass displacement directly after the last piling phase for Västlänken, Model 3.*

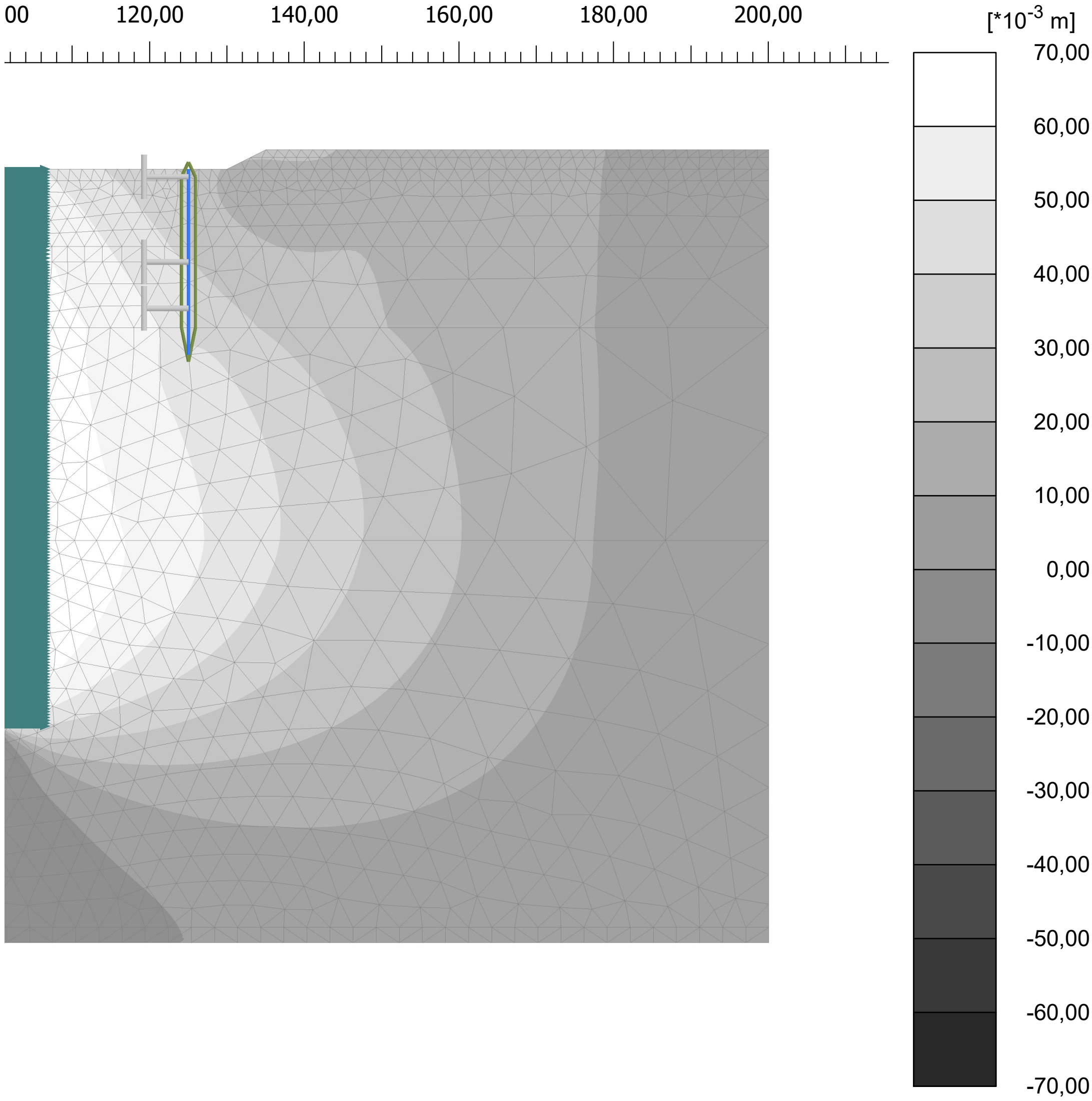

Figure C.3: *Horizontal mass displacement directly after the last piling phase for Västlänken, Model 2.*

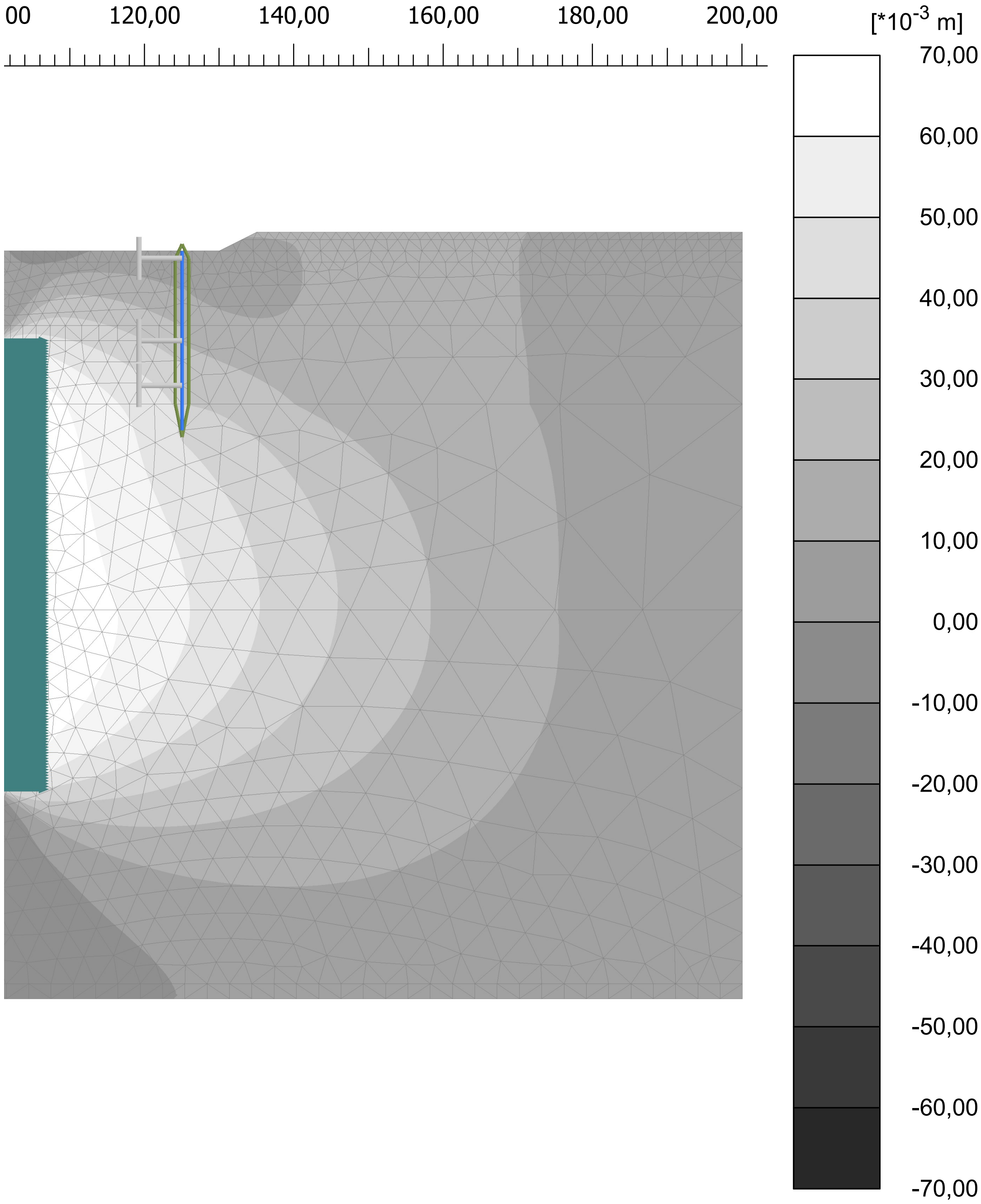

Figure C.4: *Horizontal mass displacement directly after the last piling phase for Västlänken, Model 3.*

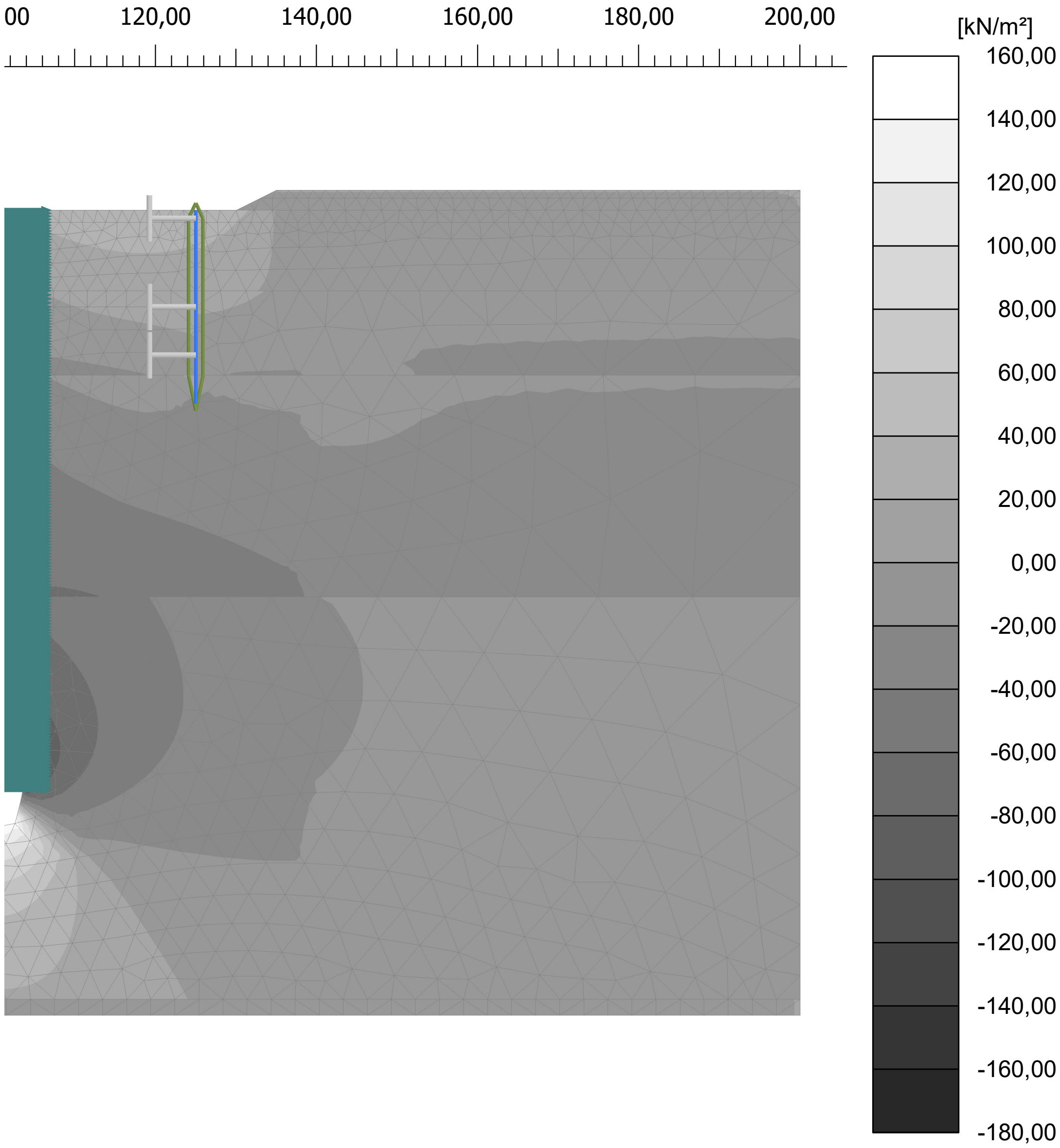

Figure C.5: *Excess pore pressure directly after the last piling phase for Västlänken, Model 2.*

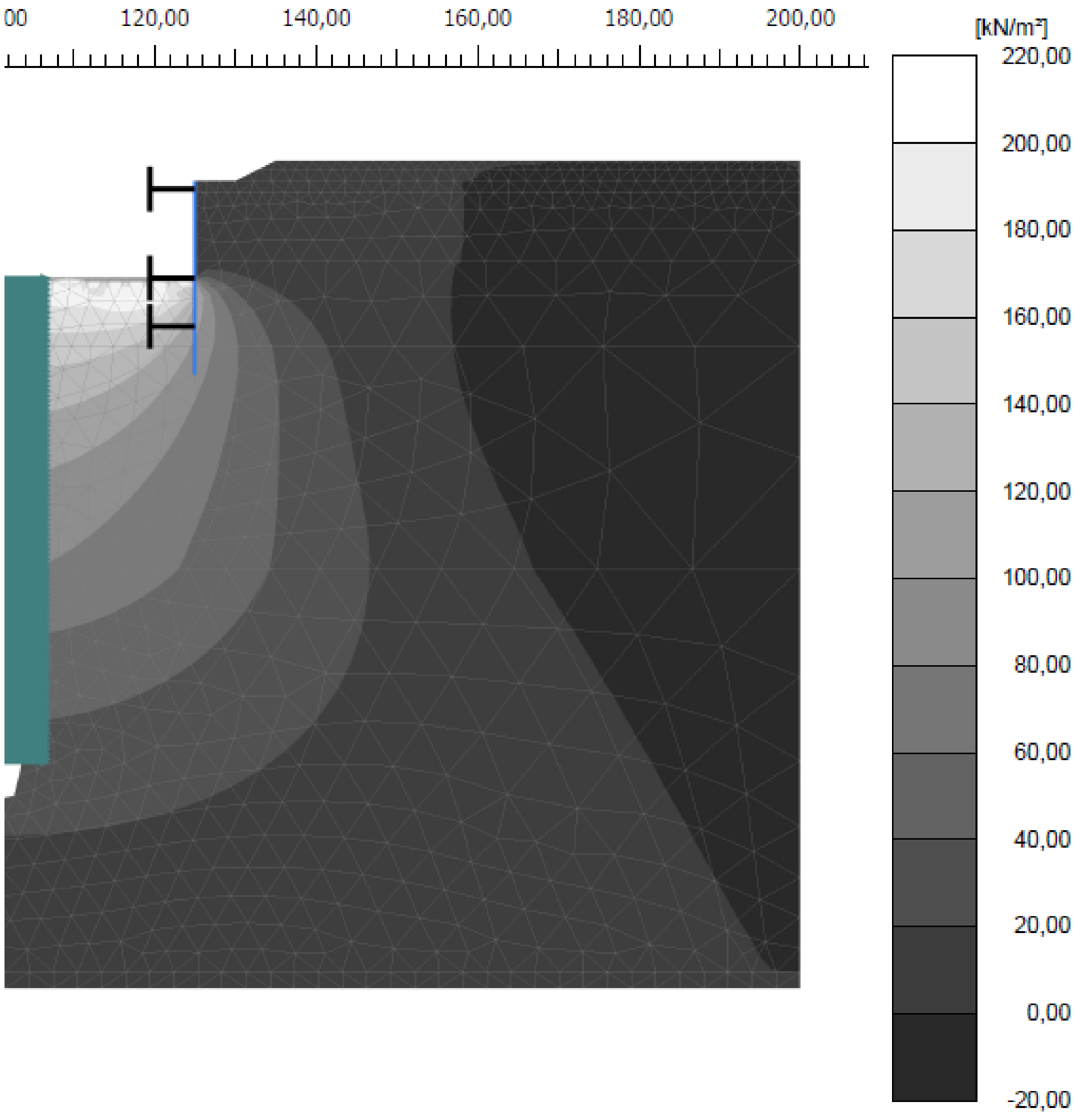

Figure C.6: *Excess pore pressure after 80 years of consolidation for Västlänken, Model 2.*

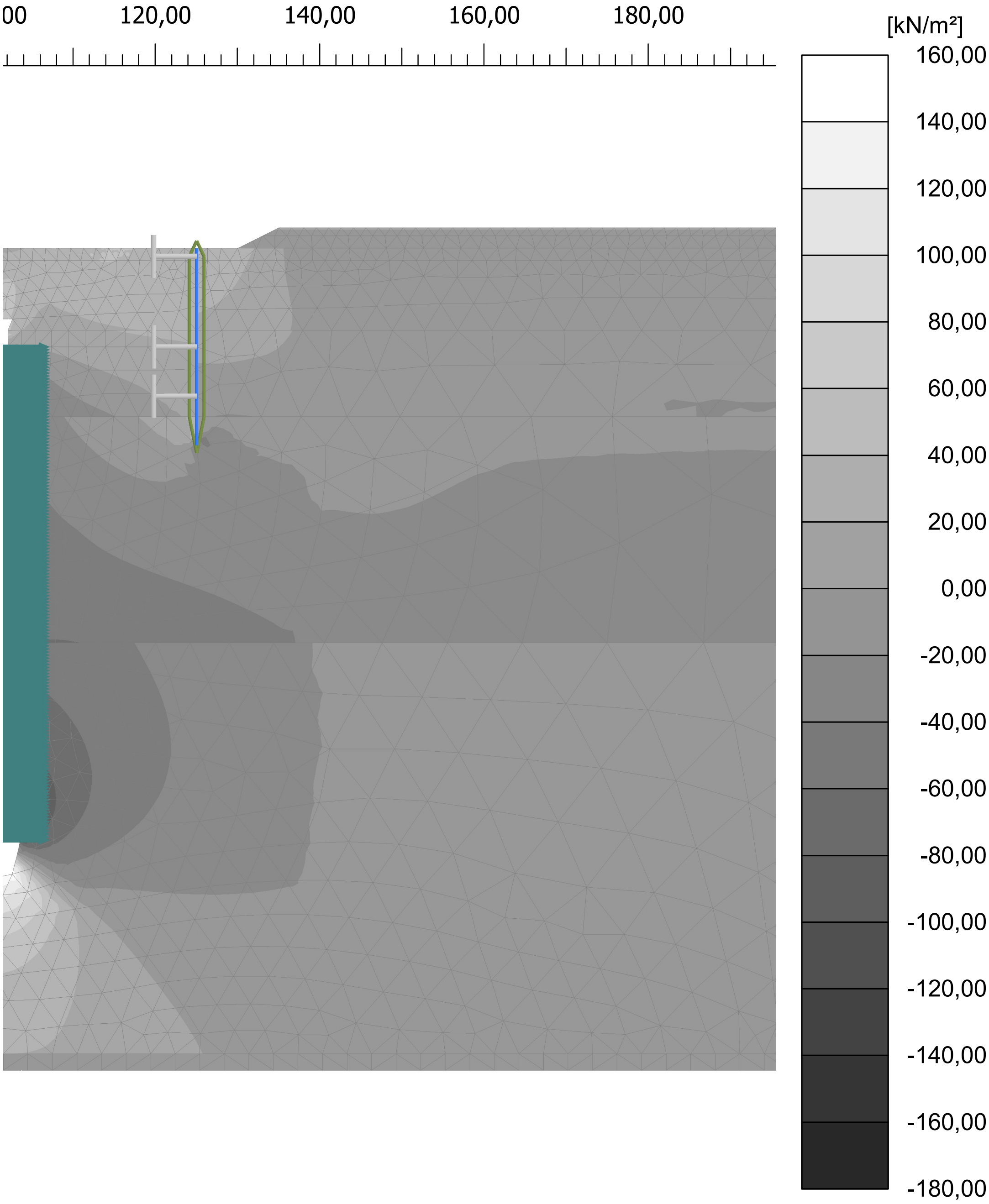

Figure C.7: *Excess pore pressure directly after the last piling phase for Västlänken, Model 3.*

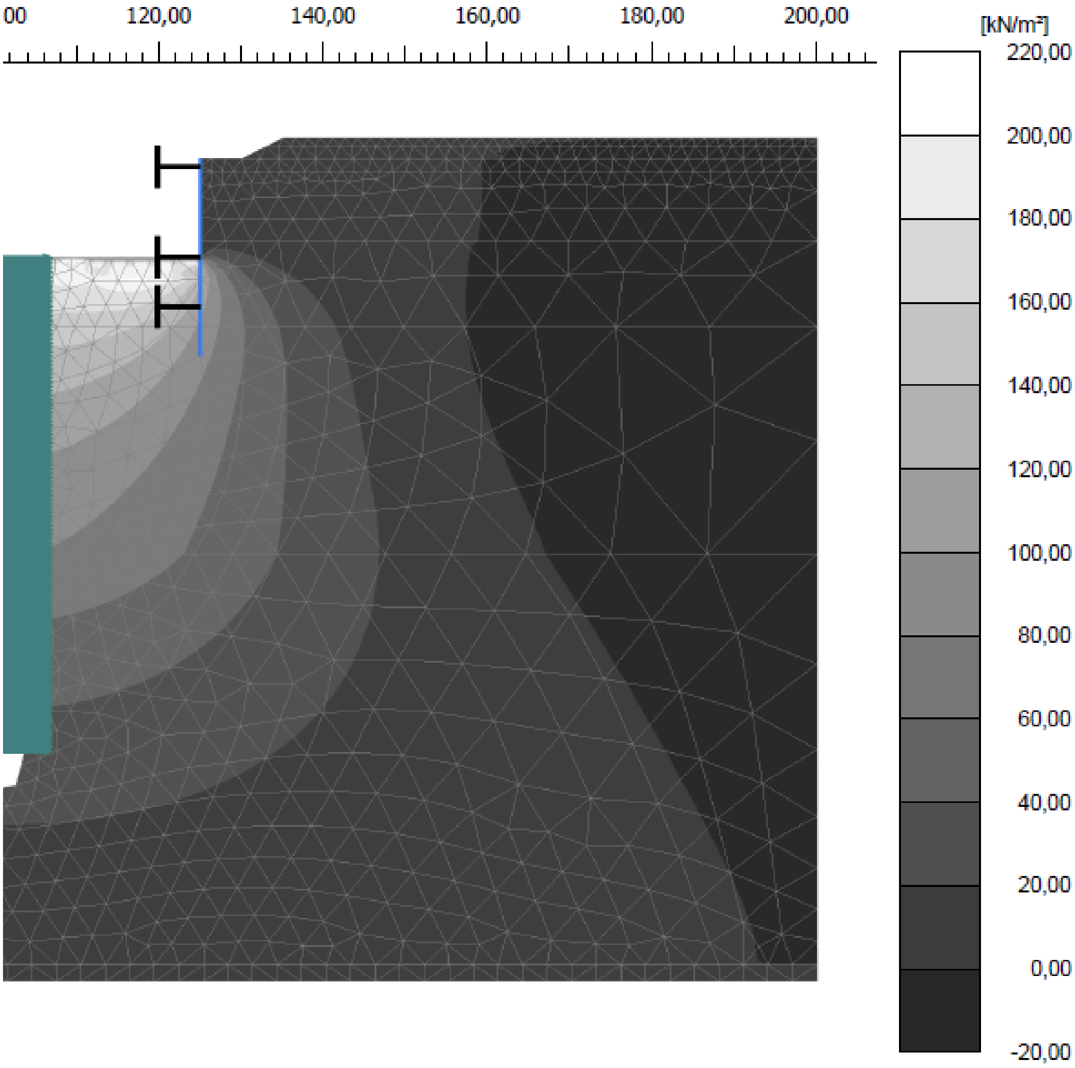

Figure C.8: *Excess pore pressure after 80 years of consolidation for Västlänken, Model 3.*